Development and optimisation of colourimetric microfluidic sensors for water quality monitoring.

Gillian Duffy, B.Sc. (Hons)

Thesis submitted in partial fulfilment of the requirements for the degree of

Doctor of Philosophy

to

Dublin City University

September 2017

Supervisor: Prof. Fiona Regan

School of Chemical Sciences

Co-supervisor: Prof. Dermot Diamond

School of Chemical Sciences

Declaration

I hereby certify that this material, which I now submit for assessment on the program of study leading to the award of Doctor of Philosophy is entirely my own work, and that I have exercised reasonable care to ensure that the work is original, and does not to the best of my knowledge breach any law of copyright, and has not been taken from the work of others save and to the extent that such work has been cited and acknowledged within the text of my work.

Signed: _____

Gillian Duffy

ID No: 59374515

Date:

Acknowledgements

I would like to thank my supervisor Prof. Fiona Regan for her support throughout my PhD, for giving me the freedom to pursue what interested me and for giving me the opportunity to work in such an interesting and exciting field. Thank you for all of the travel that you allowed me do during my PhD, and for your endless positivity, even when things went wrong.

Thank you to my co-supervisor Prof. Dermot Diamond for his help and advice throughout the last few years.

Thank you to Prof. Jennifer Tank for hosting me in the University of Notre Dame, and to all members of the Tank lab for their help and friendship during my visits.

Many thanks to the Naughton Foundation and to DCU for funding my PhD and giving me the opportunity to pursue my ambitions.

A massive thank you must go to Ivan Maguire, without whom I would not have this thesis. Thank you for always finding the time to help and for laughing at the failures with me.

A big thank you to Peter, Nigel, Cormac, and everybody who helped with the autonomous phosphate sensor, for the massive team effort.

Lisa, Maria, and Alan, thank you for your friendship and support every single day. It wouldn't have been possible without you.

Thanks to Brendan and Ciprian for your help whenever I needed it. Thanks to all members of the Regan and Diamond groups, past and present, and everyone who had involvement, for your help and friendship over the past few years. Thanks to Berni for your support and encouragement.

Thanks to all chemistry postgrads and technical staff, past and present, for the friendship and fun every day. Thanks to the NRF staff and Pat Wogan for all the help.

A big special thank you to Emer and Matt for their support and advice throughout my PhD. 36E holds a lot of good memories!

Finally, a massive thank you to my wonderful parents, John and Bernie, for their endless support, encouragement and unwavering belief in me. Thank you for being the best parents and friends I could ever imagine. This thesis is dedicated to you.

"The only source of knowledge is experience"

Albert Einstein

Table of Contents

Declaration i
Acknowledgements ii
List of publications and presentations x
List of Figures xvi
List of Abbreviations xxi
Publications and Author Contribution 1
Thesis Outline 2
Abstract x
Chapter 1: 6
Introduction 6
1.1 The Challenge 7
1.2 Internet of Things (IoT) 10
1.3 Analytes of Interest 11
1.4 Chemical sensors 12
1.5 Fundamentals of spectroscopy 14
1.5.1 Electronic transitions 17
1.5.2 The Beer-Lambert Law 19
1.5.3 UV-visible light absorbance 20
1.6 Low-cost components 22
1.6.1 Light emitting diodes 23
1.6.2 Photodiodes 25
1.7 Microfluidics 25
1.7.1 Valves 27
1.7.2 Mixing 27
1.9 Limitations of colourimetric chemical sensors for deployment 29
1.10 Common sensing methods for P and Cr (III) and (VI) 30
1.11 History of the development of an autonomous phosphate sensor 31

1.11.1 First generation of the phosphate sensor 31
1.11.2 Second generation of the phosphate sensor 34
1.11.3 Summary and future perspectives for phosphate sensor 36
References 37
Aims of the Thesis 43
Chapter 2: 44
Recent developments in optical sensing methods for the determination of eutrophying nutrients for 'smart farming' applications 45
Abstract 46
2.1 Introduction 46
2.1.1 Research drivers 48
2.1.2 Nitrogen 49
2.1.3 Approaches to nitrate monitoring 50
2.1.4 Phosphorus 51
2.1.5 Approaches to phosphate monitoring 51
2.1.6 Types of systems 52
2.1.7 Microfluidic technology for sensor development 53
2.1.8 Agricultural applications of autonomous sensors 54
2.1.9 Aesthetics of an autonomous sensor 58
2.2 Traditional analysis methods 58
2.2.1 Standard methods of analysis for Phosphates 58
2.2.3 Standard methods of analysis for Nitrates 62
2.3 Recent approaches to phosphate monitoring 63
2.3.1 Electrochemical detection 64
2.3.2 Fluorescence detection 65
2.3.3 Colourimetric Detection 67
2.4 Recent approaches to nitrate monitoring 79
2.4.1 Optical detection 79
2.4.2 Electrochemical detection 81
2.4.3 Surface Enhanced Raman Spectroscopic detection 83

2.5 Commercial Nitrate Sensors 91
2.6 Conclusions 92
Notes and references 93
Chapter 3: 109
PhosphaSense: A fully integrated, portable lab-on-a-disc device for phosphate determination in water. 110
Abstract 111
3.1 Introduction 112
3.2 Materials and Methods 113
3.2.1 Chemicals 113
3.2.2 Instrumentation 114
3.2.3 Disc design and fabrication 115
3.2.4 PhosphaSense system design and fabrication 119
3.2.5 Optimisation of optical path length 121
3.2.6 Analytical method 122
3.2.7 Signal processing 122
3.3 Results and discussion 123
3.3.1 Calibration and evaluation of analytical performance 123
3.3.2 Application of PhosphaSense to phosphate determination in environmental water samples 126
3.3.3 Path length optimisation 127
3.4 Conclusions 129
References 130
Chapter 4: 135
ChromiSense: A colourimetric lab-on-a-disc sensor for chromium speciation in water. 136
Abstract 138
4.1 Introduction 139
4.2 Experimental 142
4.2.1 Materials and methods 142
4.2.2 Instrumentation 143

4.2.3 Disc design and fabrication 143
4.2.4 Integrated device prototype 145
4.2.5 Measurement on-disc 147
4.3 Results and discussion 149
4.3.1 Calibrations and real samples 149
4.3.2 Reusable calibration disc 152
4.3.3.System design and fabrication 154
4.3.4 Analytical method development 157
4.4 Conclusion 159
Notes and references 160
Chapter 5: 164
Field-based assessment of the analytical performance of novel phosphate sensors for water monitoring. 165
Abstract 167
5.1 Introduction 168
5.2 Experimental 171
5.2.1 Reagents and standards 171
5.2.2 AutoPhos system 171
5.2.3 AutoPhos Chip 173
5.2.4 PhosphaSense 174
5.3 Experimental 176
5.3.1 Sensor validation 176
5.3.2 Sensor calibration 176
5.3.3 Off-chip mixing 177
5.3.4 Field Deployment 177
5.3.5 Pulse addition method 177
5.4 Results and discussion 179
5.4.1 Calibration of AutoPhos sensor 179
5.4.2 Off-chip mixing 180
5.4.3 Calibration of PhosphaSense 183

5.4.4 In-field measurements 185
5.5 Conclusions 186
Acknowledgements 187
Notes and references 187
Chapter 6: 192
Conclusion 192
Overall Summary & Conclusion 193

Abstract

Development and optimisation of colourimetric microfluidic sensors for water quality monitoring.

Gillian Duffy

The development of low-cost environmental sensors is essential for effective management of our valuable water resources. Traditional water analysis involves manual collection of samples, transport and subsequent analysis in the laboratory. This is time and labour intensive, expensive and requires highly qualified personnel. Automation of this process enables more frequent analysis, saving time and money for researchers, industries and governing bodies. There is a huge and growing demand for low-cost water sensors as legislation becomes more stringent and as more frequent monitoring becomes essential for legislative compliance.

The aim of this thesis was to develop low-cost colourimetric sensors for the determination of water quality in situ. Microfluidic technology was employed to facilitate miniaturisation of colourimetric analytical methods onto a portable sensing device, enabling mixing of small volumes of water with chemical reagents to form a coloured product in the presence of the analyte of interest.

Two fully integrated centrifugal microfluidic sensors were designed and fabricated for rapid on-site water analysis. These sensors were developed for the determination of phosphate and chromium speciation in fresh water. Each sensor consisted of a microfluidic disc for method automation, a motor, absorbance based detection system, electronics board and was connected to a laptop for data collection. They were both validated against the standard

colourimetric method, and applied to the measurement of river water and waste-water effluent samples.

A fully autonomous phosphate sensor was designed, fabricated, validated and deployed in an agricultural catchment site. This sensor employed a microfluidic chip coupled with syringe pumps for fluid manipulation. It incorporated its own power supply and was programmed to take periodic unassisted measurements, with on-board data storage.

Important considerations for sensor design included the sensitivity and selectivity of the analytical method, reagent stability, optical path length, material compatibility with reagents, use of low-cost components and overall robustness.

List of publications

1. Gillian Duffy, Ivan Maguire, Brendan Heery, Charles Nwankire, Jens Ducrée, Fiona Regan. PhosphaSense: A fully integrated, portable lab-on-a-disc device for phosphate determination in water, Sensors and Actuators B: Chemical. 246 (2017) 1085–1091. doi:10.1016/j.snb.2016.12.040.

2. Gillian Duffy, Fiona Regan. Recent Developments in Sensing Methods for Eutrophying Nutrients with a Focus on Automation for Environmental Applications, The Analyst, (2017). doi: 10.1039/C7AN00840F

3. Gillian Duffy, Ivan Maguire, Brendan Heery, Pauline Gers, Jens Ducrée, Fiona Regan. ChromiSense: A colourimetric lab-on-a-disc sensor for chromium speciation in water. Talanta, (2017). doi: 10.1016/j.talanta.2017.09.066

4. Gillian Duffy, Peter McCluskey, Ursula H. Mahl, Nigel Kent, Southampton people, Jennifer Tank, Dermot Diamond and Fiona Regan. Analytical performance characterisation of microfluidic, colourimetric-based phosphate sensors for water analysis. (2017). (Prepared for submission)

5. B. Heery, C. Briciu-Burghina, D. Zhang, G. Duffy, D. Brabazon, N. O'Connor, F. Regan, ColiSense, today's sample today: A rapid on-site detection of β-d-Glucuronidase activity in surface water as a surrogate for E. coli, Talanta. 148 (2016). doi:10.1016/j.talanta.2015.10.035.

Oral Presentations

1. Gillian Duffy, Brendan Heery, Ivan Maguire, Charles Nwankire, Jens Ducrée, Fiona Regan "A fully integrated centrifugal microfluidic device for in situ measurement of water quality parameters" Analytical Research Forum 2016, London, United Kingdom.

2. Gillian Duffy, Brendan Heery, Ivan Maguire, Charles Nwankire, Jens Ducrée, Fiona Regan "A centrifugal lab-on-a-disc device for determination of phosphate in water", YoungChem 2015, Krakow, Poland.

3. Gillian Duffy, Brendan Heery, Ivan Maguire, Charles Nwankire, Jens Ducrée, Fiona Regan "A centrifugal lab-on-a-disc device for the in situ determination of dissolved reactive phosphate in water", EuroAnalysis 2015, Bordeaux, France.

4. Gillian Duffy, John Cleary, Cormac Fay, Kevin Murphy, Fiona Regan, Dermot Diamond "On-chip optical sensing methods for determination of phosphates in freshwater" Association for the Sciences of Limnology and Oceanography meeting 2015, Granada, Spain.

5. Gillian Duffy, John Cleary, Fiona Regan, Dermot Diamond "The development of a low-cost, autonomous phosphate sensor for freshwater monitoring" AECOM Student Environmental Award 2014, Sligo, Ireland.

6. Gillian Duffy, John Cleary, Fiona Regan, Dermot Diamond "A low-cost autonomous phosphate sensor for quantifying the influence of agriculture on river water" Environ 2014, Dublin, Ireland.

Poster Presentations

1. Europt[r]ode 2016, Graz, Austria: A fully integrated centrifugal lab-on-a-disc platform for on site measurement of phosphate in water.

2. Diffuse Pollution and Catchment Management 2016, Dublin, Ireland: ChromiSense: A fully integrated optical sensor for rapid on-site speciation of chromium in water.

3. Napes Workshop, 2017, Dublin, Ireland. Poser presentation: A fully integrated centrifugal lab-on-a-disc platform for on-site measurement of phosphate in water.

4. CASi 2016, Dublin, Ireland. Poster presentation: A microfluidic lab-on-a-disc device for in situ measurement of phosphate in water.

5. 67th Chemistry Colloquium 2015, Maynooth, Ireland: An autonomous phosphate sensor for remote continuous monitoring.

6. SmartOcean Forum 2014, Belfast, Ireland. Poster presentation: Autonomous sensors for nutrient monitoring

7. Beaufort Review, 2014, Dublin City University: Autonomous sensors for nutrient monitoring.

8. Environ 2015, Sligo, Ireland: The optimisation of an autonomous phosphate sensor for remote continuous monitoring.

Workshops

1. Autonomous nutrient sensors. International Association of Hydrogeologists (IAH) 2016, Tullamore, Ireland.

Awards

1. Europt[r]ode 2016 Analyst poster prize, Graz, Austria.
2. AECOM student award 2014, for oral presentation.
3. Travel bursary from Royal Society of Chemistry for Analytical Research Forum, 2016.

List of Figures

1. Page 8, Fig. 1.1. The wide range of disciplines required for development of autonomous optical chemical sensors.
2. Page 13, Fig. 1.2. A schematic of a chemical sensor, adapted from reference 22.
3. Page 15, Fig. 1.3. The electromagnetic spectrum, showing the electric and magnetic field oscillation planes.
4. Page 17, Fig. 1.4. Scale showing the wavelength range for each type of electromagnetic radiation, highlighting the visible region at 400 to 700 nm.
5. Page 18, Fig 1.5. The Jablonski diagram, where radiative processes are denoted with straight arrows, and non-radiative processes are shown with curvy arrows.
6. Page 20, Fig. 1.6. An exemplar absorbance spectrum, showing an absorbance maximum at approximately 550 nm.
7. Page 21, Fig. 1.7. The electron transitions possible from UV-visible light excitation, adapted from reference 23.
8. Page 24, Fig. 1.8. Diagram of an LED/laser composition, showing the P-doped and N-doped regions, separated by an active region, from which photons are released when current flows, using gallium arsenide as a material example, adapted from reference 27.
9. Page 26, Fig. 1.9. A diagram showing the rotation of the disc at angular velocity (ω), and a resulting centrifugal force in the direction shown, from the centre to the outer edge of the disc.
10. Page 38, Fig. 1.10. The mixing of phenolphthalein and sodium hydroxide in a straight channel, a square-wave channel and a three-dimensional serpentine channel.

11. Page 32, Fig. 1.11. (A) The microcontroller and GSM modem mounted in the lid, the solenoid pumps, microfluidic chip, LED and photodiode on the mounting plate. (B) The storage bottles and battery in the lower part of the case, all contained in the 'Pelicase'.
12. Page 33, Fig. 1.12. Image of the microfluidic chip consisting of six inlets, one waste outlet, a serpentine channel for mixing of sample and reagent, and a cylindrical optical cuvette.
13. Page 35, Fig. 1.13. The second generation phosphate sensor. (1) Sample inlet (2) control board, detection system (3) peristaltic pumps (4) reagent bags and (5) enclosure.
14. Page 53, Fig. 2.1. A schematic of an autonomous water nutrient sensor, showing examples of the possible functions and requirements.
15. Page 57, Fig. 2.2. A diagram showing N and P from agricultural sources entering the water system, representing an ideal deployment site for nutrient sensor networks.
16. Page 118, Fig. 3.1. (Left) Rendered image showing each layer of the microfluidic disc, where (i) is a PMMA layer with air vents and fluid inlets; (ii) is a PSA layer with microfluidic channels; (iii) is a PMMA layer with microfluidic channels; (iv) is a PSA layer with an air ventilation system; and (v) is a base PMMA layer. (Top right) Rendered image of the microfluidic disc showing thickness; (bottom right) schematic of the microfluidic disc, which consists of a mixing reservoir (R) with inlets for sample and reagent loading, a microfluidic channel through which the fluids flow into the 75 mm long optical detection zone (ODC), and an air vent (V) to release trapped air. The disc includes three alignment slots for precise optical alignment with the stage in Fig. 3.2.
17. Page 120, Fig. 3.2. (Left) Rendered image of the PhosphaSense system where (a) is the lid for ambient light exclusion; (b) is the optical detection

system; (c) is the motor; (d) is the microfluidic disc; and (e) is the compartment for electronics. (Right) Rendered images of the 3D printed stage components of PhosphaSense, where the top image shows the stage component of the system, with the motor top piece, and the bottom image shows how the optical alignment stage is fitted on top of the primary stage. The pillars on this stage line up with slots on the microfluidic disc shown in Fig. 3.1 to facilitate precise alignment with the detection system.

18. Page 121, Fig. 3.3. Rendered image of the 3D printed cuvette holder with two light sources (an LED and a laser) and two detectors (photodiodes), precisely aligned for absorbance measurements over a range of optical path lengths.
19. Page 123, Fig. 3.4. Calibration curve obtained on the PhosphaSense system using prepared phosphate standards, where error bars show one standard deviation, with a slope of 0.003 AU.L.μg^{-1} and an R^2 of 0.9958.
20. Page 124, Fig. 3.5. Correlation plot for the measurement of the phosphate standards on PhosphaSense (n=3) and on a spectrophotometer (n=3), where each point is labelled with the concentration in $\mu g.L^{-1}$. Error bars show one standard deviation in blue for PhosphaSense and in red for the spectrophotometer, with an R^2 value of 0.9915 and a slope of 4.71.
21. Page 141, Fig. 4.1. Reaction of Cr (III) with 2 molecules of PDCA to form [Cr(PDCA)2]-.
22. Page 141, Fig. 4.2. Reaction of Cr (VI) with DPC to form $[Cr(DPCO)]^+$.
23. Page 144, Fig. 4.3. (Left) A rendered image of the five disc layers, made from PMMA (shown in purple) and PSA (shown in red), where (i) contains inlets and air outlets; (ii) contains large reservoir features and air vents; (iii) contains large reservoir features; (iv) contains large reservoir features

and microfluidic channels; (v) acts as the base. (Right) a schematic of the centrifugal disc (120 mm diameter), showing the sample reservoir (SR); reagent reservoir (RR); 500 µm wide micro-channels (MC); 5 x 50 mm optical detection zone (ODZ) with bubble traps; and 500 µm wide air ventilation system (AV). The light path for absorbance measurements is illustrated by an arrow through the ODZ, with LED and PD positions shown.

24. Page 147, Fig. 4.4. A rendered image of the ChromiSense system (measuring 20 x 18 x 15 cm in total) where (a) is the lid for ambient light exclusion during optical measurements; (b) is the disc; (c) is the optical detection system consisting of an LED and PD couple; (d) is the compartment for storage of electronic components; (e) is the heating pads attached to heat sinks; (f) is the secondary stage for precise alignment of discs with the optical detection system.
25. Page 149, Fig. 4.5. Calibration curves for Cr(VI) (a) and Cr(III) (b), and correlation plots for the measurement of the Cr(III) (c, R^2=0.995) and Cr(VI) (d, R^2=0.999) standards on ChromiSense vs. using a spectrophotometer, where n=3.
26. Page 152, Fig. 4.6. Calibration curves for Cr(VI) (a) and Cr(III) (b) at 535 nm (solid line) and Cr(III) at 330 nm (dotted line for linear range, dashed line for exponential fit) using the calibration disc and ChromiSense optical detection system, n=3.
27. Page 156, Fig. 4.7. A bar chart depicting the improved filling capability of the shield-shaped reservoir for low viscosity fluids, compared to that of the circle-shaped reservoir.
28. Page 158, Fig. 4.8. The absorbance spectra of [$Cr(PDCA)_2$] (a) showing a freshly made and a 1 month old solution of the purple coloured complex, and [Cr(DPC)] (b) showing a freshly made, a 1 day old and a 1 month old

solution of the pink coloured complex, with calibration curves for freshly made and 1 month old solutions of [$Cr(PDCA)_2$] (c) and [Cr(DPC)] (d).

29. Page 172, Fig. 5.1. A schematic of the syringe pump system, where the motor rotates a metal screw, which moves the 3D printed syringe holder up and down along the crew threads, along the metal rods.
30. Page 174, Fig. 5.2. A schematic of the microfluidic chip, showing 6 inlets, 1 outlet, 3 T-junctions for mixing, and 1 optical detection channel with an LED-PD pair for absorbance measurements.
31. Page 175, Fig. 5.3. A schematic of the steps involved for AutoPhos to make a measurement.
32. Page 176, Fig. 5.4. A schematic of the steps involved for PhosphaSense to make a measurement.
33. Page 179, Fig. 5.5. A correlation plot between the calibration carried out on the AutoPhos system in Ireland vs. that carried out in the USA, yielding an R^2 value of 0.998, where the phosphate concentration is shown in mg L^{-1}, and error bars represent standard deviation, where n=3.
34. Page 180, Fig. 5.6. On-chip mixing, off-chip mixing and UV-vis absorbance measurements for a range of phosphate concentrations, with error bars showing the standard deviation, where n=3.
35. Page 182, Fig. 5.7. Calibration curve including standards below the calculated LOQ, with and R^2 value of 0.999, where n=3.
36. Page 183, Fig. 5.8. A correlation plot for PhosphaSense between calibration carried out in Ireland (previously published)7 vs. that carried out in the USA with an R^2 of 0.997, where the phosphate concentration is shown in µg L^{-1}, and error bars represent standard deviation, where n=3.
37. Page 185, Fig. 5.9. A plot of the data obtained by measuring field samples in-field and in the lab on the AutoPhos sensor, on PhosphaSense, and on the Lachet system.

List of Abbreviations

AAS	Atomic absorbance spectroscopy
COP	Cyclic Olefin Polymer
DPC	1,5-diphenyl carbazide
HAB	Harmful Algal Bloom
IC	Internal conversion
ICP-AES	Inductively coupled plasma-atomic emission spectroscopy
ICP-MS	Inductively coupled plasma-mass spectrometry
IoT	Internet of things
IP	Ingress protection
ISC	Intersystem crossing
LED	Light emitting diode
LOAD	Lab-on-a-disc
LOD	Limit of detection
LOQ	Limit of quantitation
LWCC	Liquid waveguide capillary cell
MEMS	Microelectromechanical system
N	Nitrogen
ODZ	Optical detection zone
P	Phosphorus
PD	Photodiode
PDCA	2,6-pyridine dicarboxylic acid
PEDD	Paired emitter detector diode
PMMA	Polymethyl methacylate
PSA	Pressure sensitive adhesive
R	Reservoir
SERS	Surface enhanced Raman spectroscopy

SIA	Sequential injection analysis
SRP	Soluble reactive phosphate
TP	Total phosphorus
TRL	Technology readiness level
USDA	US Department of Agriculture
V	Vents
WFD	Water framework directive
WHO	World Health Organisation
WSN	Wireless Sensor Networks
WWTP	Waste Water Treatment Plant
µTAS	Micro-total analysis system

Publications and Author Contribution

This thesis includes two original manuscripts published in peer-reviewed journals and two chapters that are submitted/ prepared for submission to peer-reviewed journals. The core of the thesis is the development of low cost microfluidic based analysers for water quality analysis. The ideas, development and writing up of all manuscripts in the thesis were the principal responsibility of me, the candidate, working within the School of Chemical Sciences under the supervision of Prof. Fiona Regan. The inclusion of co-authors in Chapter 3 to 5 reflects the fact that part of the work came from active collaborations between researchers. In the case of these chapters, my contribution to the work involved the following:

Chapter	Sensor	Nature and extent of candidate's work
3	PhosphaSense	First author, initiation, key ideas, input into sensor design, disc fabrication, data collection and analysis, manuscript development and writing up.
4	ChromiSense	First author, initiation, key ideas, input into sensor design, disc fabrication, data collection and analysis, manuscript development and writing up.
5	Autonomous phosphate sensor	First author, initiation, some engineering, field work, data collection and analysis, and writing up.

Signed: _____ Date: _____

Gillian Duffy

Signed: _____ Date: _____

Prof. Fiona Regan

Thesis Outline

A detailed overview of each chapter is given below:

Chapter 1

This chapter provides the background information and theory relating to the research carried out in this thesis. An introduction to the interdisciplinary nature of sensor development, to spectroscopy, sensors, low-cost components, microfluidics and the history of autonomous phosphate sensor development in DCU is given.

Chapter 2

This chapter presents a published literature review article that examines the potential of both standard water analysis methods, and of novel analysis methods for automation as sensors for continuous, real-time monitoring of eutrophying nutrients. It also compares the performance of several commercially available sensors for these analytes, and promising novel analysis methods reported in the last 5 years with standard analysis methods and state-of-the-art-sensor technology to give a present-day perspective on the development of autonomous sensors for eutrophying nutrients. A 'smart farm' concept was included as an application with great potential for autonomous nutrient sensor deployment. Prior to this publication, there was a gap in the literature for a dedicated review that addresses autonomous technology with a focus on monitoring eutrophication.

Chapter 3

This chapter presents the design, fabrication and performance of a portable, centrifugal microfluidic sensor for phosphate measurement in water. The sensor, called PhosphaSense, is made up of two components: a disposable microfluidic disc and a complementary system. The microfluidic disc contains a reservoir for sample and reagent insertion, microchannels, an optical detection zone where absorbance measurements are made, and air vents to prevent bubble formation in the measurement zone. The complementary system contains a motor for disc rotation, creating centrifugal force that pumps fluids from the reservoir to the detection zone. It also contains an LED and PD pair for absorbance measurements, a stage for precise alignment of the disc with the detection system, and an electronics board to control the sensor and to log data to a computer via USB cable. The system uses the ascorbic acid method for phosphate determination, coupled with a long optical path length of 75 mm to maximise sensitivity. It was applied to the measurement of phosphate in both river water and waste water treatment plant effluent. The low measurement range of this system is typically not achieved by commercial sensors, particularly low-cost ones such as the Hach® handheld system, which measures from 20 $\mu g\ L^{-1}$, more than double the LOD of PhosphaSense. This work has the potential to become a fully portable colourimetric sensor that can be brought to a sampling site for rapid on-site analysis.

Chapter 4

This chapter presents the design, fabrication and performance of a portable, centrifugal sensor system for chromium speciation in water. This sensor, called ChromiSense, is made up of a centrifugal disc and a complementary system. The

disc contains reservoirs for sample, reagent and buffer, microchannels, and optical detection zone with bubble trap features, and air vents. The complementary system contains an LED and PD couple for absorbance measurements, heating pads and heat sinks for a heating step in the method, a stage for precise alignment of the disc with the detection system, and an electronics board for controlling the system, as well as data logging with a computer via USB cable. The system carries out two different colourimetric methods simultaneously on one disc in order to measure chromium III and VI in each sample. The system was applied to the measurement of spiked river water samples. It can measure lower concentrations than the Hach® handheld analyser for low-range Cr(VI) measurement, and has a wider measurement range than this and wider than the combined range of Hanna® Instruments low and high level handheld analysers. Cr(III) is typically inferred by measurement of total Cr and Cr(VI), followed by subtraction. This sensor uses a separate colourimetric method to measure Cr(III) directly, which is a novel approach to monitoring Cr(III) in a handheld system. The only centrifugal speciation of chromium in the literature uses a separation step followed by ICP-MS as the detection method, making this system exceptionally low-cost for its purpose.

Chapter 5

This chapter presents the performance comparison of two novel colourimetric-based, microfluidic phosphate sensors. These sensors were applied to the measurement of field samples collected from an agricultural stream in Indiana, USA, as part of a collaboration with Prof. Jennifer Tank's group in University of Notre Dame. The first sensor, PhosphaSense, was presented in Chapter 3. The second is an autonomous sensor that was developed in collaboration with Prof.

Dermot Diamond's group in DCU. The autonomous sensor consists of syringe pumps for delivery of sample and reagent from storage containers to the microfluidic chip. This chip, made from tinted PMMA, contains an LED and PD pair for absorbance measurements. The system measures phosphate using the vanadamolybdophosphoric acid method. While this method is not as sensitive as other colourimetric methods for phosphate determination, the reagent stability is excellent, making it suitable for use on long-term deployable systems. A sample intake system was incorporated, as well as a programmable electronics board, which allowed for system control, data storage on an SD card, and connection via USB cable with software for real-time data visualisation and system control. In-field performance of this sensor was demonstrated. This work contributes to the large research effort towards developing low-cost, wet chemistry-based deployable sensors for water quality monitoring. The advantages and disadvantages of the vanadomolybdophosphoric acid method were shown (high detection limit, wide linear range, excellent reagent stability), as well as the ascorbic acid method (low detection limit, narrower linear range, poor reagent stability). The field work demonstrated sensor performance in an agricultural stream water matrix, using a nutrient pulse method to provide samples over a wide range of concentrations to demonstrate performance of both sensor systems. The deployment time of the Cycle-P phosphate sensor from Wet Labs is 3 months due to its reagent stability. The deployment time of this sensor has the potential to be greater than 1 year, based on reagent stability.

Conclusion

A summary of the work carried out in this thesis is given in order to conclude the work.

Chapter 1:

Introduction

1.1 The Challenge

The demand for more frequent and more extensive environmental measurements is growing steadily as populations grow, farming intensifies, and water resources become even more precious. A 'grand challenge' was posed to analytical chemists by Prof. Royce Murray, editor of Analytical Chemistry, in 2010. This challenge was to "develop a capability for sampling and monitoring air, water, and soil much more extensively and frequently than is now possible".[1] More frequent monitoring and improved sensors are important over a wide range of applications. Some applications of wireless sensor networks to date include the monitoring of submarines by the military in the 1950s[2], air quality monitoring within cities[3], to monitor volcanic eruptions[4], to monitor the behaviour of ice caps and glaciers[5], to detect forest fires[6], to detect traffic, meter water/gas/electricity, as well as to monitor processes in large industries.[2] In order to extend the application of wireless sensor networks to new applications or analytes, a great deal of research and development is required. As the emphasis on water management is growing globally, the need for and market for reliable sensors for water quality monitoring is growing as well.

Traditional water analysis is time and labour intensive, expensive and requires highly trained personnel. It involves sample collection, transport, storage and subsequent analysis in a laboratory. As a result, it is performed as infrequently as possible.[7]

Autonomous sensors capable of long-term, unattended measurements are the ideal solution to this problem. This 'deploy and forget' philosophy removes the time intensive aspect of analysis. Real-time data communication allows scientists to simply download environmental data onto their computer, saving them valuable time that can then be used for large data set analysis and informed decision making.

However, the development of autonomous sensors is no simple task. It requires collaboration between a wide range of different disciplines, as highlighted in Fig. 1.1 using the example of autonomous optical sensors.

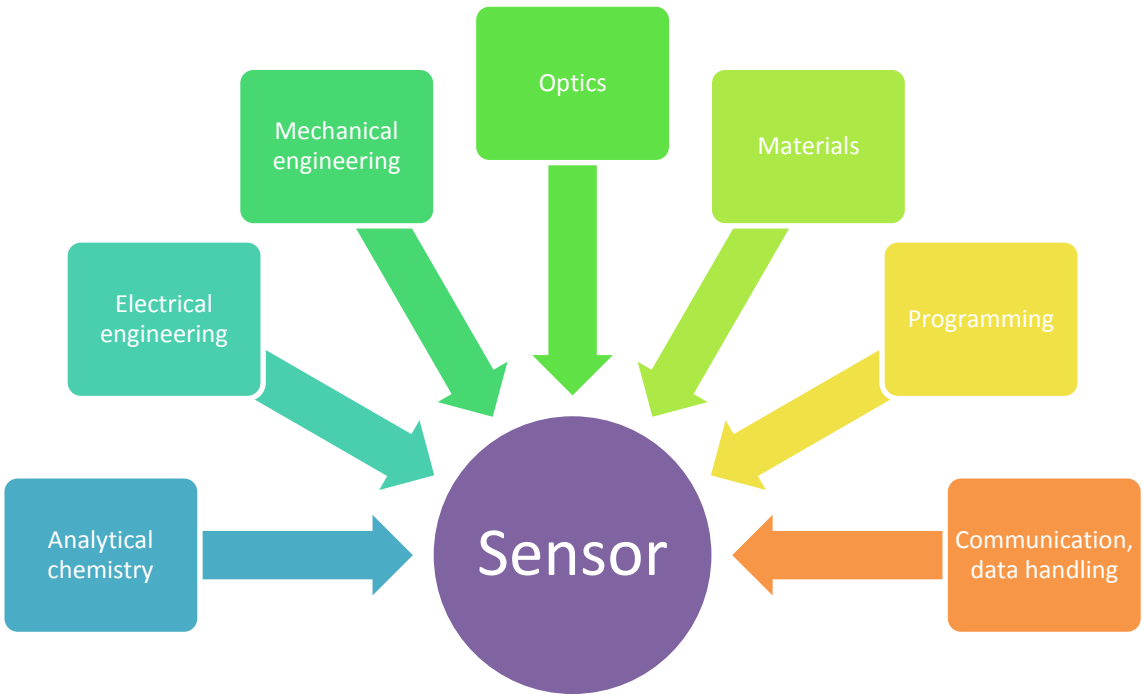

Fig. 1.1. The wide range of disciplines required for development of autonomous optical chemical sensors.

As a result of the wide range of disciplines and technologies required for their development, commercially available autonomous sensors are expensive. In order for their adoption into routine use, the cost per sensor and per measurement must decrease. Chapter 2 to 5 of this thesis focus on low-cost sensor development and its importance for environmental monitoring.

Another option for low-cost and more convenient environmental monitoring, compared to the traditional approach, involves the use of *in situ* sensors. These sensors perform analysis on-site, yielding rapid results. This concept is similar to

that of point-of-care diagnostics, where medical tests are performed rapidly at a patient's bedside. While the scientists must still travel to the sampling site, the steps of sample storage, transport and preparation in the laboratory are eliminated. These steps leave the samples prone to contamination and degradation if care is not taken.[8]

The great importance of water sensors is clear, whether they are fully autonomous and performing unaccompanied measurements or they are *in-situ* sensors for use at the sampling site. Both sensor types have advantages and disadvantages associated with their development and implementation. While autonomous sensors are the ideal end product, their development is complicated. Some important considerations for water quality sensors include:[9,10,11]

- Low component cost
- Low cost per measurement
- High sensitivity
- High selectivity
- High resolution
- Low power requirements
- Rugged, robust housing
- High repeatability
- Reagent stability
- Internal calibration

Sensors are used across a wide range of applications, including clinical diagnostics, environmental monitoring, electronic devices, vehicles, in industries and much more. While continuous measurement is the golden standard for all applications, it is not always straightforward to develop or implement. Each application comes with its own challenges. For example in clinical diagnostics, continuous monitoring is subject signal drift, with challenges in miniaturisation of the whole device for comfort and aesthetics.[12] In environmental monitoring, sensors can be larger, but are subjected to storms and harsh weather, curious animals and even vandalism, making robustness a major concern.

1.2 Internet of Things (IoT)

The Internet of Things is an important concept in the field of sensor deployments in terms of decision support and water catchment management. It has been defined as a "world of interconnected, sensor-laden devices and objects".[13] It involves the use of a range of different sensors to monitor an environment or process, providing a comprehensive visualisation of the system in question. One example of IOT would be the FitBit bracelet, which senses the physical activity and sleeping patterns of individuals. ARGO floats are another example. This global array of 3,800 profiling floats provides continuous measurement of temperature and salinity in the ocean. Understanding and predicting changes in both the atmosphere and ocean are essential for informed action, to optimise policy and to inform industrial strategies. In order for these types of predictions to be made, improved models of climate and of the entire earth system are needed.[14]

Coupling of environmental sensors to wireless connectivity allows the user to download their data, supporting decision making and making process

management easier. An example described in Chapter 2 shows how a range of different sensors from soil moisture or cattle feed levels to smoke alarms can all be used for efficient management of a farm, ensuring that crops have sufficient water, animals have sufficient food, and a fire is rapidly detected.[15,16]

1.3 Analytes of Interest

There is a wide range of compounds to be found in the natural water bodies of the world. For some of these compounds, such as pharmaceuticals, they are not naturally present, and there is a great research effort towards monitoring, towards determining their impact, towards developing new detection methods and towards more stringent legislation to manage their levels.[17-19]

In other cases, the contaminants are in fact nutrients that are essential for life. The issue arises when the levels of these nutrients become elevated. Eutrophying nutrients, such as N and P, are examples of this, where their presence at higher levels stimulates excessive growth of plants and algae. On decomposition of this large biomass, dissolved oxygen in the water is used up in the process, leading to hypoxic or anoxic water and subsequent death of aquatic animals. This process of eutrophication can have large environmental impacts, from toxic algal blooms polluting drinking water, to nuisance blooms affecting leisure activities.[20-22] The occurrence of these eutrophying nutrients in water is described in more detail in Chapter 2.

Another example of water contamination issues, examined in Chapter 4 of this thesis, is encountered when the oxidation state of the nutrient drastically changes its properties. Chromium is a famous example of this, where chromium (III) is an essential micronutrient in the human diet, while chromium (VI) exhibits carcinogenic and mutagenic properties.[23,24] This is further described in Chapter 4.

Currently, there is no legislative limit for phosphate in water as it does not harm humans or animals in drinking water unless extremely high levels are reached,[25] however 0.1 mg L^{-1} PO_4-P is stated to indicate algal bloom. However, blooms have also been reported at levels below this.[26] Phosphate enters water systems through the application of fertilisers to farm land, industrial effluent and waste water treatment plant effluent.[27]

Chromium has lower legislative limits than phosphorus due to its carcinogenic nature in the Cr(VI) form. The US EPA has a total chromium limit of 0.1 mg L^{-1} in drinking water, as Cr(III) and Cr(VI) can convert from one form to another in water and in the human body.[28] Most countries implement a limit of 0.05 mg L^{-1} of chromium in drinking water.[29] Sources of chromium are mainly due to human activity and include effluent waters from metal smelting, electroplating, tanning, metallurgy and dye industries.[23]

Other heavy metals than can be found in water include iron, copper, lead, mercury, and zinc. While some contaminants, such as iron, are visible to the naked eye at high levels, contaminants such as chromium (VI) are invisible. This highlights the huge importance of low-cost sensor development towards monitoring drinking water and environmental waters for these contaminants. The information gained by the utilisation of sensors can be used to efficiently manage drinking water systems, to predict pollution events, and aid in decision making.

1.4 Chemical sensors

According to the International Union of Pure and Applied Chemistry (IUPAC), a chemical sensor “is a device that transforms chemical information, ranging from

the concentration of a specific sample component to total composition analysis, into an analytically useful signal".[30]

A sensor contains two basic functional units. The receptor transforms chemical information from the analyte into energy that can then be measured by the transducer. The transducer converts this primary form of energy into a corresponding signal that can be processed to give information on the analyte.[30]

A simple schematic of a chemical sensor is shown in Fig. 1.2.

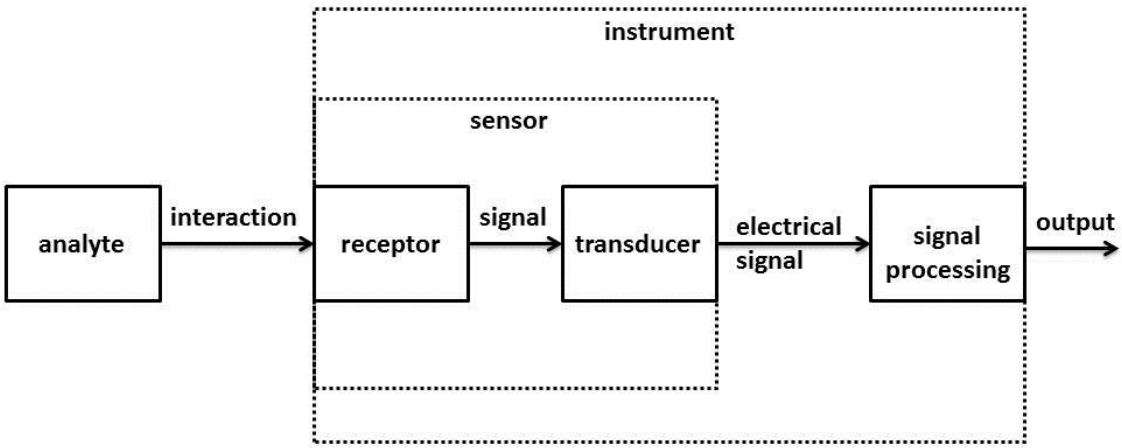

Fig. 1.2. A schematic of a chemical sensor, adapted from reference 31.

Typical transduction methods for sensors include electrochemical, optical, mechanical, thermal, etc. The focus of this thesis was on the development of colourimetric-based chemical sensors for the determination of phosphate and chromium ions in water. Important considerations for this type of chemical sensors include:

For the chemical method:

- High sensitivity

- High selectivity
- Wide linear range
- Low limit of detection
- Low limit of quantitation
- Stability of reagents
- Stability of coloured chemical product

For the instrument:

- Low-cost
- Simplicity
- Robustness of housing
- Waterproof housing
- Long battery life
- Low power requirements
- Reagent compatible materials
- Exclusion of ambient light
- On-system calibration method
- Portability

1.5 Fundamentals of spectroscopy

Optical sensors are based on the principle of spectroscopy. Spectroscopy is defined as the study of the interaction of electromagnetic radiation with matter. A ray of light consists of oscillating electric and magnetic fields.[32] Both fields

travel in a plane perpendicular to the direction of the light ray, as illustrated in Fig. 1.3.

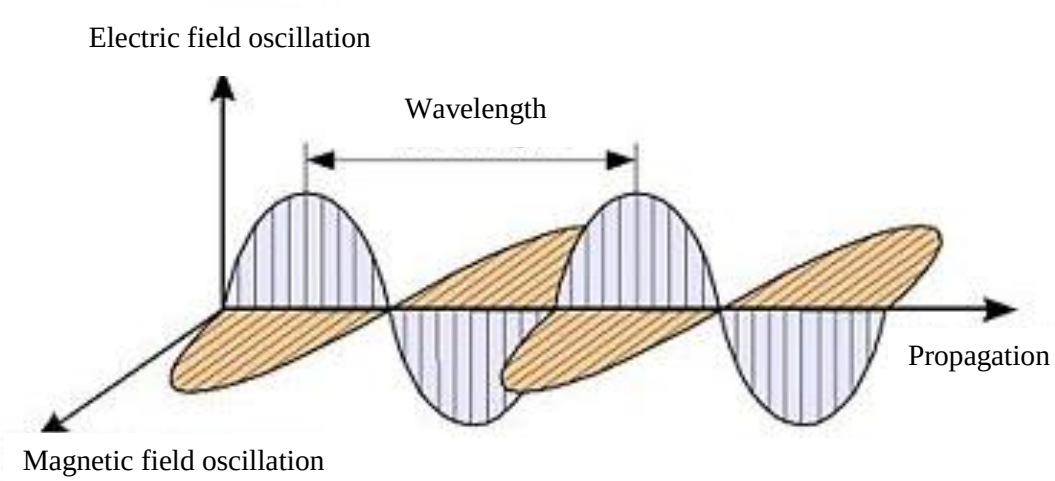

Fig. 1.3. The electromagnetic spectrum, showing the electric and magnetic field oscillation planes.[33]

Within a molecule, energy changes are quantised. This means that molecules can only exist in a certain states. These states are separated by an energy difference, or a quantum of energy. Transition of the molecule from one of these states to another involves the addition or removal of a quantum of energy, meaning the absorption or emission of electromagnetic radiation.[32] The energy of this radiation can be calculated using Eq. 1.1, where E = energy (J), h = Planck's constant (6.626×10^{-34} m^2 kg s^{-1}), and ν = frequency (s^{-1}).

Equation 1.1: $E = h\nu$

The wavelength of a photon can be calculated from its frequency by using Eq. 1.2, where λ = wavelength (m), c = speed of light (m/s) and ν = frequency (per second).

Equation 1.2: $\lambda = c/\nu$

The absorbance of light by matter is the analytical basis for this thesis. Absorbance is defined as 'a measure of the capacity of a substance to absorb light of a specified wavelength'. It is also defined by Eq. 1.3, where A is absorbance, I_0 is incident light, and I is transmitted light.[34] Absorbance is a unitless number, however 'absorbance units' or 'AU' are used.

Equation 1.3: $A = \log_{10}\frac{Io}{I}$

When incoming light interacts with a molecule, certain wavelengths of that light will be absorbed. While visible and ultraviolet light stimulate electronic transitions within a molecule, microwave radiation causes molecular rotations and infrared light causes molecular vibrations. The wavelength ranges of these types of electromagnetic radiation are indicated in Fig. 1.4. These interactions of light with matter have led to the field of spectroscopy - the study of these interactions. These analytical techniques provide an array of analytical

information, from molecular structure information and elemental analyses to methods for qualitative and quantitative analyses.[32,34]

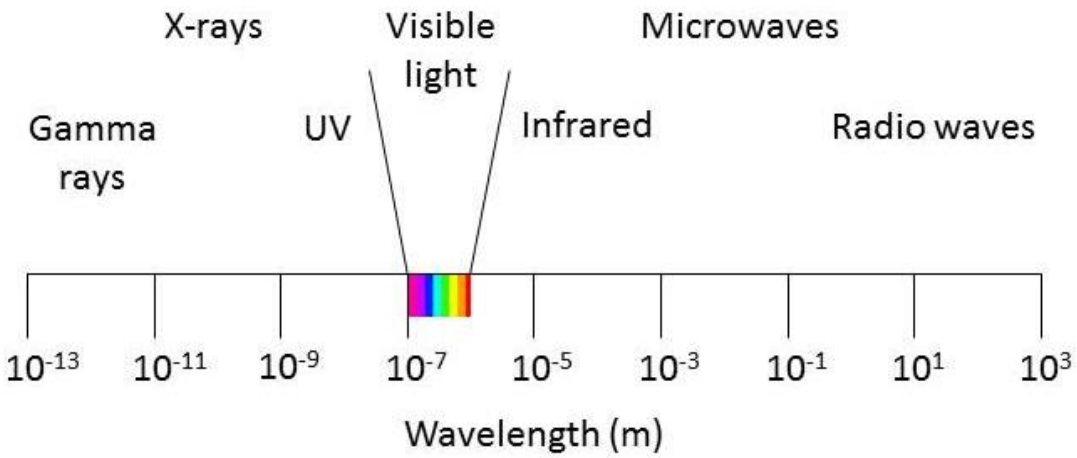

Fig. 1.4. Scale showing the wavelength range for each type of electromagnetic radiation, highlighting the visible region at 400 to 700 nm.

1.5.1 Electronic transitions

Visible and UV light stimulate electronic transitions within molecules. The energy of light at this wavelength must match exactly the energy required by a valence electron to be excited to a higher energy level. After excitation, this electron then undergoes relaxation via a number of different processes.[34] This is illustrated in the Jablonski diagram shown in Fig 1.5.

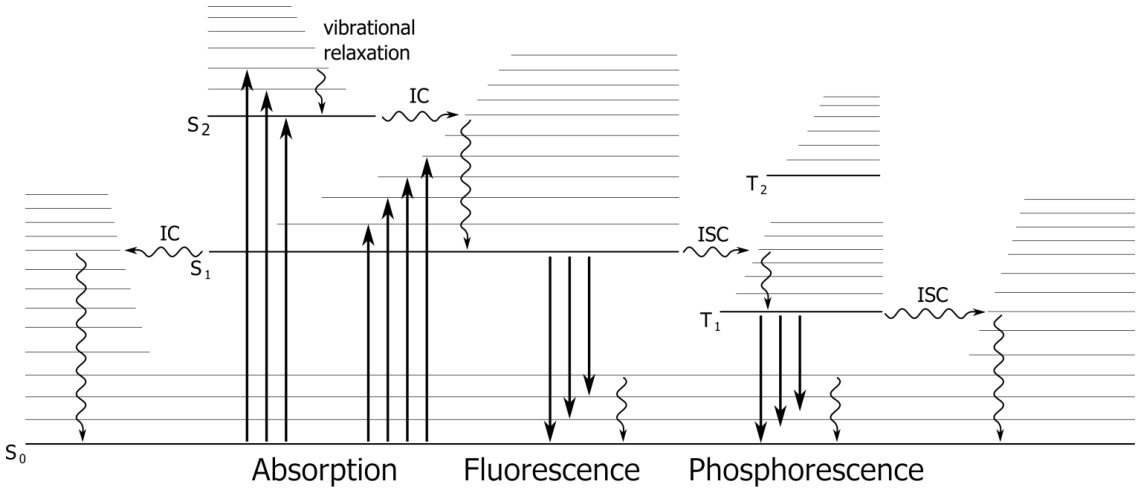

Fig 1.5. The Jablonski diagram, where radiative processes are denoted with straight arrows, and non-radiative processes are shown with curvy arrows.

The Jablonski diagram shows a number of different pathways that an electron can take to undergo relaxation from its excited state (S_1 or S_2) to the ground state (S_0) after the absorbance of energy. Vibrational relaxation refers to the process by which the molecule releases energy via vibration. This is a non-radiative mode of relaxation, and is the mode of relaxation commonly used. However, certain molecules can release their excitation energy by rapid emission of a photon. This is called fluorescence. If intersystem crossing (ISC) occurs within a molecule, relaxation occurs from the triplet state (T_1), and the release of this photon is slower. This process is called phosphorescence. Internal conversion (IC) is a radiationless transfer from a higher to a lower electronic state (eg. S_2 to S_1).[32]

1.5.2 The Beer-Lambert Law

The interaction of UV-vis light with matter can be used for quantitative analysis. This is described by the Beer Lambert law. This law relates the radiant power in a beam of electromagnetic radiation to the path length of the beam within an absorbing medium, and to the concentration of that absorbing species.[35] This is shown in Eq. 1.4, where A is the absorbance at a single wavelength (AU), ε is the molar extinction coefficient of the absorbing species at the given wavelength (L mol^{-1} cm^{-1}), C is the concentration of absorbing species (M) and l is the path length of light through the absorbing species (cm).

Equation 1.4: $A = \varepsilon c l$

From this equation, it can be seen that the absorption of light for a given analyte concentration increases with path length. This characteristic features strongly within this thesis, as simply increasing the optical path length allows for an increase in sensitivity of a colourimetric method. The more sensitive the method is, the lower the concentrations that it can measure.

Fig. 1.6 shows an exemplar absorbance spectrum, with an absorbance maximum at approximately 550 nm, which is within the visible region of the spectrum. In order to maximise sensitivity of absorbance measurements, the wavelength of maximum absorbance is used for measurement.

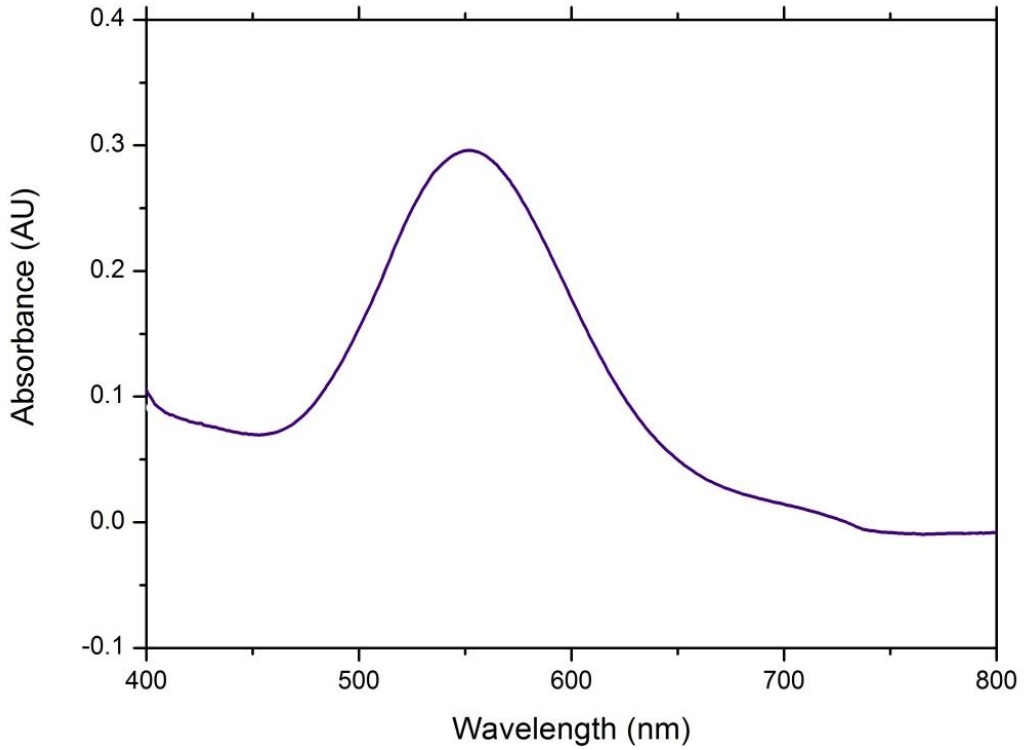

Fig. 1.6. An exemplar absorbance spectrum, showing an absorbance maximum at approximately 550 nm.

1.5.3 UV-visible light absorbance

In order for a molecule to absorb light in the UV-visible region of the spectrum, it must contain electronic energy levels that are separated by an energy difference equal to that of the incoming photons, as stated in Eq. 1.1. Typically, conjugated systems, molecules containing benzene rings, lone pairs (eg. from nitrogen, oxygen or halogens) and those containing nitrate groups are likely to absorb light within this wavelength region. Conjugated molecules contain alternating single and double bonds. This leads to the delocalisation of electrons within the conjugated system, meaning that they require lower energy to be promoted to

an excited state. The more conjugated the system, the lower the energy required for excitation.[32]

The most common electron transitions are from π or n orbitals to antibonding orbitals, as shown in Fig. 1.7, meaning that the molecule must contain double bonds or lone pairs in order for this excitation to occur.

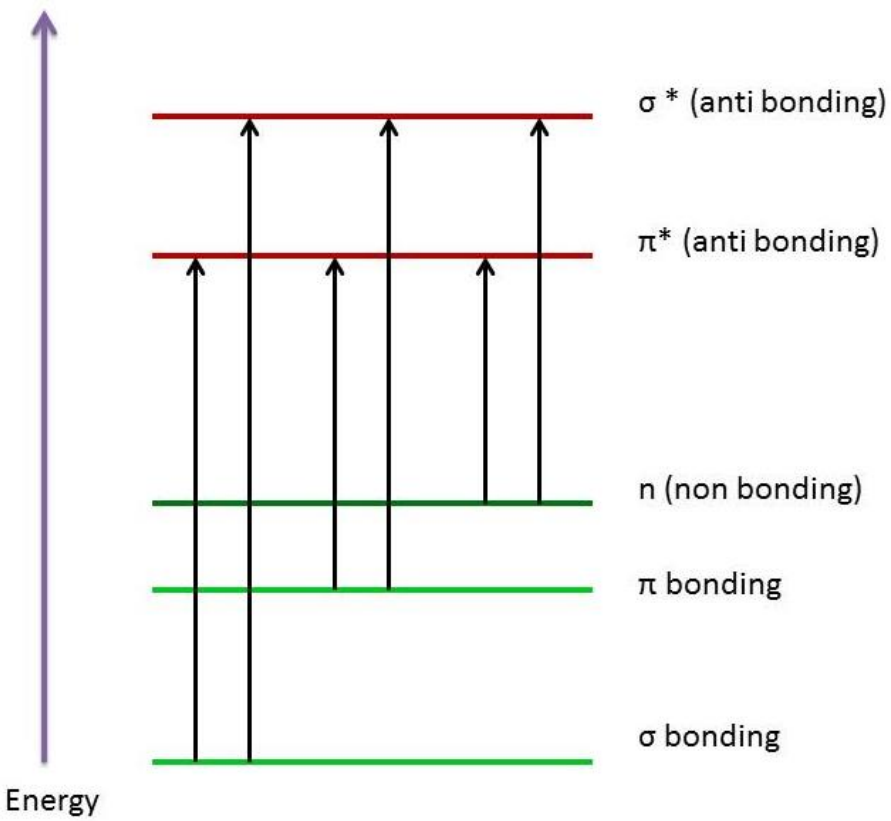

Fig. 1.7. The electron transitions possible from UV-visible light excitation, adapted from reference 32.

1.6 Low-cost components

Low-cost components are essential to the development of low-cost sensors. The sourcing of low-cost components for these systems can be time consuming and require expertise in several different fields. This is where the collaborative aspect of the project was hugely beneficial.

The use of light emitting diodes (LEDs) as a light source in colourimetric sensors provides a number of advantages. LEDs do not contain a filament that can burn out like a standard light bulb. They operate via the transfer of electrons through the semiconductor material. This means that they surpass the lifetime of standard incandescent bulbs by thousands of hours.[18] LEDs require less power for their operation, which is a huge advantage for battery driven field sensors.

The use of photodiodes for light detection also provides several advantages. A photodiode is a semiconductor device that converts light into current. They are also low-cost, small in size with low mass, low power requirements and rapid response times.

As well as using low-cost detection systems, additional cost reductions can be achieved by sourcing low-cost materials, power supplies, rugged housing, fluid pumps, and electrical components. The fluid pumping mechanisms used in the sensors presented here involved either simple motors (Chapter 3 and 4) or motor-driven syringe pumps (Chapter 5). Microfluidic pumps were previously found to be the most expensive component of the autonomous phosphate sensor systems developed in DCU, described in section 1.11.

Miniaturisation of the chemical method onto a microfluidic chip or disc allows for a reduction in the volume of reagent used and waste produced, leading to additional running cost reductions.

1.6.1 Light emitting diodes

Light can be generated in semiconductor materials (such as GaN or AlInGaP) by the injection of electrons into the conduction band of the material. This provides lower-energy sites, or 'holes', in the valence band for the electrons to 'fall' into. This creates light with colour corresponding to the energy gap between the conduction band and valence band, also called the bandgap.[18]

LEDs are made up of three different types of materials, layered on top of each other. The bottom layer has free electrons in high concentration (for example n-type GaN doped with Si). This is followed by multiple alternating thin layers (1–30 nm) of material with a smaller bandgap (InGaN/GaN), also called quantum wells. Enclosing a smaller-bandgap material (InGaN) between layers of larger-bandgap material (GaN) creates a well that traps electrons and holes, allowing for efficient recombination. This results in the emission of energy in the form of light, with wavelength of the smaller band-gap material. Above this 'active layer', there is a layer of material with a high concentration of holes (p-type GaN doped with Mg).[36]

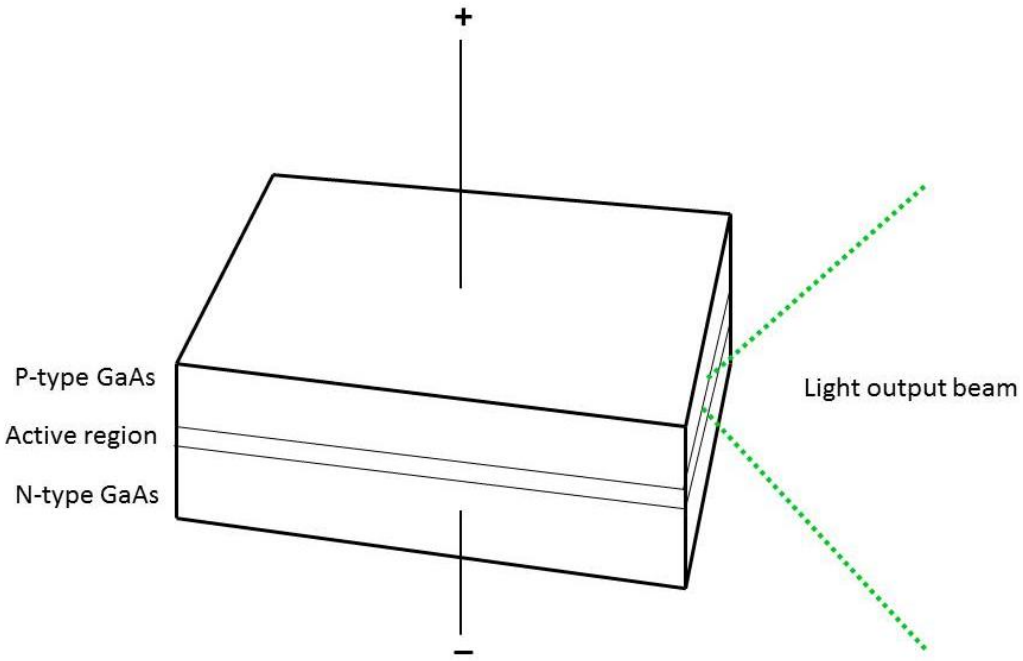

Fig. 1.8. Diagram of an LED/laser composition, showing the P-doped and N-doped regions, separated by an active region, from which photons are released when current flows, using gallium arsenide as a material example, adapted from reference 36.

A schematic of an LED is shown in Fig. 1.8. When current flows, electrons from the N-doped junction are injected at high density into the P-doped junction, and holes from the P-doped region are injected into the N-doped region. When these electrons and holes recombine, photons are emitted.[36]

1.6.2 Photodiodes

A photodiode is a semiconductor that converts light into current. Photodiodes operate based on the principle of photoemission. The energy to free electrons within the semiconductor material comes from incident photons. If the incoming energy is sufficient, electrons move from the valence band to the conduction band, forming an electron-hole pair, with the hole in the valence band. The incoming light is focussed onto the junction between the P and N regions. If an external electric field is applied, the electron moves to the cathode and holes move towards the anode, forming a photocurrent.[36]

1.7 Microfluidics

The field of microfluidics has been a focus of major research for over 40 years. It allows for the miniaturisation and automation of laboratory protocols and analysis. It has attracted wide interest in both academic and industrial fields.[11,37] Micro-Total Analysis Systems (μTAS) have been under development for over 20 years, and aim towards integrated microfluidic systems for automating all stages of a given process. Applications for microfluidic systems include point-of-care diagnostics, fundamental research and in-field environmental monitoring.[12,11,37]

In this work, two different types of microfluidic systems were fabricated: a chip and a disc. The microfluidic chip requires tubing to connect it to the fluid pumping system and waste container. A centrifugal microfluidic disc simply requires a motor. When the disc is rotated at a high frequency, a centrifugal force is created, that pumps these fluid through the microchannels.[11] The direction of this force is illustrated in Fig. 1.9.

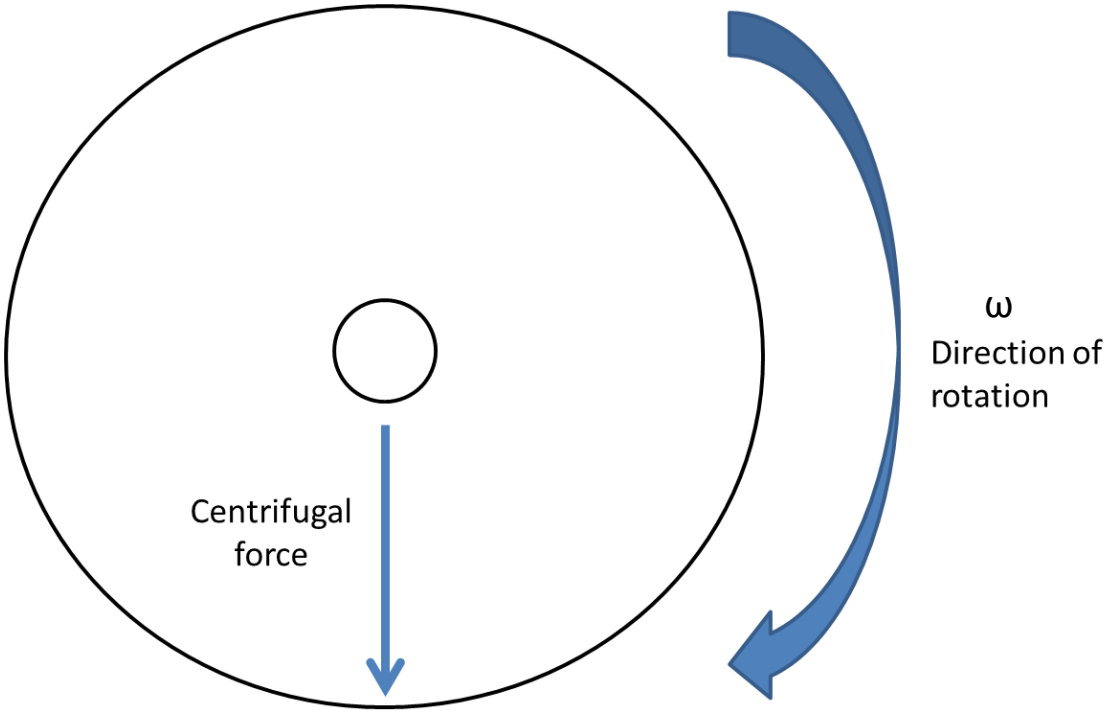

Fig. 1.9. A diagram showing the rotation of the disc at angular velocity (ω), and a resulting centrifugal force in the direction shown, from the centre to the outer edge of the disc.

The centrifugal force drives fluid radially outwards from the centre to the edges of the disc. The average velocity of this fluid depends on many parameters including the fluid's viscosity and density, its distance from the centre of the disc, the cross sectional area of the channel and channel wetness.[11]

A wide range of functions have been successfully implemented on microfluidic platforms for the automation of biological and chemical assays and analyses. These functions include fluid mixing techniques, on-chip valving, cell lysis, and chemical or physical separations. When coupled with optical or electrochemical

detection methods, these systems can fully automate chemical or biological analyses.

1.7.1 Valves

Sophisticated fluid manipulation can be achieved on a microfluidic chip through the incorporation of valves. The purpose of a valve is to prevent fluid flow in a given direction. This can be accomplished in a number of ways; capillary valves are one example. They operate based on the balance between capillary pressure induced by surface tension and pressure induced by the centrifugal force or pump system. Once the force overcomes the capillary pressure, the fluid passes through the valve. Centrifugal force is increased by increasing the angular velocity of the disc. Other common types of valves include hydrophobic valves, siphon valves and sacrificial valves.[11]

1.7.2 Mixing

Mixing can be difficult on microfluidic platforms as it is limited by diffusion and convection artifacts, which can be very slow.[38] When channels are tens of micrometers wide, diffusional mixing of molecules can take seconds. However when the dimensions are larger, in the range of several hundred micrometers wide, this mixing can take tens of seconds.[39] For chemical reactions with slow kinetics, such as the colourimetric methods for Cr(III) described in Chapter 4 or phosphate in Chapter 5, this means that the reaction could take even longer on-chip than using benchtop methods. Mixing can be enhanced through the inclusion of mixers in the channels. There are two types of mixers: active and passive. Active mixers exert control over the fluid flow via a moving part or varying pressure gradients, while passive mixers do not require any extra energy

input.[39] Passive mixers are simpler and more practical to implement onto these devices, as simplicity, low-cost and low power consumption were all important design characteristics. An example of passive mixers would be a square wave configuration, or a serpentine or 'twisted pipe' configuration, illustrated in Fg. 1.10.[39]

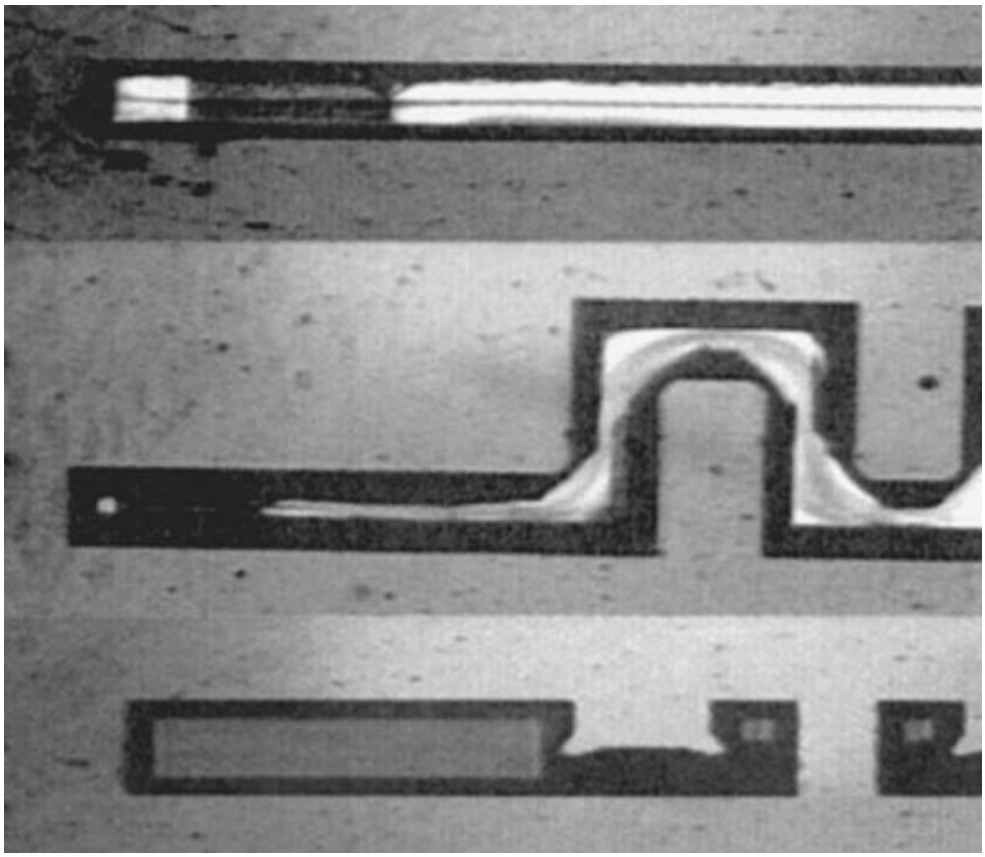

Fig. 1.10. The mixing of phenolphthalein and sodium hydroxide in a straight channel, a square-wave channel and a three-dimensional serpentine channel.[39]

From Figure 1.10, the mixing capability of three channel types is shown, with poor mixing in the straight channel, improved mixing in the square-wave channel and the best mixing was reported for the 3D serpentine channel. Passive mixing was achieved on the devices in this thesis by varying channel widths (on centrifugal platforms) or employing T-junctions (on chip platforms).

1.9 Limitations of colourimetric chemical sensors for deployment

There are several disadvantages to colourimetric chemical sensing for either handheld or autonomous sensors. For autonomous systems, sampling frequency depends on the time taken for development of coloured product (reaction kinetics) and on how much reagent can be stored on the system to last for a given period of time (eg. a 3 month deployment). The longer the system can be deployed for, the less frequently it must be removed from the water for maintenance or reagent changes. This makes it less time consuming and labour intensive for the user, compared to traditional analysis methods which required more frequent field trips for sample collection. Additionally, battery life will limit the sampling frequency. Deployment time of the sensor also relies on the stability of the reagent. If the reagent expires in a short period of time, the sensor cannot be deployed for longer than this as the results will no longer be reliable or meaningful. Reagent stability is less of an issue for hand-held systems, however battery life is also an important factor for these. Materials used for both types of sensors depend on chemical compatibility. Chemically resistant material can be expensive.

The LOD is limited by the sensitivity of the method, the length of the optical path, and the amount of light loss or signal noise that occurs. Sensitivity of colourimetric methods will not reach that of fluorescent methods, however colourimetric methods are much better validated and well-studied, while fluorescence methods are more novel, making colourimetry a better, more reliable choice for automation.

From the Beer-Lambert Law, it is clear that in order to detect a water pollutant using colourimetric methods, a sensor requires:

1. A ligand that complexes the analyte to yield a complex with a high molar absorptivity;
2. A long optical path length to maximise sensitivity for trace analysis;
3. The complex to absorb in the visible region of the spectrum, allowing for low cost LEDs to be used;
4. A low number of steps in the analytical protocol, to simplify automation;
5. As few complex steps as possible (eg. acid digestion, solute extraction, heating), to simplify automation.

1.10 Common sensing methods for P and Cr (III) and (VI)

The typical methods for phosphate measurement are either colourimetry or ion chromatography. The standard method using ion chromatography reached and LOD of 0.1 mg L^{-1}. As this is high in terms on environmental phosphate levels (typically 0-100 µg L^{-1}), colourimetric methods are favoured.[20]

Chromium analysis in water is typically carried out using AAS, ICP-MS, ICP-AES or spectrophotometry, following a separation of the chromium species.[23]

Concentration ranges that these methods range from ng L^{-1} (AAS, ICP-MS) up to mg L^{-1} (AAS, spectrophotometry). While the spectrophotometric methods for Cr(VI) are very sensitive, the sensitivity of Cr(III) methods is poor in the visible region of the spectrum, as shown in Chapter 4. Analysis methods for chromium speciation was reviewed by Gomez *et al.* in 2006.

1.11 History of the development of an autonomous phosphate sensor

There are only a small number of different autonomous phosphate sensors in development. Wet Labs have a commercially available system called Cycle-P, which is further described in Chapter 2. Research groups such as the NOC in Southampton[13,40], or Garcon *et al*. in France[41,42] have published literature on their autonomous phosphate systems with deployment data. These systems use a range of either colourimetric or electrochemical determination methods. The sensor described in Chapter 5 is the 3rd generation of an autonomous sensor that has been under development for over 10 years in DCU.[43-48] This section looks at the variety of design changes that have taken place from prototype one to prototype two, which will give an introduction into the design process behind the sensor generation presented in Chapter 5, which was inspired by these previous works.

1.11.1 First generation of the phosphate sensor

The early prototype of the phosphate sensor, shown in Figure 1.11 (A) and (B), held the reagent, calibration solutions and cleaner in bottles. Solenoid pumps were used to pump each liquid onto the microfluidic chip, on which the yellow

method for phosphate quantitation was carried out. A water sample was pumped into the sample port through a filter membrane. It mixed with the reagent in a T-mixer on-chip, and then passed through a serpentine channel to allow time for colour development. A 370 nm light-emitting diode (LED) and a photodiode were positioned at the serpentine channel to take absorbance measurements. Waste was collected in a waste storage container after analysis. A microcontroller was used to control the system components and for data acquisition. This data was stored on a flash memory unit, and a GSM modem allowed for communication of the data via SMS to a laptop. To protect these components from the environment, a water-tight propylene 'Pelicase' was used.

Fig. 1.11. (A) The microcontroller and GSM modem mounted in the lid, the solenoid pumps, microfluidic chip, LED and photodiode on the mounting plate. (B) The storage bottles and battery in the lower part of the case, all contained in the 'Pelicase'.[46]

Figure 1.12 shows an image of the microfluidic chip used on the sensor. This chip was milled from polymethyl methacrylate (PMMA) and bonded using pressure sensitive adhesive (PSA).

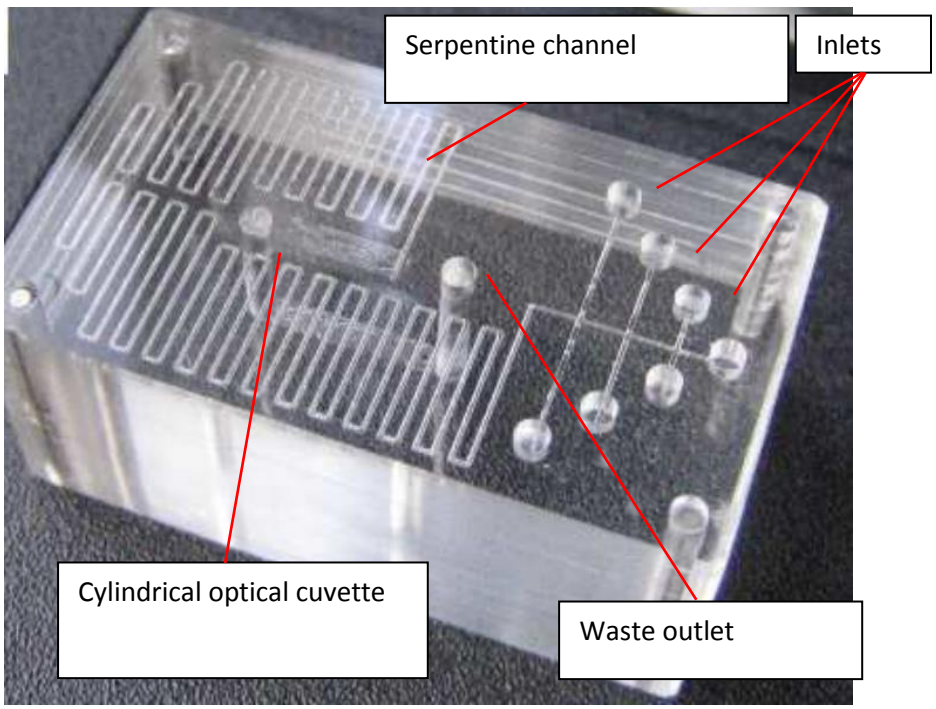

Fig. 1.12. Image of the microfluidic chip consisting of six inlets, one waste outlet, a serpentine channel for mixing of sample and reagent, and a cylindrical optical cuvette.

1.11.2 Second generation of the phosphate sensor

This phosphate sensor underwent a redesign with the aim of reducing the cost per unit to less than €200 and improving analytical performance.[43] This second generation system, shown in Figure 1.13, incorporated the following changes that contributed to reduced cost, improved analytical performance and improved compactness.

- Improved bubble detection and removal from the microfluidic system;
- the reagent, calibrant and waste bottles were replaced with collapsible polypropylene bags;
- a folded sheet metal frame was used to mount the internal components;
- a low-cost dual channel peristaltic pump in place of solenoid pumps;
- the design of the sample inlet filter was altered to reduce biofouling.

The data was remotely accessible using ZigBee® radio, providing real time data as well as allowing the user to change the setup parameters of the sensor remotely. The correlation between sensor measurements and measurements of grab samples analysed using a Hach-Lange DR890 Portable Colourimeter improved from 0.908 on the first generation system to 0.9706 on the second generation system.

Fig. 1.13. The second generation phosphate sensor. (1) Sample inlet (2) control board, detection system (3) peristaltic pumps (4) reagent bags and (5) enclosure.[43]

This system was more compact due to the space saved by the collapsible reagent bags. As the reagent bags emptied, the waste bag filled, meaning that minimal space was required.

1.11.3 Summary and future perspectives for phosphate sensor

The first generation phosphate sensor costed approximately €2,000. The second generation sensor costed approximately €200. This reduction in cost of autonomous sensors for environmental monitoring is essential. Data on the spatial variation of phosphate in a water body is limited by the number of sensors within that water body. Reduction in cost per unit means that these sensors can be deployed on a large scale, forming a sensor network. Spatial data can provide insights into point and diffuse pollution sources, allowing for their identification and management. It also allows for the detection of discreet pollution events which could be missed entirely when using traditional grab sampling methods.

The LOD of phosphate using this sensor is 0.1 mg L^{-1} $P\text{-}PO_4^{3-}$. According to the European Directive 91/676/EE, 0.1 mg P L^{-1} is an indication of excessive algal growth. This limits the applicability of the sensor to waters with high levels of phosphate, such as those found in a waste water treatment plant, in industry or in known polluted waters. There are significant applications for the sensor in waste water treatment plants or industries for monitoring of in-process and discharged effluent, where phosphate levels are typically higher, and in known polluted surface waters.[44]

The third generation phosphate sensor development aimed to improve the sensor's analytical performance, in order to extend its applicability to less polluted waters, and improve marketability thorough redesign took place in order to facilitate the new low-cost syringe pump components and the new microfluidic chip. The size of the sensor increased to accommodate the long-length syringe pumps.

Commercially available phosphate sensors for water analysis are described in Chapter 2. Their market cost is currently more than triple the component cost of these phosphate sensors.

References

1. Royce Murray, Challenges in Environmental Analytical Chemistry, Anal. Chem., 2010, 82 (5), pp 1569–1569.
2. Silicon Laboratories Inc., The Evolution of Wireless Sensor Network, 2013, available from: https://www.silabs.com/documents/public/white-papers/evolution-of-wireless-sensor-networks.pdf (accessed on 22/08/17)
3. M.I. Mead, O.A.M. Popoola, G.B. Stewart, P. Landshoff, M. Calleja, M. Hayes, J.J. Baldovi, M.W. McLeod, T.F. Hodgson, J. Dicks, A. Lewis, J. Cohen, R. Baron, J.R. Saffell, R.L. Jones, The use of electrochemical sensors for monitoring urban air quality in low-cost, high-density networks, Atmos. Environ. 70 (2013) 186–203. doi:10.1016/j.atmosenv.2012.11.060.
4. G. Werner-Allen, J. Johnson, M. Ruiz, J. Lees, M. Welsh, Monitoring volcanic eruptions with a wireless sensor network, Wirel. Sens. Networks, 2005. Proceeedings Second Eur. Work. (2005) 108–120. doi:10.1109/EWSN.2005.1462003.
5. K. Martinez, J.K. Hart, R. Ong, Environmental sensor networks, Computer (Long. Beach. Calif). 37 (2004) 50–56. doi:10.1109/MC.2004.91.
6. J. Granda Cantuña, D. Bastidas, S. Solórzano Lescano, J.-M. Clairand, Design and Implementation of a Wireless Sensor Network to Detect

Forest Fires, 2017 Third Int. Conf. eDemocracy eGovernment. 2 (2017) 15–21. doi:10.1109/ICEDEG.2017.7962508.

7. A.T. Law Al, S.B. Adeloju, Progress and recent advances in phosphate sensors: A review, Talanta. 114 (2013) 191–203. doi:10.1016/j.talanta.2013.03.031.
8. A.M. Nightingale, A.D. Beaton, M.C. Mowlem, Trends in microfluidic systems for in situ chemical analysis of natural waters, Sensors Actuators B Chem. 221 (2015) 1398–1405. doi:10.1016/j.snb.2015.07.091.
9. S. Berchmans, T.B. Issa, P. Singh, Determination of inorganic phosphate by electroanalytical methods: A review, Anal. Chim. Acta. 729 (2012) 7–20. doi:10.1016/j.aca.2012.03.060.
10. V.S. Palaparthy, M.S. Baghini, D.N. Singh, Review of polymer-based sensors for agriculture-related applications, Emerg. Mater. Res. 2 (2013) 160–180. doi:10.1680/emr.13.00010.
11. R. Gorkin, J. Park, J. Siegrist, M. Amasia, B.S. Lee, J.-M. Park, J. Kim, H. Kim, M. Madou, Y.-K. Cho, Centrifugal microfluidics for biomedical applications., Lab Chip. 10 (2010) 1758–1773. doi:10.1039/b924109d.
12. D. Rodbard, Continuous Glucose Monitoring: A Review of Successes, Challenges, and Opportunities., Diabetes Technol. Ther. 18 Suppl 2 (2016) S23–S213. doi:10.1089/dia.2015.0417.
13. A. H. Tran, (2017). The internet of things and potential remedies in privacy tort law. Columbia Journal of Law and Social Problems 50(2), 263-298.
14. ARGO floats reference
15. P. Rajalakshmi, S.D. Mahalakshmi, IOT Based Crop-Field Monitoring And Irrigation Automation, 10th Int. Conf. Intell. Syst. Control. (2016) 1–6. doi:10.1109/ISCO.2016.7726900.

16. M.H. Memon, W. Kumar, A.R. Memon, M. Aamir, P. Kumar, Internet of Things (IoT) Enabled Smart Animal Farm, Int. Conf. Comput. Sustain. Glob. Dev. 7 (2016) 2067–2072.
17. R.P. Deo, R.U. Halden, Pharmaceuticals in the built and natural water environment of the United States, Water. 5 (2013) 1346–1365. doi:10.3390/w5031346.
18. S. Pimputkar, J.S. Speck, S.P. DenBaars, S. Nakamura, Prospects for LED lighting, Nat. Photonics. 3 (2009) 180–182. doi:10.1038/nphoton.2009.32.
19. A. Nikolaou, S. Meric, D. Fatta, Occurrence patterns of pharmaceuticals in water and wastewater environments, Anal. Bioanal. Chem. 387 (2007) 1225–1234. doi:10.1007/s00216-006-1035-8.
20. V.H. Smith, Eutrophication of freshwater and coastal marine ecosystems: a global problem., Environ. Sci. Pollut. Res. Int. 10 (2003) 126–139. doi:10.1065/espr2002.12.142.
21. D.W. Schindler, The dilemma of controlling cultural eutrophication of lakes, Proc. R. Soc. B Biol. Sci. 279 (2012) 4322–4333. doi:10.1098/rspb.2012.1032.
22. J. Heisler, P.M. Glibert, J.M. Burkholder, D.M. Anderson, W. Cochlan, W.C. Dennison, Q. Dortch, C.J. Gobler, C.A. Heil, E. Humphries, A. Lewitus, R. Magnien, H.G. Marshall, K. Sellner, D.A. Stockwell, D.K. Stoecker, M. Suddleson, Eutrophication and harmful algal blooms: A scientific consensus, Harmful Algae. 8 (2008) 3–13. doi:10.1016/j.hal.2008.08.006.
23. V. Gomez, M.P. Callao, Chromium determination and speciation since 2000, Trends Anal. Chem. 25 (2006) 1006–1015. doi:10.1016/j.trac.2006.06.010.
24. K.-C. Hsu, C.-C. Sun, Y.-C. Ling, S.-J. Jiang, Y.-L. Huang, An on-line microfluidic device coupled with inductively coupled plasma mass

spectrometry for chromium speciation, J. Anal. At. Spectrom. 28 (2013) 1320–1326. doi:10.1039/c3ja50030f.

25. M.S. Razzaque, Phosphate toxicity: new insights into an old problem, Clin. Sci. 120 (2011) 91–97. doi:10.1042/CS20100377.
26. EPA Report on the Environment, “Nitrogen and Phosphorus in Agricultural Streams”, available from: https://cfpub.epa.gov/roe/indicator_pdf.cfm?i=31 (accessed on 09/08/17)
27. P.J.A. Withers, H.P. Jarvie, Delivery and cycling of phosphorus in rivers: A review, Sci. Total Environ. 400 (2008) 379–395. doi:10.1016/j.scitotenv.2008.08.002.
28. US EPA, “Chromium in Drinking Water”, 2017, available from: https://www.epa.gov/dwstandardsregulations/chromium-drinking-water (accessed on: 09/08/17)
29. Lenntech, Chromium (Cr) and water, “Chromium and water: reaction mechanisms, environmental impact and health effects”, 2017, available from : http://www.lenntech.com/periodic/water/chromium/chromium-and-water.htm (accessed on 09/08/17)
30. Z. Hugh Fan, Chemical Sensors and Microfluidics, J. Biosens. Bioelectron. 4 (2013) 1–2. doi:10.4172/2155-6210.1000e117.
31. R.D. Prien, The future of chemical in situ sensors, Mar. Chem. 107 (2007) 422–432. doi:10.1016/j.marchem.2007.01.014.
32. P.S. Sindhu, Elements of Molecular Spectroscopy, 2011, New Age International, New Delhi.
33. University of Washington, Electromagnetic Radiation, “Electric and Magnetic waves”, available from: http://depts.washington.edu/cmditr/modules/lum/index.html (accessed on 09/08/17)

34. L. D. Field, S. Sternhell, J. R. Kalman, Organic Structures from Spectra, 5th ed., John Wiley & Sons Ltd., 2013.
35. D.F. Swinehart, The Beer-Lambert Law, J. Chem. Educ. 39 (1962) 333. doi:10.1021/ed039p333.
36. Optics and Photonics: An Introduction - F. Graham Smith, Terry A. King, Dan Wilkins.
37. R. Burger, L. Amato, A. Boisen, Detection methods for centrifugal microfluidic platforms, Biosens. Bioelectron. 76 (2016) 54–67. doi:10.1016/j.bios.2015.06.075.
38. M.C. Shastry, S.D. Luck, H. Roder, A continuous-flow capillary mixing method to monitor reactions on the microsecond time scale., Biophys. J. 74 (1998) 2714–2721. doi:10.1016/S0006-3495(98)77977-9.
39. R.H. Liu, M.A. Stremler, K. V. Sharp, M.G. Olsen, J.G. Santiago, R.J. Adrian, H. Aref, D.J. Beebe, Passive mixing in a three-dimensional serpentine microchannel, J. Microelectromechanical Syst. 9 (2000) 190–197. doi:10.1109/84.846699.
40. F.E. Legiret, V.J. Sieben, E.M.S. Woodward, S.K. Abi Kaed Bey, M.C. Mowlem, D.P. Connelly, E.P. Achterberg, A high performance microfluidic analyser for phosphate measurements in marine waters using the vanadomolybdate method, Talanta. 116 (2013) 382–387. doi:10.1016/j.talanta.2013.05.004.
41. J. Jońca, V. León Fernández, D. Thouron, A. Paulmier, M. Graco, V. Garçon, Phosphate determination in seawater: Toward an autonomous electrochemical method, Talanta. 87 (2011) 161–167. doi:10.1016/j.talanta.2011.09.056.
42. D. Thouron, R. Vuillemin, X. Philippon, A. Lourenço, C. Provost, A. Cruzado, V. Garçon, An autonomous nutrient analyzer for oceanic long-

term in situ biogeochemical monitoring, Anal. Chem. 75 (2003) 2601–2609. doi:10.1021/ac020696+.

43. J. Cleary, D. Maher, D. Diamond. 2013. Development and deployment of a microfluidic platform for water quality monitoring. In: Mukhopadhyay, Subhas C. and Mason, Alex, (eds.) Smart Sensors for Real-Time Water Quality Monitoring. Smart Sensors, Measurement and Instrumentation. Springer-Verlag, Berlin Heidelberg 2013, 125-148.
44. M. Bowden, D. Diamond, The determination of phosphorus in a microfluidic manifold demonstrating long-term reagent lifetime and chemical stability utilising a colorimetric method, Sensors Actuators, B Chem. 90 (2003) 170–174. doi:10.1016/S0925-4005(03)00024-8.
45. M. Bowden, M. Sequiera, J.P. Krog, P. Gravesen, D. Diamond, Analysis of river water samples utilising a prototype industrial sensing system for phosphorus based on micro-system technology., J. Environ. Monit. 4 (2002) 767–771. doi:10.1039/b200330a.
46. C. Slater, J. Cleary, C.M. McGraw, W.S. Yerazunis, K.T. Lau, D. Diamond, Autonomous field-deployable device for the measurement of phosphate in natural water, Roc. SPIE 6755, Adv. Environ. Chem. Biol. Sens. Technol. (2007). doi:10.1117/12.733754.
47. J. Cleary, C. Slater, C. McGraw, D. Diamond, An autonomous microfluidic sensor for phosphate: On-site analysis of treated wastewater, IEEE Sens. J. 8 (2008) 508–515. doi:10.1109/JSEN.2008.918259.
48. C. Slater, J. Cleary, K.T. Lau, D. Snakenborg, B. Corcoran, J.P. Kutter, D. Diamond, Validation of a fully autonomous phosphate analyser based on a microfluidic lab-on-a-chip, Water Sci. Technol. 61 (2010) 1811–1818. doi:10.2166/wst.2010.069.

Aims of the Thesis

This project had the overall objective of developing low-cost, microfluidic, colourimetric sensors for environmental water quality monitoring. It focussed on sensors for the measurement of phosphate and of chromium species in water. The **low-cost** factor was achieved by taking an interdisciplinary approach to keep the fabrication costs low, using low-cost materials and components. Microfluidics was the ideal tool for miniaturisation and automation of colourimetric laboratory based protocols, also reducing running costs due to minimisation of reagent consumption and waste production. **Sensitivity** was a major focus for these systems, and it was maximised by optimising the wet chemistry methods and by incorporating long optical path lengths for absorbance measurements. In order to develop viable sensors for the intended application, **reliability** was essential. This was maintained on all systems by selecting well validated, robust wet chemistry methods that could be automated with ease, with no complicated steps such as acid digestions or pre-concentrations. The less complex sensor systems are, the more reliable they are for in-field use and long term, continuous operation. These sensors were applied to the measurement of phosphate and chromium species in environmental samples to demonstrate their performance in environmental matrices.

Chapter 2:
Review

Recent developments in optical sensing methods for the determination of eutrophying nutrients for 'smart farming' applications

Gillian Duffy and Fiona Regan

Marine Environmental Sensing Technology Hub, Dublin City University, Glasnevin, Dublin 9, Ireland

Published: The Analyst, 2017. DOI: 10.1039/C7AN00840F

Aims and Objectives

Chapter 2 reviews the current status of autonomous sensor development for the eutrophying nutrients phosphorus and nitrogen. The various detection methods for both nutrients are reviewed, from novel laboratory-based methods with potential for automation, to fully automated systems that have been deployed, as well as commercially available systems.

Abstract

The demand for autonomous sensors for unattended, continuous nutrient monitoring in water is rapidly growing with the increasing need for more frequent and widespread environmental pollution monitoring. Legislative bodies, local authorities and industries all require frequent water quality monitoring, however, this is time and labour intensive, and an expensive undertaking. Autonomous sensors allow for frequent, unattended data collection. While this solves the time and labour intensive aspects of water monitoring, sensors can be very expensive. Development of low-cost sensors is essential to realise the concept of Internet of Things (IoT). However there is much work yet to be done in this field. This article reviews current literature on the research and development efforts towards deployable autonomous sensors for phosphorus (in the form of phosphate) and nitrogen (in the form of nitrate), with a focus on analytical performance and cost considerations. Additionally, some recent sensing approaches that could be automated in the future are included, along with an overview of approaches to monitoring both nutrients. These approaches are compared with standard laboratory methods and also with commercially available sensors for both phosphate and nitrate. Application of nutrient sensors in agriculture is discussed as an example of how sensor networks can provide improvements in decision making.

2.1 Introduction

Nitrogen (N) and phosphorus (P) are essential nutrients for the growth of organisms.[1-4] Elevated levels of nutrients in a water system, in particular N

and P, stimulate excessive growth of aquatic plants such as algae and weeds.[3] The decay of this plant material can lead to depleted oxygen levels in water, resulting in the death of aquatic animals. This process, called eutrophication, has a negative impact on the environment in a number of additional ways, including the release of algal toxins, formation of 'dead zones' and pollution of drinking water supplies.[5,6]

Cultural eutrophication has been referred to as the Earth's most widespread water quality problem. It is caused by the input of nutrients from anthropogenic sources such as intensively farmed agricultural land, industrial and domestic wastewater effluent, animal manure and atmospheric deposition of N from burning fossil fuels.[5,7] These pollutants can come from point or diffuse sources. At a point source, such as a sewage treatment plant, the water quality can be monitored at one location. Diffuse sources, such as fertiliser running from land into surface waters during heavy rainfall, are more difficult to monitor. There can be multiple points of entry.[5] This introduces a need for autonomous sensors capable of providing not only temporal, but also spatial resolution on nutrient fluctuations in a water system. They allow for continuous, real time monitoring of N and P at a number of locations in a water body. In order to efficiently interpret nutrient movement in a water system, large data sets are required.[8] A network of autonomous sensors is the ideal method for obtaining this spatial resolution. A smart network can be incorporated, where a small number of sensors monitor continuously. On detection of a pollution event, downstream sensors are then activated to analyse nutrient movement throughout the water body with greater resolution.

Some previous reviews of interest on the topic of nutrient sensors include Bagshaw *et al.,*[9] Warwick *et al.,*[10] Law Al *et al.*,[11] and Campos *et al.*.[12]

2.1.1 Research drivers

The European Council Directive 91/676/EEC set the guide level of nitrate in water for human consumption as 25 mg L^{-1}, with a maximum admissible level of 50 mg L^{-1}. The maximum admissible level for nitrite and ammonium is 0.1 mg L^{-1} and 0.5 mg L^{-1}, respectively.[13] The EU regulatory directives state that 0.1 mg L^{-1} $P\text{-}PO_4^{3-}$ is an indicator for excessive algal growth.[14] No maximum acceptable limit has been set to date. Frequent water monitoring is essential to uphold these nutrient guide levels and to ensure compliance with legislation.

There have also been incentives to drive the research and development of environmental sensors forwards and fill gaps in the sensor market. Some examples of these include the Wendy Schmidt Ocean Health X-Prize for a pH sensor and the Alliance for Coastal Technologies Nutrient Sensor Challenge for nitrate and phosphate sensors. This style of competition offers a substantial monetary prize for development of a sensor that meets the set criteria.

In order to assess whether water bodies are maintaining their good status in accordance with the Water Framework Directive (WFD), continuous monitoring must be carried out.[15,16] Low-cost autonomous sensors are the ideal tool for this as they provide real time data, showing when waters are within acceptable nutrient limits, along with the precise time of pollution events. Legislation and policy are increasing the necessity of and demand for this technology, and are driving the research towards their development.

2.1.2 Nitrogen

In water, N exists in a number of chemical forms. Those of greatest interest include organic N, nitrate (NO_3^-), nitrite (NO_2^-) and ammonia (NH_3).[1] Organic N is found in compounds such as proteins, peptides, amino acids, nucleic acids and urea.[17] Sources include mammals, birds and insects. Inorganic forms of N include nitrate, nitrite, ammonia and dissolved N gas (N_2).[17] Nitrate and nitrite are the oxidised forms of N. When the concentrations of these two forms are combined, it is referred to as total oxidised N. The levels for nitrate N in drinking water have been limited by the U.S. EPA to no greater than 10 mg L^{-1}. This is to protect infants from methemoglobinemia, also known as blue baby syndrome. The condition results from oxidation of the ferrous ion in haemoglobin to the ferric ion, forming methemoglobin. Methemoglobin cannot carry oxygen, which can result in tissue hypoxemia, cyanosis and death.[18] Nitrite is an intermediate product formed during the oxidation of ammonia to nitrate or the reduction of nitrate to ammonia. Nitrites in the human digestive system can be converted into carcinogenic nitrosamines.[19] Ammonia is the reduced form of N. It is produced by the decomposition of organic N under anaerobic conditions. The concentration therefore gives an important indication of water quality.[20] Ammonium, NH_4^+, is also an acute toxin to some fish at concentrations greater than 200 µg N L^{-1}, making it an important nutrient to monitor.[21] Elevated levels of ammonia in water is an important indicator of faecal pollution.[22]

2.1.3 Approaches to nitrate monitoring

Nitrates can be detected directly using ultraviolet spectroscopy. Optical nitrate sensors are an example of reagent-free sensors. They operate by measuring the absorbance of ultraviolet (UV) light by nitrate ions. This occurs at approximately 220 nm. Measurements at additional wavelengths are used to correct for interferences such as absorbance due to dissolved organic matter.

Chemical-free optical sensors provide many advantages over those that incorporate chemical reagents. The sensor design is simpler as no reagent-sample mixing is required. No waste is produced; the sample can simply be released back into the environment after analysis. Reagent stability and storage are not a concern and the number of measurements taken does not rely on reagent volume. Longer deployment times are more achievable, with the main concerns including battery life, maintenance and biofouling. Challenges specific to ultraviolet nitrate sensors include power consumption by the light source as it limits deployment time, and interfering species such as dissolved organic matter and halides. Correction for these interferences involves measurements at additional wavelengths, further reducing battery life.

The incorporation of a digestion step into an autonomous system is complicated. As nitrate is often the largest component of total N in freshwater, it gives a good indication of changes in total N levels. Changes in nitrate levels represent the most significant water quality issues such as algal blooms and drinking water quality, making them a suitable substitute to monitor. Commercial sensors for nitrate in water are available, however the cost per sensor is too high for the deployment of sensor networks.

Several of these commercial options are shown in Table 2.5, later in this review.

2.1.4 Phosphorus

P exists in water in a number of chemical forms, the most common of which are phosphates. Phosphates occur as orthophosphates, condensed phosphates (pyro-, meta-, and poly-phosphates) and organically bound phosphates. Phosphates also occur in bottom sediments and biological sludges, either in organic compounds or precipitated in inorganic forms.[1] Condensed phosphates are added to water during a number of processes including water treatment, laundering or commercial cleaning processes. Orthophosphates used as fertilisers on land are carried into surface waters by rain, while organic phosphates are produced through biological processes, and enter the water system through body waste and food.[1,23]

2.1.5 Approaches to phosphate monitoring

There are a variety of approaches for phosphate determination in water. It cannot be detected directly, introducing the need for reagent-based methods. These include colourimetric wet chemistry based detection, electrochemical detection and fluorescence detection. Laboratory based techniques for phosphate determinations include ion chromatography and spectrophotometry. For autonomous sensor development, incorporation of reagents introduces challenges such as stability and storage, waste storage, and for colourimetric analysis, sample carryover or staining of the

optical pathway by the coloured product. Electrochemical sensors for phosphate typically also require reagents. They also face challenges in signal drift and long term stability, requiring frequent calibration.

A trend found in the literature showed that electrochemical and fluorescence detection methods were typically not yet automated, while autonomous sensors tend to use the standard colourimetric yellow or blue methods.[24,25,26,27]

Similar to N, the release of P from organic matter as orthophosphates requires a digestion step, making the analysis of total P (TP) using an autonomous sensor more complicated. Incorporation of an automated digestion step into these sensors is complicated, and has not been achieved in a deployable system in a cost effective manner to date.[28] Phosphates are therefore monitored in water to give an indication of TP levels.

2.1.6 Types of systems

Traditionally, nitrate and phosphate levels in water have been monitored by obtaining grab samples followed by analysis in a laboratory. This is time consuming, labour intensive and prone to contamination at the sample collection, transport and preparation stages. The findings are only relevant for the location of water sampled, at the time of sampling. This low frequency data has provided answers to many important questions about the dynamics of a water system. However, nutrient movement can vary widely both spatially and temporally, which is not evident from infrequent measurements where transient occurrences can be missed entirely.[29] A

network of autonomous sensors capable of continuous, unattended analysis can provide high frequency measurements to show this variation.

The intermediate option between traditional analysis and unattended autonomous sensors would be handheld analysers for on-site measurements. These systems, such as the SL1000 portable parallel Hach Analyzer, allow for rapid measurements to be collected at the sampling site, removing the need for storage and transportation to the lab.[30]

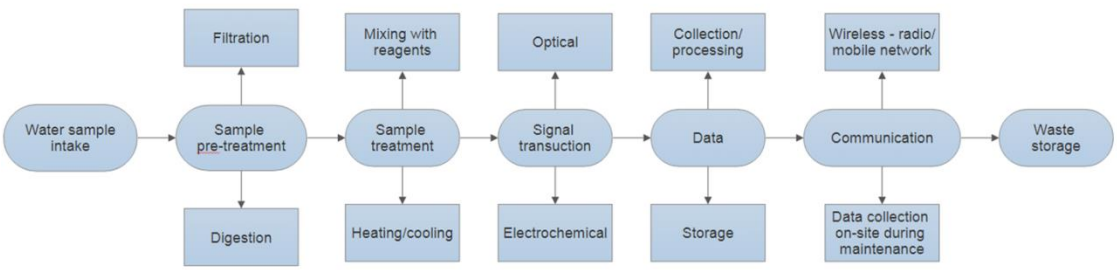

Fig. 2.1. A schematic of an autonomous water nutrient sensor, showing examples of the possible functions and requirements.

2.1.7 Microfluidic technology for sensor development

There are a number of advantages associated with using microfluidic technology for fluid manipulation if direct measurement of an analyte is not possible. It allows for the miniaturisation of analytical protocols into a sensor for compactness and portability. The low sample volume, typically within the µL range, allows for reduction in reagent consumption and waste production compared to laboratory methods. Reductions in analysis

time are also possible due to the improved efficiency of diffusional mixing in smaller volumes, enabling more frequent measurements.[31]

For environmental monitoring, microfluidic chips can also presents some drawbacks. The µL volume sample is taken to represent the entire water body. This issue can be overcome by taking frequent measurements, showing real time variations in nutrient levels. When compared to infrequent grab samples which are analysed in a laboratory, the *in situ* sensors provide more valuable data than the laboratory analysis.[32]

Microfluidic channels are also prone to blockages and bubble formation. A filtration step can minimise blockages. Bubble formation introduces interferences for optical detection, and can be avoided by careful design of the microfluidic system.[31,33,34] Advances in microfluidic technology for environmental analysis were reviewed by Jokerst *et al.* in 2012.[35]

A combination of low-cost microfluidic components with low-cost optical or electrochemical detectors allow for the manufacture of affordable sensors. Low-cost sensors are essential for the recording of large data sets within a water system, which are required for efficient interpretation of nutrient movement in water.

2.1.8 Agricultural applications of autonomous sensors

With growing interest in IoT and the concept of widely distributed low cost devices, one area where this can show real potential is in agriculture.[36-40]

Farm management practices can have a profound impact on ground and surface water quality in a catchment. Outdated farm management practices include excessive fertiliser application, the use of pesticides and herbicides, poor management of livestock, and traditional irrigation

practices.[36] The application of surplus fertiliser occurs in order to maximise crop yields. However, not all of the nutrients applied to the soil can be taken up by the crops. Irrigation and rainfall cause excess nutrients to leach into the drainage water. This water eventually connects with streams and rivers, leading to eutrophication within the water catchment. This not only has a negative impact on the environment, but it is also inefficient, and a waste of farming resources. This creates an opportunity for sensor development experts, environmental scientists and farmers to work together in a mutually beneficial manner.

Wireless Sensor Networks (WSNs) are highly promising tools in the advanced automation of chemical analysis processes.[37] Interest in 'smart farming' is growing as technological advances are made in the area of autonomous sensors. Smart farming involves the use of autonomous sensor technology to remotely monitor farming processes and to make informed decisions based on the collected data. Incorporation of an Internet of Things (IOT) approach can allow for alert generation and even automated response systems. Smart Agriculture helps to reduce waste production, allows for effective usage of fertiliser and increases crop yields. In one example of smart farming, sensors were used to monitor soil moisture, temperature, humidity, and light in a crop field in order to automate the irrigation system. The collected data was wirelessly sent to a web server database, and notifications were sent to farmers' phones periodically. The irrigation was automated if soil moisture and temperature dropped below a certain threshold. Light intensity can be automated in greenhouses, alongside irrigation automation. This system was found to be 92% more efficient than the conventional approach, highlighting the huge potential of smart farming.[38]

An IoT based smart animal farm was designed cost effectively to monitor and operate the farm remotely. This design used microcontrollers, water level sensors, ultrasonic sensors, gas sensors, temperature sensors, humidity sensors, and an IP Camera, as well as connectivity with devices such as smart phones or computers, with a cost of $300. This system can provide feed and water to animals as required, exhaust the excess of biogas produced by the animals, and detect fire in the farm.[39]

The US Department of Agriculture (USDA) is working to develop a total "Smart Field System" that automatically detects, locates, reports and applies water, fertilisers and pesticides.[40]

Poor management of livestock can result in leaching of animal waste into the water system. Not only does this have an impact on the nutrient levels in the water, but it also carries pathogens.

Monitoring the drainage system of a farm allows for the assessment of its impact on the surrounding environment and water quality of the catchment. In order to effectively assess this impact, frequent measurements are required. The only method to feasibly achieve this level of monitoring in a farm setting, which is typically remote, is to automate it. This is where the cost per sensor comes into sharp focus. Pollutants from farmland can have multiple points of entry, requiring multiple sensors to effectively monitor the process.

Phosphate and nitrate sensors are currently too expensive (typically from $20,000 upwards) to be applied to this type of practice. In order for them to be adopted into sensor network applications, the cost per unit must be reduced.

Previous deployments of nutrient sensors in environmental settings are described after Table 2.3 and 2.4.

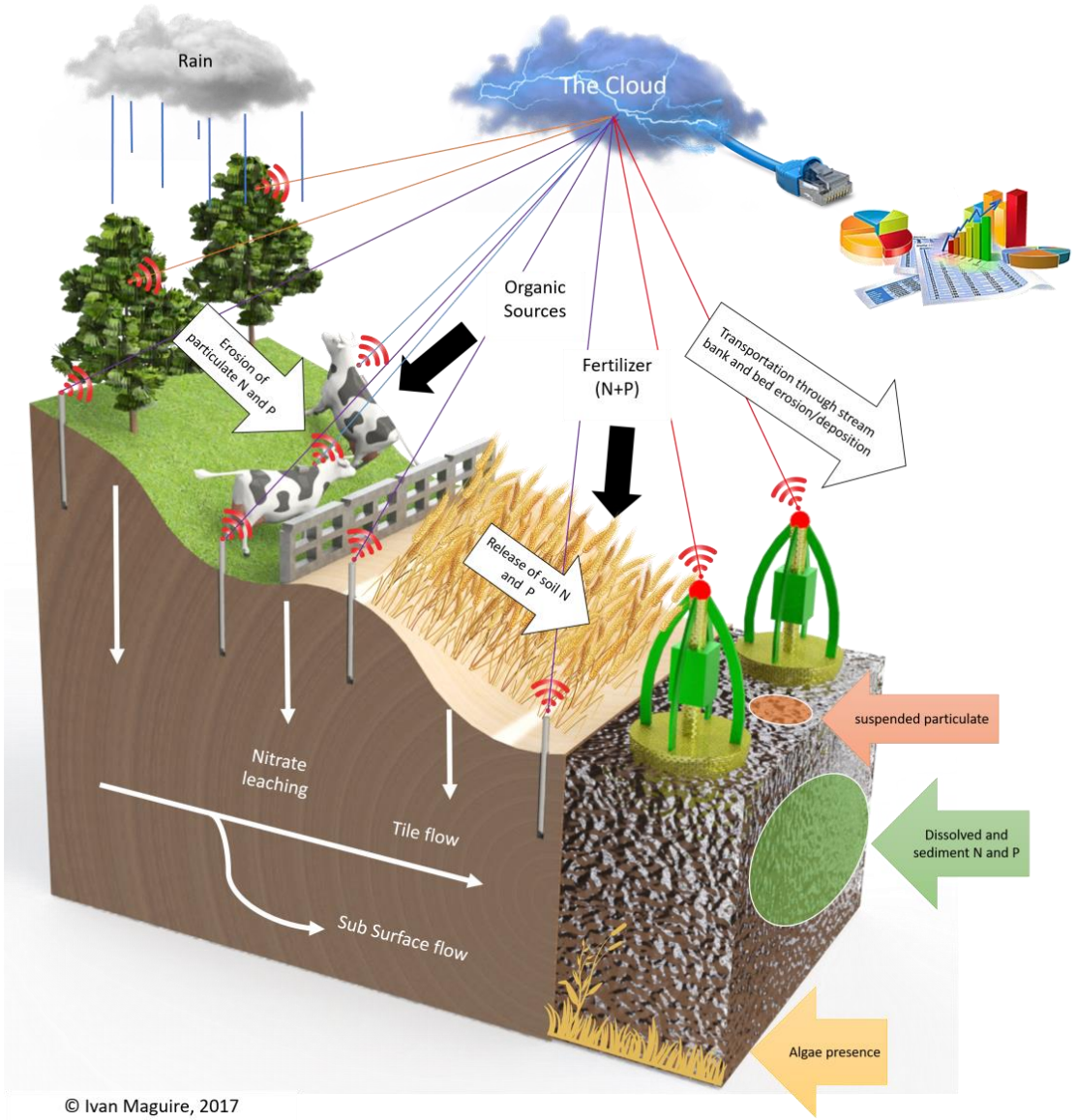

Fig. 2.2. A diagram showing N and P from agricultural sources entering the water system, representing an ideal deployment site for nutrient sensor networks.

2.1.9 Aesthetics of an autonomous sensor

A topic not often addressed in the development of autonomous sensors is compactness and appearance. If sensors are bulky and unattractive, the public will not respond in a positive manner to the deployment of large scale sensor networks in their lakes, rivers and streams. Compactness is also an important consideration for disguising sensors for protection from vandalism or from curious animals, and for their deployment in difficult-to-reach locations. They must be rugged and very well secured for extra protection. The level of ingress protection (IP) is an important consideration for long-term deployability. This numerical based system indicates the sensor's ability to withstand different types of impact. The first number represents the degree of protection against solid objects. The second number indicates its protection against the ingress of water. The third number is rarely used. It represents the degree of impact an object can sustain while still maintaining normal function.[41]

Technology readiness level (TRL) of a sensor is an important consideration for the developers. This scale is widely used to determine the maturity of technology, from basic research to a commercialisable product.

Some examples of deployed systems are described in Table 2.3 and 2.4.

2.2 Traditional analysis methods

2.2.1 Standard methods of analysis for Phosphates

The three standard colourimetric methods of analysis for phosphates are discussed in this section, as described in the Standard Methods for the Examination of Water and Wastewater. The selection of a method depends

on the concentration range of orthophosphate in samples to be analysed, as shown in Table 2.1. An extraction step can be included if levels are low or interferences are present. An alternative method, not listed in the Standard Methods for the Examination of Water and Wastewater, is the malachite green method, based on the formation of a strongly absorbing species from reaction of phosphomolybdate with malachite green.[42] A variation on the stannous chloride was also included, which uses hydrazine as a reducing agent in place of glycerol for storage of stannous chloride.[43,44,45]

2.2.2 Sample preparation

There are three methods for sample preparation; filtration, acid hydrolysis and acid digestion. Filtration using a 0.45 µm filter removes particles for dissolved reactive phosphorus analysis. Acid-hydrolysable phosphorus includes condensed phosphates such as pyro-, tripoly-, and high molecular weight species. A digestion method is required for TP determination, to oxidise organic matter, releasing P in the form of orthophosphate.

Table 2.1. A summary of standard colourimetric methods for phosphate analysis in water, and two additional methods.

Method	Concentration range (mg PO_4^{3-} P L^{-1})	Limit of Detection (µg PO_4^{3-}-P L^{-1})	Reagent stability	Complex formation time (min)	Interfering ions	Comments toward method automation
Vanado-molybdo phosphoric acid method	1.0 - 18	200	>1 year	≥10	AsO_4^{3-}, F^-, Th, Bi, S_2^-, $S_2O_3^{2-}$, SCN^-, or excess molybdate	Most frequently used on automated sensors, poor sensitivity, good reagent stability.
Stannous chloride method	0.007 - 2	3	>6 months	>10, <12	Same as vanado-molybdo-phosphoric acid method	Good reagent stability and sensitivity, reagent viscosity makes it challenging for use in microfluidic systems.
Ascorbic	0.01 – 2.0	10	~1 week	>10, <30	AsO_4^{3-}, Cr^{6+},	Most frequently used on

acid method					NO_2^-	in-line sensors. Good sensitivity, poor reagent stability.
Variation on stannous chloride method [43]	0.001 – 0.8 mg PO_4^{3-} L^{-1} *	2.4 µg PO_4^{3-} L^{-1} *	Not stated	Similar to stannous chloride method	SiO_4^-. Tartaric acid used to overcome this.	Less viscous solvent makes it more suitable for use in microfluidics and flow systems.
Malachite green method [46]	Up to 2.9 µmol L^{-1} **	0.17 µmol L^{-1} **	>1 year	10	ArO_4^{3-} [47]	Good reagent stability and stability. More frequently used for biological analyses than for water.

*Using a 100 mm path length. Other measurements are for standard 10 mm path length in a spectrophotometer.

**5 mm long flow cell

2.2.3 Standard methods of analysis for Nitrates [1]

There are six standard methods of analysis for nitrates (NO_3^-) included in this section.[1] The selection of a method is done based on a screening of the sample. A method is selected in order to minimise interferences from the sample matrix and to measure within the concentration range of the samples to be analysed. Methods are summarised in Table 2.2.

Table 2.2. A summary of standard methods of nitrate analysis.[1]

Method	Concen-tration range (mg NO_3^--N L^{-1})	Reagent stability	Measure-ment time (min)	Comments towards method automation
UV spectro-photometry screening	0 - 11	N/A	<1 min	No reagents required. Power hungry, relatively expensive light sources Need multiple wavelengths
Ion chromato-graphy	From 0.1	N/A	N/A	Complicated, expensive instrumentation, high LOD
Nitrate electrode	0.14 – 1400	N/A	~1 min	Calibration required multiple times daily
Cadmium	0.01 – 1.0	Approx. 1	<15 min,	Difficult to automate –

reduction		month	post reduction column	multiple steps, column maintenance
Titanous chloride reduction	0.1 – 20	Stable	Until electrode stabilises	Calibration required
Automated hydrazine reduction	0.01 - 10	Approx. 1 month	10 min for colour development, post reduction	Extra heating step required

2.3 Recent approaches to phosphate monitoring

There are a great number of alternative methods for phosphate determination in the literature that could be applied to autonomous sensing. Some of these methods have been compiled in Table 2.3, indicating the LOD and linear range of each method, as well as whether the method has been automated or deployed in water as a sensing device. While many of these methods have not been automated, it shows the great efforts underway for development of new detection methods, and also the wide variety of approaches taken.

2.3.1 Electrochemical detection

The overall trend visible from Table 2.3 is that a lot of promising electrochemical sensors are under development. Not many electrochemical sensors have been incorporated into autonomous systems to date, compared to the number of colourimetric systems. The focus of research in this area seems so be on optimisations of novel electrochemical sensors, with a prediction of their usefulness in autonomous systems. The LOD of the methods shown in Table 2.3 are similar to those for fluorescence and for colourimetric detection.

Challenges common to many of these examples included overcoming interferences and improving sensitivity and selectivity. While the developed electrodes are suggested as viable options for automation, not many have been automated to date. Important considerations for their automation include calibration or signal drift, lifetime and ruggedness of the sensors. Electrochemical sensors are already frequently employed in environmental monitoring, for example for pH, dissolved oxygen and trace metals.[48] However signal drift presents a challenge for long term deployment.[49,50,51]

Phosphate has been measured using a number of different electrochemical techniques such as potentiometry, voltammetry and amperometry.[52] While electrodes can offer faster measurement times and lower LODs than colourimetric methods, they still require the addition of reagents. Phosphate is not an electro-active species; however it can be detected electrochemically in acidic conditions in the form of phosphomolybdate, similar to colourimetric methods.

A flow injection analysis system was employed to achieve continuous measurement capabilities.[53,54] A portable 'PhosQuant' electrochemical

detection system suitable for use in-field was created, comprising of a potentiostat, screen printed electrodes, a tablet for readout display and a power supply housed together in an acrylic box. A droplet of water was placed on the SPE system for measurement.[55]

An electrochemical sensor for phosphate determination in seawater was reported in 2012, with an LOD of 0.11 µM, showing good accuracy and reproducibility.[48] The method was optimised to overcome interferences from silicate.

A microelectromechanical system (MEMS) for phosphate determination was reported in 2010.[74] This sensor consists of a microfluidic chip incorporating a phosphate sensitive electrode made of cobalt. This was shown to respond linearly to phosphate ion concentration. A micro-digestion system was incorporated onto the chip design for measurement of TP. A heating electrode will be incorporated, coupled with a micro temperature sensor to control heating and pressure.

A gold microelectrode with gold nanoparticles was incorporated to increase the surface area of the electrode.[57, 58] The LOD reported in 2014 was 1.2×10^{-7} mol L^{-1}.[58] This will be integrated with the micro-digestion system to create an autonomous TP sensor, suitable for water pollution monitoring.[74]

2.3.2 Fluorescence detection

Fluorescence detectors are an excellent option for phosphate sensors as they can achieve high sensitivity, and reach lower limits of detection than colourimetric methods. They are typically based on fluorescence recovery by replacing a competing ion in the fluorescent complex, quantum dot or

nanoparticle with phosphate. Sensitivity can be further improved by the use of light filters or lenses[69], however this will increase the sensor cost. Automation of fluorescence sensors to date has been with flow systems, where reagents are mixed together in tubing and reaches the detector for measurements. This could be incorporated into an autonomous system in the same manner that colourimetric methods have been automated for deployments in the environment.

A sequential injection analysis system (SIA) for simultaneous phosphate and ammonia determination in marine and river waters was reported in 2006.[75] Phosphate is reacted with acidic molybdate to form phosphomolybdate, which forms non-fluorescent ion pairs with rhodamine 6G. The remaining rhodamine is detected by excitation at 470 nm and measurement of fluorescence at 550 nm. The detection limit for this method was reported as 0.3 µM phosphate. The range for phosphate detection is small due to the very effective quenching of rhodamine fluorescence by phosphomolybdate. To overcome this, three sample volumes (50, 17 or 8 µL) can be used, depending on the expected concentration of phosphate. The limit of detection for 50 µL volume in the laboratory was 0.04 µM. Using the 8 µL volume, concentrations up to 4 µM can be measured. These detection limits are low compared to the yellow colourimetric detection methods but are higher than the electrochemical detection limits described here.

Future work on this sensor aims towards size reduction of the pump and detectors for integration with a tow-fish. It would also be suitable for automated continuous monitoring as it incorporates low reagent consumption, rapid measurement times and good sensitivity.[76]

As mentioned in Table 2.3, a low-cost fluorescence detector, also based of quenching of rhodamine 6G with molybdophosphate, was developed for

FIA applications. It has a low LOD of 0.45 µg L^{-1} PO_4-P compared to other sensing methods, however it also has a very narrow sensing range. Suggested applications for the sensor includes surface or underway monitoring in seawater.[71]

2.3.3 Colourimetric Detection

It is clear from Table 2.3 that colourimetric detection methods have been the most favoured detection approach for automation in deployable sensors. These methods are well validated and have been used in laboratories all over the world. One obstacle for colourimetric detection is the lifetime of the reagents. Some methods with preferable characteristics are ruled out as potential candidates for deployable sensors due to their short reagent lifetime, for example, the more sensitive ascorbic acid method. This is detailed in Table 2.1. The yellow method has excellent reagent stability, while its corrosive nature and the low molar extinction coefficient of the product compared with other colourimetric methods presents challenges for automation such as sourcing low-cost, highly sensitive optical detection components and acid resistant materials.

The micro total analysis system (µTAS) idea originated in 1990.[77] These systems require microfluidic components in order to minimise laboratory processes onto a small chip. This is where the term lab-on-a-chip comes from. Some early applications of microfluidic technologies for nutrient analysis were seen from Daykin *et al.* in 1995, [78] who used a micro flow injection manifold for spectrophotometric detection of orthophosphate, from Petsul *et al*. in 1999,[79] who reported a µTAS for spectrophotometric determination of nitrite, and from Petsul *et al. in* 2001,[80] for the

development of an on-chip micro-flow injection analysis system for nitrate determination.

The development of a microfluidic platform for the detection of phosphate in marine waters was reported by Legiret *et al*. in 2013.[25] The incorporation of tinted PMMA and polished fluidic channels resulted in a limit of detection of 52 nM phosphate, with a range of 0.1-60 µM. Due to reagent stability, the yellow method for phosphate detection is used. After the formation of vanadomolybdophosphoric acid, the absorbance of the yellow complex was measured at 375 nm in a 25 mm long absorbance cell, using an LED and photodiode. A water sample was pumped into the system using a syringe pump. Mixing of sample and reagent occurred in the mixer on-chip. A reference absorbance cell was used for background absorbance correction.

This sensor was deployed in 2010 to carry out a sampling transect off the coast of England, and in 2011 it was connected to the underway system of a ship. For each deployment, no statistical difference was seen between the sensor measurements and discreet samples analysed with bench top equipment at 95% confidence. Due to low power consumption, stability of reagents and the low reagent volume required per measurement, this sensor can be deployed for long periods of time.

A microfluidic approach was also taken by Cleary *et al.,* reported in 2008. This colourimetric sensor, also based on the yellow method, was deployed in wastewater, freshwater and estuarine locations.[24] The system was compact, containing reagents, calibrant solutions and waste in collapsible polypropylene bags, a microfluidic chip and low cost peristaltic pumps. A 3 mm long optical path length was incorporated on chip for absorbance measurements with the LED-photodiode detection system. It was self-calibrating and self-cleaning for long term deployments. Data from the

sensor was accessed remotely using ZigBee® radio, providing real time information as well as allowing the user to change the setup parameters of the sensor remotely. The limit of detection of phosphate using this sensor was 0.3 mg PO_4^{3-} L^{-1}, or 0.1 mg PO_4^{3-}-P L^{-1}, with a linear range of 0.1-1.6 mg PO_4^{3-}-P L^{-1}. This sensor would be suitable for waste water treatment plants or industrial effluent, where phosphate levels are typically higher, and in known polluted surface waters.[14,24,32,81,82]

In 2016, as summarised in Table 2.3, an autonomous sensor for TP analysis with component cost less than $3000 was developed. While this system has not yet been deployed, it is **a** great step forward, towards TP analysis using low-cost autonomous systems.[28]

The ANAIS analyser, reported in 2003, measured phosphate, nitrate and silicate. Phosphate measurements were based on stannous chloride method with hydrazine sulphate. Solenoid-driven diaphragm pumps were used to propel the sample or standards, along with the reagents, through a micro-conduit, flow injection-style thermostated manifold. An LED and photodiode were used for detection, along with an interference filter and a convex lens to select and focus monochromatic light. An LOD of 0.1 µM for phosphate was achieved, with a measurement range up to 5 µM. This sensor was deployed in the surface ocean. It was then implemented on top of a YOYO vertical eulerian profiler for deployment in the northwestern Mediterranean Sea over a 15-day period.[83]

A compact, portable flow injection analysis instrument for filterable reactive phosphate (0.2 µM filter) was reported in 2002 for phosphate measurement in marine waters. Gas pressure was used for fluid propulsion, with a solid state LED photometer to detect phosphate via the stannous chloride

Table 2.3. Recent approaches to phosphate sensing showing LOD and linear range, and whether the sensor was automated or tested for water monitoring.

Transduction method	Ref.	Characteristics	LOD	Linear range	Autonomous	Tested
Electrochemical	[56], [48]	Differential pulse voltammetry was used to detect the phosphomolybdate complex, formed by oxidation of molybdenum and subsequent complexing with phosphate. No reagent addition required. No silicate interference. As no reagent storage is required, this could be more compact than reagent based sensors, where deployment time is limited by the volume of reagent stored.	0.19 µM	Covers range found in the open ocean	No	No
	[57]	Electrochemical microsensor based on reduction of the molybdophosphate complex on the gold working electrode, where the reducing current is measured. With a digestion step, TP determination was measured.	0.66 µM	~1-500 µM	No	No

[58]	Same operating principle as [32]. The gold electrode was modified with gold nanoparticles to increase surface area, improving sensitivity. TP determination with digestion step.	$1.2x10^{-7}$ M	$3x10^{-7}$ to $3x10^{-4}$ M	No	No
[59]	Reagentless detection with long lifetime based on a liquid junction potential formation. Improved selectivity coefficients compared to other ISEs (except bare cobalt electrode).	Not stated	10^{-4}-10^{-1} M PO_4^{3-}	No	No
[53], [54]	3 electrode system with flow injection analysis, using oxalate to mask silicate interference.	4.0 µg P L^{-1}	0-1 mg PO_4-P L^{-1}	Yes	No
[60], [61]	A thiourea based molecularly imprinted polymer with conductance based transduction. No sample filtration required. Rinsing of membranes between samples required. Longevity of membranes was not determined beyond 10 uses within 3-5 days.	0.16 mg P L^{-1}	0.66-8 mg P L^{-1}	No	No
[62]	Paper-based sensor with wax channels, impregnated with reagents to form electroactive phosphomolybdic complex. Detected by cyclic voltammetry with screen printed 3-electrode	4 µM	Up to 300 µM	No	No

		system. Long storage stability. No reagent addition required. No pre-treatment required. A large number of paper strips would be required for a deployable system.				
	[55]	Indirect measurement of phosphate using a screen printed 3-electrode system with a graphite working electrode, where reduction of phosphomolybdate is achieved electrochemically. The reduction peak of the cyclic voltammogram is measured.	0.3 µg P L^{-1}	0.5-20 µg P L^{-1}	Semi – portable sensor, sample prep. required.	No
Fluore-scence	[63], [64]	Based on quenching of dye fluorescence by formation of ion pairs between molybdophosphoric acid and rhodamine B. Applied to soil and human serum analysis. Low-cost micro-solenoid pumps and valves, and low-cost detection system used. As water samples require even less sample preparation than blood and soil samples, this could easily be adapted to water analysis.	3.6 µM in serum 0.013 – 0.04 mg P L^{-1} in soil, depending on	12-60 µM 0.019–10 mg P L^{-1}, across all extraction media	No Automated extraction and determination	No No

			extraction medium			
	[65]	Thiol capped cadmium telluride quantum dots form a complex with europium nitrate, which quenches their fluorescence. Addition of phosphate results in recovery of fluorescence.	Not stated	In physiological range (~ 0.85-2.4 mM)	No	No
	[66]	Mono and di- octamethylcalix[4]pyrrole substituted diketopyrrolopyrrole based anion sensors for detecting selective anions. Measurable response colorimetrically and fluorometrically.	1.15 ppm PO_4^{3-} in visible light and 0.025 ppm PO_4^{3-} under UV light	Not stated	No	No
	[67]	Graphene quantum dots based upconversion	100 nM	1-12 µM	No	No

		fluorescent sensor for detection of phosphate. The upconversion fluorescence of graphene quantum dots with emission wavelength at 407 nm was quenched by Eu^{3+}. Fluorescence was recovered on addition of phosphate. Applied to measurement of phosphate in river water samples. High stability of the method was reported, making long term storage on a deployable system feasible.				
	[68]	An off–on fluorescence probe for PO_4^{3-} based on quenching of the tannic acid-stabilized copper nanoclusters (TA-Cu NCs) by Eu^{3+} via static quenching mechanism. After adding PO_4^{3-}, the quenched fluorescence recovered due to higher affinity of Eu^{3+} ions for the oxygen-donor atoms in PO_4^{3-} than for the carboxylate groups on the TA-Cu NCs surface. Applied to water sample measurements for eutrophication diagnosis. Stable fluorescence for at least 2 months of storage.	$9.6x10^{-3}$ µM	0.07 - 80 µM	No	No
	[69]	A flow-through optoelectronic detector with 4	Photome	11.3-	Yes – flow	No

	LEDs, capable of both photometric and fluorimetric measurements. Photometric measurements are based on the ascorbic acid method, while the fluorimetric method is based on quenching of rhodamine G with the phosphomolybdenum complex. Applied to analysis of soft drinks and postdialysis fluid produced by artificial kidney. This flow cell would be suitable for water samples also.	tric: 5.5 mg L^{-1} PO_4^{3-} Fluorime tric: 10.4 µ L^{-1} PO_4^{3-}	300mg L^{-1} PO_4^{3-} 33.5-1000 µg $L^{-1}PO_4^{3-}$	through cell	
[70]	Inorganic phosphate displaced Fe^{3+} in a complex, causing fluorescence enhancement, with visible light excitation and emission. Applied to aqueous solutions and incorporated in flow cytometry for intracellular measurements.	1.5 µM	0 - 20 µM	No	No
[71]	Fluorescence of Rhodamine 6G quenched by phosphomolybdate. A reversed flow injection analysis system was designed for decoupling the analytical setup from environmental pressure for in situ applications. Sampling frequency of up to 300 samples per hour.	0.22 µg L^{-1} PO_4-P (pure water) 0.45 µg L^{-1} PO_4-P	0 - 40 µg L^{-1} PO_4-P	Yes	No

			(seawater)			
Colouri-metric	[28]	Low cost autonomous, in-situ analyser for orthophosphate and TP. Based on stannous chloride method, incorporating a heated peroxodisulphate digestion step for TP determination. 5 cm long optical path length for absorbance measurements. Sequential injection analysis (SIA) fluid handling system with syringe pumps. Component cost <$3000, not including submersible housing.	TP: 29 µg P L^{-1} PO_4^{3-}: 34 µg P L^{-1}	Up to 200 µg P L^{-1}	Yes	No
	[25]	Autonomous microfluidic chip-based analytical system based on the yellow method. Low reagent consumption of 340 µL per sample. Low power consumption. The low LOD was achieved by incorporating tinted PMMA and polished fluidic channels. Up to 20 samples per hour.	52 nM	0.1-60 µM	Yes	b, c
	[27]	The commercially available Hydrocycle-PO4 developed by WetLabs, based on the ascorbic acid	2.3 µg P L^{-1}	Up to 0.3 mg L^{-1}	Yes	a, b, c

		method, incorporating a 5 cm optical path length for absorbance measurements. Reagent lifetime has been extended to 5 months, compared to the previously stated 3 months for the Cycle-PO4 sensor. Up to 4 samples per hour.		PO_4-P		
	[72]	A sequential injection system based on the ascorbic acid blue method. Two different detection systems with differing LOD and linear range were incorporated: a spectrophotometer with a commercial flow cell, and a multi-reflective flow cell with a photometric detector. 37 samples per hour.	0.007 µM	0.024-9.5 µM	Yes	No
	[73]	A photometric detector made up of an organic LED and organic PD was applied to phosphate determination using flow injection with a 5 mm path length. Based on the malachite green colourimetric method. Applied to river water samples.	0.02 ppm PO_4^{3-}	Up to 0.2 ppm PO_4^{3-}	Yes	No

[a] Tested in freshwater; [b] Tested in saltwater; [c] Unattended deployment

method with hydrazine sulphate. This sensor was capable of 225 measurements per hour. An LOD of 0.15 µM and range of 0.81-3.23 µM was reported.[84]

Zimmer *et al.* reported a spectrometric detection method for nanomolar concentrations of phosphate in ocean surface waters in 2012.[85] This real-time, continuous monitoring sensor incorporates a liquid waveguide capillary cell (LWCC): a fibre optic cell with a long optical path length allowing for small sample volumes compared to traditional cuvette volumes. The ascorbic acid molybdenum blue method was used. Use of a LWCC is a reliable technique for measurement of phosphate on the nanomolar scale without a pre-concentration step. A limit of detection of 0.8 nM phosphate was reported which is very low compared to the electrochemical, fluorescence and yellow colourimetric detection methods. Real-time monitoring for up to 16 consecutive hours was possible from a shipboard tow-fish. A reference channel with DI water and reagents is used to minimise baseline drift.

Wet Lab's Cycle-PO4 is a commercially available phosphate sensor that incorporates microfluidics with optical detection.[80] It is based on the ascorbic acid method, however it reported a reagent stability of 5 months.[27] The reagent responsible for this extended lifetime is withheld as a trade secret in the data sheets provided. The system has been deployed in marine and freshwater environments with reported precision and accuracy are 50 nM and <150 nM,

respectively, a limit of detection of 0.023 µM and a typical concentration range of 0.113-47.8 µM.[86] The sensor contains a standard solution for on-board calibration, and incorporates 'smart sampling' to minimise power consumption, making it suitable for long term deployments.[27] A

deployment of four weeks with continuous testing was reported.[87] During deployments described in the Performance Demonstration Statement, the optical sensors were cleaned daily to remove biofouling.[87] This is not ideal as one aim of autonomous sensors is to eliminate the need for frequent visits to the deployment site.

2.4 Recent approaches to nitrate monitoring

There are also a wide range of alternative methods for nitrate determination in the literature that could be applied to autonomous sensing. Some of these methods have been summarised in Table 2.4, with the same information for each method as in table 2.3. As nitrate can be detected directly using multiple wavelengths of UV light, sensor development was more straightforward. There are already a number of commercial sensors for nitrate monitoring based on this mode of detection, some of which are discussed in this section. The use of reagents or electrochemical methods means that sensor development is more complicated and takes more time. Many of these methods have already been automated, however only a small number have been deployed as a functioning autonomous sensor.

2.4.1 Optical detection

Early developments in deployable optical nitrate sensors were reported in 1998.[88] Finch *et al.* developed a UV nitrate sensor that utilised a xenon flash lamp light source, fused silica windows and lenses, a grating

spectrometer and UV enhanced silicon photodiode detectors.[88] Sample absorbance was recorded at three wavelengths. This provided one wavelength at which nitrate and halide absorb significantly, one at which halide absorbance is very small, and one where absorbance is affected primarily by obscuring particles which acts as a reference. The minimum concentration change this sensor was capable of resolving was >0.21 μM. To improve definition of spectral changes associated with changes of interfering species, the use of six wavelengths (205, 220, 235, 250, 265 and 280 nm) was proposed.[88]

In 2002, the design for an *in situ* sensor for nitrate, bromide and bisulfide in ocean water was reported. This *in situ* ultraviolet sensor (ISUS) is composed of four main components; a UV light source, an optically coupled sensing probe, a high resolution spectrometer and a low power instrument controller with data storage.[89]

A Heraeus Fiberlight was used as an alternative to the xenon flash lamp due to the low light intensity of the xenon flash lamp below 220 nm, the variability in the lamp spectra with temperature changes, and the solarisation of optical fibres caused by the high intensity of the lamp light. These issues were not experienced with the Fiberlight. This light source is a continuous wave deuterium light source, requiring low power (3 W), similar to the xenon flash lamp which required 3-4 W.[88,89] A high resolution (approximately 1 nm) spectrometer with a The estimated sensitivity of ISUS is ±0.25 mM. This is not as sensitive as the sensor developed in 1998. However, the ISUS was capable of a longer deployment time of >3 months, an improvement upon the 10 day deployment time by Finch *et al.*

In 2012, a lab-on-a-chip optical nitrate and nitrite sensor was reported, with a limit of detection of 0.025 μM for nitrate and 0.02 μM for nitrite,

detecting both analytes up to 350 µM, making it suitable for deployment in a variety of natural waters.[90]

This sensor detects nitrate using a cadmium tube for reduction to nitrite. The Griess assay is then carried out on-chip, forming an intensely coloured azo dye. A green 525 nm LED and photodiode measure the absorbance of the reacted sample. The chip contains three cells for absorbance measurements; a 25 mm reference cell, a 25 mm cell for measuring concentrations below 30 µM, and a 2.5 mm cell for measuring concentrations above 30 µM. During deployments, the data is stored on a flash memory card, while data can also be streamed over an RS-232 connection for real time data monitoring. The sensor is small with a power consumption of 1.5 W. 1.5 W is low compared to the UV optical nitrate sensors discussed previously, which were 4 W and 3 W. This is due to the use of an LED and photodiode for absorbance measurements. A 26 day deployment of the sensor was reported.

2.4.2 Electrochemical detection

An electrochemical based nitrate sensor called iNits (Illinois Nitrate Sensor) has been developed for nitrate quantitation in water.[91] This sensor works by reducing nitrate to nitrite in a two electron transfer process. Oxygen was found to interfere with this measurement, meaning that dissolved oxygen in water reduces the sensitivity of the method. Solid metal electrodes are used: the working and reference electrodes are made of silver and the counter electrode is made of gold. The sensor contains a low-cost, portable potentiostat, a sensor interface for input and output of parameters, a low-cost processor and Imote2, a wireless communication

device. Its small size compared to optical sensors makes it an attractive option for sensor networks. Suggested applications for this low-cost sensor include nitrate monitoring in drinking water, wastewater, food and ground water. The main application discussed in this article is 'smart farming', where the sensors show nutrient levels in a field, enabling adjusted fertiliser application.[91]

A potentiometric sensing array based on polymeric membrane materials for continuous monitoring of nutrients and chemical species in freshwater was reported in 2015. It operates autonomously, carrying out measurement, calibration, fluidic control and acquisition. It was deployed for continuous monitoring of pH, calcium, nitrate and carbonate levels at the EAWAG monitoring platform on the lake Greifensee (Switzerland), in parallel with scanning low cytometer measurements. Continuous calibration of potentiometric sensors between the measurements of water samples provided more reliable data compared to ISE arrays using relatively infrequent calibration in field conditions.[92]

Sequential injection analysis was used as a method of automating analysis using novel electrochemical detection methods.[73,94] While this works well in a laboratory environment, it would not be ideal for long term deployable systems due to the significant consumption of solvents compared to alternative methods, as it runs on a continuous flow principle. It is an improvement upon its predecessor, FIA, which used more sample and reagents, resulting in greater waste production.[94]

2.4.3 Surface Enhanced Raman Spectroscopic detection

A surface enhanced Raman spectroscopy (SERS) technique coupled with a gold nanosubstrate was reported in 2012, for nitrate and nitrite measurement in water and wastewater.[95] Raman spectroscopy measures the inelastic scattering of light resulting from molecular vibration. SERS enhances Raman signals due to the excitation of localised surface plasmons, where the local electromagnetic field is enhanced greatly. SERS has the ability to detect single molecules.[95] The incorporation of a coating of commercial gold nanosubstrate, including a SERS-active area, onto the silicon wafer allowed for an enhancement in Raman signals by a factor of approx. 104. The detection limits for this method in water and wastewater samples were reported to be 0.5 mg L^{-1} NO_3^-, using laboratory solutions of nitrate. The range within which nitrate could be detected was 1-10,000 mg L^{-1} in water, and 1-100 mg L^{-1} in wastewater. A reduction in nitrate signal intensity was seen in the presence of interfering anions, which was dependent on the concentration of the anions. As the nitrite signal was found to be too weak to be detected in the presence of interfering anions, this method is unsuitable for nitrite detection in water systems.[95] This sensor has not been automated. The method is advantageous for deployment as no waste is generated, and

sample pre-treatment is not required. The sample is simply air dried at room temperature onto the gold surface. SERS detection is rapid, taking 15 minutes from time of sampling to completion of analysis for 9 samples loaded on one substrate.

Table 2.4. Recent approaches to nitrate sensing showing LOD and linear range, and whether the sensor was automated or tested for water monitoring.

Transduction method	Ref.	Characteristics	LOD	Linear range	Autonomous	Tested
Electrochemical	[91]	The iNits sensor - a three electrode nitrate microsensor coupled with a miniaturised, portable potentiostat, where the current produced by the reduction of nitrate using cyclic voltammetry is measured. This was integrated with a wireless network, allowing for commands to be sent to the sensor, and also for data to be collected.	0.4 µM	5-500 µM, 500 µM-50 mM	Yes	No
	[94]	A sequential injection analysis system incorporating a microfluidic chip with an embedded ion selective electrode (ISE) for detection. Applied to the measurement of nitrate in environmental water samples. Approx.	7.0×10^{-6} M	1.0×10^{-5} - 1.0×10^{-1} M	Yes	No

	12 samples per hour. Low reagent and sample volumes and automated operation.				
[96]	A sequential injection analysis technique for continuous nitrate determination using a three-electrode-system (Pt–Pt–Ag/AgCl), in which the Pt working electrode was modified with renewable copper nano-clusters. The developed system was used to detect nitrate in real freshwater samples. The continuous renewal of copper sensing material on the working-electrode surface meant that each measurement was performed on a fresh copper surface, allowing for continuous nitrate determination for long term operations.	Not stated	Up to 12.1 mg L^{-1}	Yes	No
[92]	A self-contained instrument that operates autonomously, with measurement, calibration, fluidic control and acquisition triggers.	$>10^{-6}$ M	Millimolar range	Yes	a, c

		Experimental validation was performed on an automated monitoring platform on lake Greifensee (Switzerland) using potentiometric sensors selective for nitrate, and also for hydrogen ions, carbonate, calcium and ammonium. The sensor alternated between calibration mode and experiment mode, allowing for a two point calibration before and after profiling. While the measurement range was high, the system integration was impressive.				
Colouri-metric	[97]	The CMAS analysis system is a portable centrifugal microfluidic system for on-site measurement of nitrite. Required manual loading of sample. Wet chemistry based analysis using Griess reagent to form coloured species. Absorbance measurements made at 540 nm with a paired emitter detector diode (PEDD).	9.31 µg L^{-1}	89 – 1,200 µg L^{-1}	No	No

	[98]	This autonomous nitrate and nitrite microfluidic analyser was deployed in an estuarine environment. The microfluidic chip allows for mixing of water sample and reagents to perform the Griess method for nitrite quantitation. A cadmium tube was incorporated for nitrate reduction to nitrite. Absorbance measurements were recorded within the microfluidic chip using a 525 nm LED and photodiode.	0.0016 mg NO_3^- L^{-1} 0.00092 mg NO_2^- L^{-1}	Up to 21.7 mg L^{-1}	Yes	a, b, c
	[99]	This injection flow analysis system uses a micro column containing zinc granules to reduce nitrate to nitrite. Nitrite is then quantified using the Griess reagent followed by absorbance measurements at 520 nm using an LED and photodiode. The sensor was tested on-board a ship, carrying out over 3000 measurements.	1.3 µg NO_3^--N L^{-1}	3-700 µg NO_3^--N L^{-1}	Yes	a, b, c
	[100]	An automated system for nitrate, nitrite and	0.0207	0.14-1.82	Yes	No

	sulphate measurements based on sequential injection analysis. Nitrite is measured using the Griess method, while nitrate is reduced to nitrite using a cadmium column, with subsequent determination in the same way. Sulphate is measured turbidimetrically.	mg NO_3^- L^{-1} 0.0022 mg NO_2^- L^{-1}	mg NO_3^- L^{-1} 0.01-0.42 mg NO_2^- L^{-1}		
[101], [102]	A fully integrated nitrate sensing platform based on a modified chromotropic method, with a sample inlet with filter, storage units for reagent and standards for self-calibration, pumping system, a microfluidic mixing and detection chip, and waste storage, and waterproof housing. The optical detection system consists of a LED light source with a photodiode detector. Reagent stability of up to 6 months is reported. This was applied to the analysis of standards in deionised water and seawater matrices.	0.70 mg NO_3^- L^-	0.9 – 80 mg NO_3^- L^-	Yes	No

Ultraviolet	[103]	A flow system consisting of a peristaltic pump and a single-reflection flow-through cell for the measurement of nitrate. Total nitrogen was quantified by using alkaline peroxodisulfate photo-digestion with an ultra-violet photo-reactor, a hollow-fibre filter and a debubbler in the flow system. The nitrate system featured a data acquisition time of 1.5 s per spectrum. Total nitrogen had a throughput of 5 samples per hour.	0.04 mg NO_3^--N L^{-1} 0.05 mg N L^{-1}	0–2.0 mg NO_3^--N L^{-1} 0–2.0 mg N L^{-1}	Yes	No
Fluore-scence	[104]	An aggregation-induced emission fluorescent probe for detection of trace nitrite and nitrate ions in water. The probe, a monoamine of tetraphenylethylene, spontaneously detects nitrites (or nitrates) by a fluorescence “turn-off” method via diazotization followed by formation of a non-fluorescent TPE-azodye. Nitrate must be reduced to nitrite using zinc powder before it is detected. The sensor was used to measure	$6x10^{-7}$ M NO_2^-	Below micro-molar range	No	No

	real samples from sources such as rivers, paddy fields, and aquaria.				
[105]	A hyperbranched polyethyleneimine protected silver nanocluster based nanosensor for nitrite detection. Firstly, nitrite reacts with hydrogen peroxide to generate peroxynitrous acid. This induces aggregation and fluorescence quenching of the nanoclusters. The sensor was used to measure lake water, tap water and seawater samples.	100 nM	Up to 7 µM	No	No
[106]	Graphene oxide (GO) was used for detection of nitrite and nitrate. The GO was synthesized via an improved Hummers' method. The emission sites of the GO were monitored at 567 nm, which corresponded to the oxygen functional groups. Both nitrite and nitrate ions resulted in fluorescence quenching of the GO.	Not stated	1-10 mM	No	No

[a] Tested in freshwater; [b] Tested in saltwater; [c] Long term deployment

2.5 Commercial Nitrate Sensors

There are numerous commercial nitrate sensors capable of autonomous monitoring available. Table 2.5 shows five of these commercially available nitrate sensors, comparing the limit of detection, range, accuracy and operating principle.

YSI do not state the LOD of their ISE on their website. One publication showed the YSI sensor to have an LOD of 142.5 µM.91 Similarly, it is not stated for ISUS V3, however an LOD from older literature stated that it was approx. 1.5 µM.89 These sensors are currently expensive, meaning that their incorporation into sensor networks is not feasible.

Table 2.5. Specifications of five commercial nitrate sensors.

Sensor	LOD	Range	Accuracy	Operating principle
YSI 6884 [107]	Not stated	0-200 mg NO_3^- L^{-1}	±10%	Ion selective electrode
SUNA V2 [108]	0.007 mg N L^{-1} using a 10 mm path length	Up to 42 mg N L^{-1}	±10%	UV absorbance
	0.0028 mg N L^{-1} using a 5 mm path length (for high turbidity)	Up to 56 mg N L^{-1}		
ISUS V3 [109]	Not stated	0.007 to 28 mg N L^{-1}	±10%	UV absorbance

EcoLAB 2[110]	Not stated	0-5 mg NO_3^- L^{-1}	Not stated	Wet colourimetric method
Systea WIZ probe[111]	0.02 µM	0-1000 ppb NO_2^-	Not stated	Wet colourimetric method

2.6 Conclusions

Commercially available nutrient sensors for water are currently high in cost, making them impractical for use in farming, environmental monitoring or research applications, where large scale sensor networks are required. The spatial resolution of data is dependent on the cost per sensor, making it a key consideration for sensor development. Low-cost nutrient sensors from the literature have been described in this review, as well as some commercial sensors and some novel approaches to nutrient monitoring. A low limit of detection is essential for these sensors to be applicable in environmental monitoring. Achieving a limit of detection comparable to those of the expensive commercial sensors is challenging, however, it has been achieved by some of the sensors described.

The prospects of further reductions in cost and LOD make this an exciting field for researchers to work in. The research for fluorescence and electrochemical sensors is quite focused on method improvement, while methods such as colourimetric and UV detection have been automated into deployable sensors for almost two decades. The incorporation of microfluidic technology and low-cost fluidic handling components and detection systems has made these systems excellent contenders in the race to produce the next generation of nutrient sensors.

Notes and references

[a] *Water Institute, School of Chemical Sciences, Dublin City University, Dublin, Ireland.*

1. A. E. Greenberg, L. S. Clesceri, A. D. Eaton. *Standard Methods for the Examination of Water and Wastewater.* 18th ed. 1992.
2. G. C. Gerloff. *Nutritional ecology of nuisance aquatic plants.* 1975.
3. J. Heisler, P.M. Glibert, J.M. Burkholder, D.M. Anderson, W. Cochlan, W.C. Dennison, Q. Dortch, C.J. Gobler, C.A. Heil, E. Humphries, A. Lewitus, R. Magnien, H.G. Marshall, K. Sellner, D.A. Stockwell, D.K. Stoecker, M. Suddleson, Eutrophication and harmful algal blooms: A scientific consensus, Harmful Algae. 8 (2008) 3–13. doi:10.1016/j.hal.2008.08.006.
4. V.H. Smith, Eutrophication of freshwater and coastal marine ecosystems: a global problem, Environ. Sci. Pollut. Res. Int. 10 (2003) 126–139. doi:10.1065/espr2002.12.142.
5. R.J. Diaz, R. Rosenberg, Spreading dead zones and consequences for marine ecosystems, Science, 321 (2008) 926–929. doi:10.1126/science.1156401.
6. F.M. Van Dolah, Marine Algal Toxins: Origins, Health Effects, and Their Increased Occurrence, Environ. Health Perspect. 108 (2000) 133–141. doi:10.1289/ehp.00108s1143.
7. D.W. Schindler, The dilemma of controlling cultural eutrophication of lakes, Proc. R. Soc. B Biol. Sci. 279 (2012) 4322–4333. doi:10.1098/rspb.2012.1032.
8. J. Buffle, G. Horvai. *In-Situ Monitoring of Aquatic Systems: Chemical Analysis and Speciation*, 6th ed, 2000. Chichester: John Wiley & Sons, LTD.

9. E. Bagshaw, A. Beaton, J. Wadham, M. Mowlem, J.Hawkings, M.Tranter, Chemical sensors for in situ data collection in the cryosphere, Trends Anal. Chem. 82 (2016) 348-357.
10. C. Warwick, A. Guerreiro, A. Soares, Sensing and analysis of soluble phosphates in environmental samples: A review, Biosens. Bioelectron. 41 (2013) 1-11.
11. A. T. Law Al, S. B. Adeloju, Progress and recent advances in phosphate sensors: A review, Talanta. 114 (2013) 191-203.
12. C.D.M. Campos, J.A.F. da Silva, Applications of autonomous microfluidic systems in environmental monitoring, RSC Adv. 3 (2013) 18216-18227.
13. Council Directive 91/676/EE of 12 December 1991 concerning the protection of waters against pollution caused by nitrates from agricultural sources, available at: http://eur-lex.europa.eu/legal-content/en/ALL/?uri=CELEX:31991L0676 (accessed 13/05/17)
14. C.M. McGraw, S.E. Stitzel, J. Cleary, C. Slater, D. Diamond, Autonomous microfluidic system for phosphate detection, Talanta. 71 (2007) 1180–1185. doi:10.1016/j.talanta.2006.06.011.
15. Directive 2000/60/EC of the European Parliament and of the Council of 23 October 2000 establishing a framework for Community action in the field of water policy Official Journal L 327 , 22/12/2000 P. 0001 – 0073.
16. P. P. Quevauviller, P. Roose and G. Verreet, *eds. Chemical marine monitoring: policy framework and analytical trends. Vol. 28. John Wiley & Sons, 2011.*
17. T. Saeed, G. Sun, A review on nitrogen and organics removal mechanisms in subsurface flow constructed wetlands: Dependency on environmental parameters, operating conditions and supporting media, J. Environ. Manage. 112 (2012) 429–448. doi:10.1016/j.jenvman.2012.08.011.

18. D.M. Manassaram, L.C. Backer, R. Messing, L.E. Fleming, B. Luke, C.P. Monteilh, Nitrates in drinking water and methemoglobin levels in pregnancy: a longitudinal study., Environ. Heal. 9 (2010) 60. doi:10.1186/1476-069X-9-60.
19. M. Badea, A. Amine, G. Palleschi, D. Moscone, G. Volpe, A. Curulli, New electrochemical sensors for detection of nitrites and nitrates, J. Electroanal. Chem. 509 (2001) 66–72. doi:10.1016/S0022-0728(01)00358-8.
20. S.M. Gray, P.S. Ellis, M.R. Grace, I.D. McKelvie, Spectrophotometric Determination of Ammonia in Estuarine Waters by Hybrid Reagent-Injection Gas-Diffusion Flow Analysis, Spectrosc. Lett. 39 (2006) 737–753. doi:10.1080/00387010600934766.
21. D. Senthamilselvan, A. Cheznian, Ammonia Induced Biochemical Changes on the Muscle Tissue of the Fish Cyprinus carpio FT-IR Study, Res. J. Environ. Toxicol. 8 (2014) 117–123. doi:10.3923/rjet.2014.117.123.
22. Guidelines for drinking-water quality, 2nd ed. Vol. 2. Health criteria and other supporting information. World Health Organization, Geneva, 1996. Available at: http://apps.who.int/iris/handle/10665/38551 (accessed 13/05/17)
23. M.B. Young, K. McLaughlin, C. Kendall, W. Stringfellow, M. Rollog, K. Elsbury, E. Donald, A. Paytan, Characterizing the Oxygen Isotopic Composition of Phosphate Sources to Aquatic Ecosystems, Environ. Sci. Technol. 43 (2009) 5190–5196.
24. J. Cleary, C. Slater, C. McGraw, D. Diamond, An autonomous microfluidic sensor for phosphate: On-site analysis of treated wastewater, IEEE Sens. J. 8 (2008) 508–515. doi:10.1109/JSEN.2008.918259.
25. F.E. Legiret, V.J. Sieben, E.M.S. Woodward, S.K. Abi Kaed Bey, M.C. Mowlem, D.P. Connelly, E.P. Achterberg, A high performance

microfluidic analyser for phosphate measurements in marine waters using the vanadomolybdate method, Talanta. 116 (2013) 382–387. doi:10.1016/j.talanta.2013.05.004.

26. D. Thouron, R. Vuillemin, X. Philippon, A. Lourenço, C. Provost, A. Cruzado, V. Garçon, An autonomous nutrient analyzer for oceanic long-term in situ biogeochemical monitoring, Anal. Chem. 75 (2003) 2601–2609. doi:10.1021/ac020696+.

27. Sea-Bird Sientific HydroCycle-PO_4 data sheet 'In situ dissolved phosphate' 2017. Available at: http://wetlabs.com/hydrocycle (accessed 30/04/17)

28. E. Taylor, J. Bonner, R. Nelson, C. Fuller, W. Kirkey, S. Cappelli, Development of an in-situ total phosphorus analyzer, Ocean. MTS/IEEE Washingt. (2016) 1–4. doi:10.23919/OCEANS.2015.7404384

29. R.D. Prien, The future of chemical in situ sensors, Mar. Chem. 107 (2007) 422–432. doi:10.1016/j.marchem.2007.01.014.

30. Hach® "SL1000 Portable Parallel Analyzer™ (PPA)", Available at: www.hach.com/sl1000-portable-parallel-analyzer-ppa/product?id=22361943508 (accessed on 20/05/17)

31. J.M. Ottino, S. Wiggins, Introduction: mixing in microfluidics, Philos. Trans. R. Soc. London A. 362 (2004) 923–935. doi:10.1098/rsta.2003.1355.

32. Cleary, John and Maher, Damien and Diamond, Dermot (2013) Development and deployment of a microfluidic platform for water quality monitoring. In: Mukhopadhyay, Subhas C. and Mason, Alex, (eds.) Smart Sensors for Real-Time Water Quality Monitoring. Smart Sensors, Measurement and Instrumentation. Springer-Verlag, Berlin Heidelberg 2013, pp. 125-148. ISBN 978-3-642-37005-2

33. C. Lochovsky, S. Yasotharan, A. Günther, Bubbles no more: in-plane trapping and removal of bubbles in microfluidic devices, Lab Chip. 12 (2012) 595–601. doi:10.1039/c1lc20817a.
34. A.M. Skelley, J. Voldman, An active bubble trap and debubbler for microfluidic systems, Lab Chip. 8 (2008) 1733–1737. doi:10.1039/b807037g.
35. J.C. Jokerst, J.M. Emory, C.S. Henry, Advances in microfluidics for environmental analysis, Analyst. 1 (2012) 24-34.
36. H. Zia, N.R. Harris, G. V. Merrett, M. Rivers, N. Coles, The impact of agricultural activities on water quality: A case for collaborative catchment-scale management using integrated wireless sensor networks, Comput. Electron. Agric. 96 (2013) 126–138. doi:10.1016/j.compag.2013.05.001.
37. J. V. Capella, A. Bonastre, R. Ors, M. Peris, In line river monitoring of nitrate concentration by means of a Wireless Sensor Network with energy harvesting, Sensors Actuators, B Chem. 177 (2013) 419–427. doi:10.1016/j.snb.2012.11.034.
38. P. Rajalakshmi, S.D. Mahalakshmi, IOT Based Crop-Field Monitoring And Irrigation Automation, 10th Int. Conf. Intell. Syst. Control. (2016) 1–6. doi:10.1109/ISCO.2016.7726900.
39. M.H. Memon, W. Kumar, A.R. Memon, M. Aamir, P. Kumar, Internet of Things (IoT) Enabled Smart Animal Farm, Int. Conf. Comput. Sustain. Glob. Dev. 7 (2016) 2067–2072.
40. AZoNanotechnology Article: “Precision Agriculture - Nanotech Methods Used, Such as ‘Smart Dust’, Smart Fields’ and Nanosensors:” Available at: http://www.azonano.com/article.aspx?ArticleID=1318 (accessed on 30/04/17)
41. R. Repas, Sensor Sense: IP ratings for sensors, Machine Design: Technologies, available at:

http://www.machinedesign.com/technologies/sensor-sense-ip-ratings-sensors (accessed 13/05/17)

42. A.A. Baykov, O.A. Evtushenko, S.M. Avaeva, A malachite green procedure for orthophosphate determination and its use in alkaline phosphatase-based enzyme immunoassay, Anal. Biochem. 171 (1988) 266–270. doi:10.1016/0003-2697(88)90484-8.
43. M.B. Silva, S.S. Borges, S.R.W. Perdigão, B.F. Reis, Green Chemistry–Sensitive Analytical Procedure for Photometric Determination of Orthophosphate in River and Tap Water by Use of a Simple LED-Based Photometer, Spectrosc. Lett. 42 (2009) 356–362. doi:10.1080/00387010903185744.
44. L.J. Gimbert, P.M. Haygarth, P.J. Worsfold, Determination of nanomolar concentrations of phosphate in natural waters using flow injection with a long path length liquid waveguide capillary cell and solid-state spectrophotometric detection, Talanta. 71 (2007) 1624–1628. doi:10.1016/j.talanta.2006.07.044.
45. O. Tue-Ngeun, P. Ellis, I.D. McKelvie, P. Worsfold, J. Jakmunee, K. Grudpan, Determination of dissolved reactive phosphorus (DRP) and dissolved organic phosphorus (DOP) in natural waters by the use of rapid sequenced reagent injection flow analysis, Talanta. 66 (2005) 453–460. doi:10.1016/j.talanta.2004.12.032.
46. T. Uemura, T. Ogusu, M. Takeuchi, H. Tanaka, Spectrophotometric determination of trace phosphate ions by amplitude-modulated flow analysis coupled with malachite green method., Anal. Sci. 26 (2010) 797–801.
47. K.L. Linge, C.E. Oldham, Interference from arsenate when determining phosphate by the malachite green spectrophotometric method, Anal. Chim. Acta. 450 (2001) 247–252. doi:10.1016/S0003-2670(01)01388-5.

48. J. Jońca, W. Giraud, C. Barus, M. Comtat, N. Striebig, D. Thouron, V. Garçon, Reagentless and silicate interference free electrochemical phosphate determination in seawater, Electrochim. Acta. 88 (2013) 165–169. doi:10.1016/j.electacta.2012.10.012.
49. P.J. Bresnahan, T.R. Martz, Y. Takeshita, K.S. Johnson, M. LaShomb, Best practices for autonomous measurement of seawater pH with the Honeywell Durafet, Methods Oceanogr. 9 (2014) 44–60. doi:10.1016/j.mio.2014.08.003.
50. C. Fay, C. Slater, R. Buda, Sandra Teodora Shepherd, B. Corcoran, O.N. E., G.G. Wallace, A. Radu, D. Diamond, Wireless ion selective electrode autonomous sensing system, IEEE Sens. J. 11 (2011) 2374–2382.
51. S. Di Carlo and M. Falasconi (2012). Drift Correction Methods for Gas Chemical Sensors in Artificial Olfaction Systems: Techniques and Challenges, Advances in Chemical Sensors, Prof. Wen Wang (Ed.), ISBN: 978-953- 307-792-5, InTech, Available from: http://www.intechopen.com/books/advances-in-chemical-sensors/drift- correction-methods-for-gas-chemical-sensors-in-artificial-olfaction-systems-techniques-and-cha
52. S. Berchmans, T.B. Issa, P. Singh, Determination of inorganic phosphate by electroanalytical methods: A review, Anal. Chim. Acta. 729 (2012) 7–20. doi:10.1016/j.aca.2012.03.060.
53. Y. Song, C. Bian, Y. Li, J. Tong, S. Xia, Electrochemical Determination of Phosphate in Freshwater Free of Silicate Interference, J. Biomed. Sci. 5 (2016) 1–7.
54. Y. Song, C. Bian, J. Tong, Y. Li, S. Xia, Selective electrochemical sensor for phosphate determination toward a silicate interference free method in freshwater, Sensors, 2015 IEEE. (2015) 1–4. doi:10.1109/ICSENS.2015.7370477.

55. A. V. Kolliopoulos, D.K. Kampouris, C.E. Banks, Rapid and Portable Electrochemical Quantification of Phosphorus, Anal. Chem. 87 (2015) 4269–4274. doi:10.1021/ac504602a.
56. J. Jońca, V. León Fernández, D. Thouron, A. Paulmier, M. Graco, V. Garçon, Phosphate determination in seawater: Toward an autonomous electrochemical method, Talanta. 87 (2011) 161–167. doi:10.1016/j.talanta.2011.09.056.
57. Y. Bai, J. Tong, C. Bian, S. Xia, An electrochemical microsensor based on molybdophosphate complex for fast determination of total phosphorus in water, in: 8th Annu. IEEE Int. Conf. Nano/Micro Eng. Mol. Syst., 2013: pp. 41–44. doi:10.1109/NEMS.2013.6559678.
58. Y. Bai, J. Tong, J. Wang, C. Bian, S. Xia, Electrochemical microsensor based on gold nanoparticles modified electrode for total phosphorus determinations in water, IET Nanobiotechnology. 8 (2014) 31–36. doi:10.1049/iet-nbt.2013.0041.
59. L. Hsu, P.R. Selvaganapathy, Stable and reusable electrochemical sensor for continuous monitoring of phosphate in water, IEEE SENSORS 2014 Proc. (2014) 1423–1426. doi:10.1109/ICSENS.2014.6985280.
60. C. Warwick, A. Guerreiro, A. Gomez-Caballero, E. Wood, J. Kitson, J. Robinson, A. Soares, Conductance based sensing and analysis of soluble phosphates in wastewater, Biosens. Bioelectron. 52 (2014) 173–179. doi:10.1016/j.bios.2013.08.048.
61. C. Warwick, A. Guerreiro, E. Wood, J. Kitson, J. Robinson, A. Soares, A molecular imprinted polymer based sensor for measuring phosphate in wastewater samples, Water Sci. Technol. 69 (2014) 48–54. doi:10.2166/wst.2013.550.
62. S. Cinti, D. Talarico, G. Palleschi, D. Moscone, F. Arduini, Novel reagentless paper-based screen-printed electrochemical sensor to

detect phosphate, Anal. Chim. Acta. 919 (2016) 78–84. doi:10.1016/j.aca.2016.03.011.

63. M. Fiedoruk, D.J. Cocovi-Solberg, Ł. Tymecki, R. Koncki, M. Miró, Hybrid flow system integrating a miniaturized optoelectronic detector for on-line dynamic fractionation and fluorometric determination of bioaccessible orthophosphate in soils, Talanta. 133 (2015) 59–65. doi:10.1016/j.talanta.2014.05.063.
64. M. Fiedoruk-Pogrebniak, R. Koncki, Multicommutated flow analysis system based on fluorescence microdetectors for simultaneous determination of phosphate and calcium ions in human serum, Talanta. 144 (2015) 184–188. doi:10.1016/j.talanta.2015.06.001.
65. V. Borse, P. Jain, M. Sadawana, R. Srivastava, “Turn-on” fluorescence assay for inorganic phosphate sensing, Sensors Actuators, B Chem. 225 (2016) 340–347. doi:10.1016/j.snb.2015.11.054.
66. T.K. Ghorpade, M. Patri, S.P. Mishra, Highly sensitive colorimetric and fluorometric anion sensors based on mono and di-calix[4]pyrrole substituted diketopyrrolopyrroles, Sensors Actuators, B Chem. 225 (2016) 428–435. doi:10.1016/j.snb.2015.10.067.
67. S. Zhuo, L. Chen, Y. Zhang, G. Jin, Luminescent phosphate sensor based on upconverting graphene quantum dots, Spectrosc. Lett. 49 (2016) 1–4. doi:10.1080/00387010.2015.1023957.
68. H. Cao, Z. Chen, Y. Huang, Copper nanocluster coupling europium as an off-to-on fluorescence probe for the determination of phosphate ion in water samples., Talanta. 143 (2015) 450–456. doi:10.1016/j.talanta.2015.05.024.
69. M. Fiedoruk, E. Mieczkowska, R. Koncki, Ł. Tymecki, A bimodal optoelectronic flow-through detector for phosphate determination, Talanta. 128 (2014) 211–214. doi:10.1016/j.talanta.2014.04.086.
70. Q. Meng, Y. Wang, M. Yang, R. Zhang, R. Wang, Z. Zhang, A new fluorescent chemosensor for highly selective and sensitive detection

of inorganic phosphate (Pi) in aqueous solution and living cells, RSC Adv. 5 (2015) 53189–53197. doi:10.1039/C5RA08712K.

71. L. Kröckel, H. Lehmann, T. Wieduwilt, M.A. Schmidt, Fluorescence detection for phosphate monitoring using reverse injection analysis, Talanta. 125 (2014) 107–113. doi:10.1016/j.talanta.2014.02.072.
72. R.B.R. Mesquita, M.T.S.O.B. Ferreira, I. V Tóth, A.A. Bordalo, I.D. Mckelvie, A.O.S.S. Rangel, Development of a flow method for the determination of phosphate in estuarine and freshwaters — Comparison of flow cells in spectrophotometric sequential injection analysis, Anal. Chim. Acta. 701 (2011) 15–22. doi:10.1016/j.aca.2011.06.002.
73. R. Liu, R. Ishimatsu, M. Yahiro, C. Adachi, K. Nakano, T. Imato, Photometric flow injection determination of phosphate on a PDMS microchip using an optical detection system assembled with an organic light emitting diode and an organic photodiode, Talanta. 132 (2015) 96–105. doi:10.1016/j.talanta.2014.08.057.
74. J. Tong, C. Bian, Y. Li, Y. Bai, Design of a MEMS-based total phosphorus sensor with a microdigestion system, 4th Int. Conf. Bioinforma. Biomed. Eng. (2010) 1–4. doi:10.1109/ICBBE.2010.5515051.
75. C. Frank, F. Schroeder, R. Ebinghaus, W. Ruck, A fast sequential injection analysis system for the simultaneous determination of ammonia and phosphate, Microchim. Acta. 154 (2006) 31–38. doi:10.1007/s00604-006-0496-y.
76. C. Frank, F. Schroeder, R. Ebinghaus, W. Ruck, Using sequential injection analysis for fast determination of phosphate in coastal waters, Talanta. 70 (2006) 513–517. doi:10.1016/j.talanta.2005.12.055.
77. H. Fiehn, S. Howitz, M.T. Pham, T. Vopel, M. Burger, T. Wegner, (1995) Components and technology for a fluidic-ISFET-microsystem.

In: A.V.d. Berg and P. Bergfeld (eds): Micro Total Analysis Systems. Dordrecht: Kluver Academic Publ., The Netherlands, pp 289–294.

78. R. N. C. Daykin and S. J. Haswell, Development of a micro flow injection manifold for the determination of orthophosphate, *Anal. Chim. Acta*, 1995, 313, 155–159.
79. G.M. Greenway, S.J. Haswell, P.H. Petsul, Characterisation of a micro-total analytical system for the determination of nitrite with spectrophotometric detection, Anal. Chim. Acta. 387 (1999) 1–10. doi:10.1016/S0003-2670(99)00047-1.
80. P.H. Petsul, G.M. Greenway, S.J. Haswell, The development of an on-chip micro-flow injection analysis of nitrate with a cadmium reductor, Anal. Chim. Acta. 428 (2001) 155–161. doi:10.1016/S0003-2670(00)01244-7.
81. C. Slater, J. Cleary, C.M. McGraw, W.S. Yerazunis, K.T. Lau, D. Diamond, Autonomous field-deployable device for the measurement of phosphate in natural water, Roc. SPIE 6755, Adv. Environ. Chem. Biol. Sens. Technol. (2007). doi:10.1117/12.733754.
82. M. Bowden, D. Diamond, The determination of phosphorus in a microfluidic manifold demonstrating long-term reagent lifetime and chemical stability utilising a colorimetric method, Sensors Actuators, B Chem. 90 (2003) 170–174. doi:10.1016/S0925-4005(03)00024-8.
83. D. Thouron, R. Vuillemin, X. Philippon, A. Lourenço, C. Provost, A. Cruzado, V. Garçon, An autonomous nutrient analyzer for oceanic long-term in situ biogeochemical monitoring, Anal. Chem. 75 (2003) 2601–2609. doi:10.1021/ac020696+.
84. A.J. Lyddy-Meaney, P.S. Ellis, P.J. Worsfold, E.C. V Butler, I.D. McKelvie, A compact flow injection analysis system for surface mapping of phosphate in marine waters, Talanta. 58 (2002) 1043–1053. doi:10.1016/S0039-9140(02)00428-9.

85. L.A. Zimmer, G.A. Cutter, High resolution determination of nanomolar concentrations of dissolved reactive phosphate in ocean surface waters using long path liquid waveguide capillary cells (LWCC) and spectrometric detection, Limnol. Oceanogr. Methods. 10 (2012) 568–580. doi:10.4319/lom.2012.10.568.
86. WET Labs. *Case Studies of WET Labs' Cycle-PO4: Simple and Reliable Nutrient Monitoring.* 2013. Available at: http://wetlabs.com/news/case-studies-wet-labs-cycle-po4-simple-and-reliable-nutrient-monitoring (accessed on: 07/05/17)
87. Alliance for Coastal Technologies. *Performance Demonstration Statement; WET Labs Cycle-P Nutrient Analyzer*. 2008. Available at: http://drum.lib.umd.edu/bitstream/handle/1903/13730/[UMCES]CBL%2008-042.pdf;jsessionid=AAE9C76E33E14B825BE2439574C63CF6?sequence=3 (accessed 07/05/17)
88. M.S. Finch, D.J. Hydes, C.H. Clayson, B. Weigl, J. Dakin, P. Gwilliam, A low power ultra violet spectrophotometer for measurement of nitrate in seawater: Introduction, calibration and initial sea trials, Anal. Chim. Acta. 377 (1998) 167–177. doi:10.1016/S0003-2670(98)00616-3.
89. K.S. Johnson, L.J. Coletti, In situ ultraviolet spectrophotometry for high resolution and long-term monitoring of nitrate, bromide and bisulfide in the ocean, Deep. Res. Part I Oceanogr. Res. Pap. 49 (2002) 1291–1305. doi:10.1016/S0967-0637(02)00020-1.
90. A.D. Beaton, C.L. Cardwell, R.S. Thomas, V.J. Sieben, F.-E. Legiret, E.M. Waugh, P.J. Statham, M.C. Mowlem, H. Morgan, Lab-on-chip measurement of nitrate and nitrite for in situ analysis of natural waters, Environ. Sci. Technol. 46 (2012) 9548–9556. doi:10.1021/es300419u.

91. M.R. Gartia, B. Braunschweig, T.-W. Chang, P. Moinzadeh, B.S. Minsker, G. Agha, A. Wieckowski, L.L. Keefer, G.L. Liu, The microelectronic wireless nitrate sensor network for environmental water monitoring., J. Environ. Monit. 14 (2012) 3068–3075. doi:10.1039/c2em30380a.
92. N. Pankratova, G.A. Crespo, M.G. Afshar, M.C. Crespi, S. Jeanneret, T. Cherubini, M.-L. Tercier-Waeber, F. Pomati, E. Bakker, Potentiometric sensing array for monitoring aquatic systems, Environ. Sci. Process. Impacts. 17 (2015) 906–914. doi:10.1039/C5EM00038F.
93. N.W. Barnett, C.E. Lenehan, S.W. Lewis, Sequential injection analysis: an alternative approach to process analytical chemistry, Trends Anal. Chem. 18 (1999) 346–353.
94. B. Tossanaitada, T. Masadome, T. Imato, Sequential injection analysis of nitrate ions using a microfluidic polymer chip with an embedded ion-selective electrode, Anal. Methods. (2012) 4384–4388. doi:10.1039/c2ay25882j.
95. S. Gajaraj, C. Fan, M. Lin, Z. Hu, Quantitative detection of nitrate in water and wastewater by surface-enhanced Raman spectroscopy, Environ. Monit. Assess. 185 (2013) 5673–5681. doi:10.1007/s10661-012-2975-4.
96. Y. Li, H. Li, Y. Song, H. Lu, J. Tong, C. Bian, J. Sun, S. Xia, An Electrochemical Sensor System With Renewable Copper Nano-Clusters Modified Electrode for Continuous Nitrate Determination, IEEE Sens. J. 16 (2016) 8807–8814. doi:10.1109/JSEN.2016.2582038.
97. M. Czugala, D. Maher, F. Collins, R. Burger, F. Hopfgartner, Y. Yang, J. Zhaou, J. Ducrée, A. Smeaton, K.J. Fraser, F. Benito-Lopez, D. Diamond, CMAS: fully integrated portable centrifugal microfluidic analysis system for on-site colorimetric analysis, RSC Adv. 3 (2013) 15928–15938. doi:10.1039/c3ra42975j.

98. A.D. Beaton, C.L. Cardwell, R.S. Thomas, V.J. Sieben, F.-E. Legiret, E.M. Waugh, P.J. Statham, M.C. Mowlem, H. Morgan, Lab-on-chip measurement of nitrate and nitrite for in situ analysis of natural waters, iron. Sci. Technol. 46 (2012) 9548–9556. doi:10.1021/es300419u.
99. P.S. Ellis, A.M.H. Shabani, B.S. Gentle, I.D. Mckelvie, Field measurement of nitrate in marine and estuarine waters with a flow analysis system utilizing on-line zinc reduction, Talanta. 84 (2011) 98–103. doi:10.1016/j.talanta.2010.12.028.
100. A. Ayala, L.O. Leal, L. Ferrer, V. Cerdà, Multiparametric automated system for sulfate , nitrite and nitrate monitoring in drinking water and wastewater based on sequential injection analysis, Microchem. J. 100 (2012) 55–60. doi:10.1016/j.microc.2011.09.004.
101. D. Cogan, C. Fay, D. Boyle, C. Osborne, N. Kent, J. Cleary, D. Diamond, Development of a Low Cost Microfluidic Sensor for the Direct Determination of Nitrate Using Chromotropic Acid in Natural Waters, Anal. Methods. 7 (2015) 5396–5405. doi:10.1039/C5AY01357G.
102. D. Cogan, J. Cleary, T. Phelan, E. McNamara, M. Bowkett, D. Diamond, Integrated flow analysis platform for the direct detection of nitrate in water using a simplified chromotropic acid method, Anal. Methods. 5 (2013) 4798–4804. doi:10.1039/c3ay41098f.
103. B.S. Gentle, P.S. Ellis, M.R. Grace, I.D. Mckelvie, Flow analysis methods for the direct ultra-violet spectrophotometric measurement of nitrate and total nitrogen in freshwaters, Anal. Chim. Acta. 704 (2011) 116–122. doi:10.1016/j.aca.2011.07.048.
104. A. Chatterjee, D.G. Khandare, P. Saini, A. Chattopadhyay, M.S. Majik, M. Banerjee, Amine functionalized tetraphenylethylene: a novel aggregation-induced emission based fluorescent

chemodosimeter for nitrite and nitrate ions, RSC Adv. 5 (2015) 31479–31484. doi:10.1039/C4RA14765K.

105. C. Chen, Z. Yuan, H.-T. Chang, F. Lu, Z. Li, C. Lu, Silver nanoclusters as fluorescent nanosensors for selective and sensitive nitrite detection, (n.d.). doi:10.1039/c6ay00214e.

106. I.H. Tang, R. Sundari, H.O. Lintang, L. Yuliati, Detection of nitrite and nitrate ions in water by graphene oxide as a potential fluorescence sensor, IOP Conf. Ser. Mater. Sci. Eng. 107 (2016) 12027. doi:10.1088/1757-899X/107/1/012027.

107. YSI, a xylem brand 2010. *6-series multiparameter water quality sondes*. Available at: https://www.ysi.com/accessory/id-6884/6884-nitrate-ise-sensor (accessed 30/04/17)

108. SeaBird Scientific datasheet 'SUNA V2 UV Nitrate Sensor', 2017. Available at: http://satlantic.com/suna?qt-product_tabs=4#qt-product_tabs (accessed 30/04/17)

109. SeaBird Scientific datasheet 'ISUS V3 Nitrate Sensor', 2012. Available from: http://satlantic.com/sites/default/files/documents/2015_datasheet_isusv3.pdf (accessed 30/04/17)

110. EnviroTech Instruments 'EcoLab 2 – Multi-Channel Analyzer System'. Available from: http://www.labtech.com.mx/files/ecolab_2.pdf (accessed 13/05/17)

111. Systea brochure 'WIZ portable in-situ probe for water analysis' 2017. Available from: http://www.systea.it/index.php?option=com_k2&view=item&layout=item&id=293&Itemid=244&lang=en (accessed 30/04/17)

“We are the cosmos made conscious and life is the means by which the universe understands itself.”

Brian Cox

Chapter 3:
PhosphaSense

PhosphaSense: A fully integrated, portable lab-on-a-disc device for phosphate determination in water.

Gillian Duffy[a], Ivan Maguire[a], Brendan Heery[a], Charles Nwankire[a], Jens Ducrée[b] and Fiona Regan[a]

[a] Marine Environmental Sensing Technology Hub, Dublin City University, Glasnevin, Dublin 9, Ireland

[b] School of Physical Sciences, Dublin city University, Glasnevin, Dublin 9, Ireland

Published: Sensors & Actuators: B. Chemical, 2016. DOI: 10.1016/j.snb.2016.12.040

Aims and Objectives

Chapter 3 describes the design, fabrication and characterisation of a centrifugal, microfluidic sensor for determination of phosphate in water. The system was optimised for measuring low levels of phosphate, and applied to the measurement of river water and waste water treatment plant effluent.

Abstract

A portable, compact, centrifugal microfluidic system for the *in situ* quantitation of phosphate in water is reported. The device uses the ascorbic acid method, a colourimetric absorbance based assay, for phosphate determination. The integrated system consists of two components; the centrifugal microfluidic disc and the complementary system. The microfluidic disc is designed to have similar dimensions to that of a compact disc (CD), with a slightly thicker composition. Capillary active micro-channels are integrated internally, through which small and precise volumes of fluids can flow. Upon loading of the disc with a water sample and chemical reagents, the fluids can be moved through the disc using centrifugal force. This is created by rotation of the disc by the motor in the complementary system. The loaded fluids are then mixed due to rapid expansion and contraction as they are forced through the microfluidic channels and significantly larger reservoirs. Once mixing has occurred, this force will then drive the fluid into the optical detection zone. The low-cost optical detection system incorporated into the complementary system consists of an LED-photodiode transducing pair that measures the absorbance of light by the molybdenum blue complex formed at 880 nm. The total mass of 2 kg and dimensions of 20 cm x 18 cm x 14 cm make this system portable convenient for analysis at the sampling site. The limit of detection (LOD) and limit of quantitation (LOQ) of this device were 5 and 14 $\mu g.L^{-1}$ PO_4-P, respectively. The linear range of 14 – 800 $\mu g.L^{-1}$ and sensitivity of 0.003 $AU.L.\mu g^{-1}$ make it suitable for analysing water bodies with low levels of phosphate.

Keywords Phosphate, optical sensor, centrifugal microfluidics, Lab-On-A-Disc, LOAD, water quality

3.1 Introduction

Phosphorus (P) is an essential nutrient for life. It is a growth limiting nutrient, which makes it an important parameter to monitor in water.[1] Elevated levels of growth-limiting nutrients lead to algal blooms.[2] These blooms can be a nuisance, however some algal species release toxins which are harmful to humans and animals. Aside from toxicity, decay of the large amounts of organic matter associated with algal blooms leads to hypoxic or anoxic waters, forming 'dead zones' where aquatic animals cannot survive.[3] These Harmful Algal Blooms (HABs) can have devastating effects on the local ecosystem, as well as on the fishing industry, water sports and leisure activities, and drinking water supplies.

Major sources of P entry into fresh water systems include fertiliser run-off from farmlands, and effluent from waste water treatment plants and industrial plants. It exists in many different chemical forms in water.[4] The simplest method for estimating bioavailable phosphorus in water is to analyse for soluble reactive phosphate (SRP). Orthophosphates are the most abundant forms of SRP at pH levels typically encountered in natural waters.[5, 6]

Phosphate cannot be measured directly in water, introducing the need for reagent based detection. A number of different strategies have been adapted for phosphate measurements on-site, including colourimetry,[7-12] electrochemistry[13-17] and fluorescence emission spectroscopy.[18-20]

Lab-on-a-disc (LOAD) devices are an ideal means for rapid on-site measurements as they allow for miniaturisation and automation of laboratory based analytical protocols, towards the development of inexpensive, portable and compact devices.[21] The use of microlitre volumes results in a reduction in reagent consumption, waste production and analysis times compared to standard laboratory protocols. This coupled with reduced cost, work flow and lowered sample contamination risk makes disposable microfluidic devices an attractive option for water analysis.[22]

Low reagent volume requirements improve portability of the system, as larger volumes of liquid reagents are cumbersome to transport, particularly when the

sampling sites are difficult to access. Centrifugal microfluidics offers the added advantages of simplicity and low cost. In place of multiple microfluidic pumps, which are often expensive and require considerable power input, a simple motor is used for disc rotation, to generate a centrifugal force which acts from the centre of the disc, radially outwards.[23] This centrifugal force propels fluid through the microfluidic channels.

The microfluidic platform for this system was fabricated from poly(methyl methacrylate) (PMMA) and pressure sensitive adhesive (PSA). It is rotated at ~8 Hz to create the centrifugal force for fluid manipulation. The on-board microfluidic architecture, including an air ventilation system for performance enhanced mixing of sample and reagents, also enables precise fluidic manipulation. The ascorbic acid method for SRP determination was incorporated onto this device due to its high sensitivity compared to other colourimetric methods. A long optical path length of 75 mm was included in order to maximise absorbance signal, producing improved sensitivity and LOD.

There are currently few examples of LOAD devices for water quality analysis. Some parameters for water quality assessment that have been automated on-disc include pH, turbidity, nitrate, nitrite, ammonium, silicate and hexavalent chromium.[21,24-27] These devices are compared in Table 3.1.

3.2 Materials and Methods

3.2.1 Chemicals

All solutions were prepared using ultra-pure water (Elga Maxima®, 18.2 MΩ) and ACS grade reagents purchased from Sigma Aldrich, Arklow, Ireland. Working standards were prepared by dilution of a 50 µg PO_4-P.mL^{-1} stock solution, prepared from potassium dihydrogen phosphate monobasic. A 0.032 M solution of ammonium molybdate tetrahydrate, a 0.004 M solution of potassium antimonyl tartrate and a 0.1 M solution of L-ascorbic acid were prepared. A 5 M

sulphuric acid solution was prepared by adding 7 mL concentrated sulphuric acid (96%) to 50 mL of deionised water. The combined reagent was made freshly each day by mixing 5 mL sulphuric acid solution, 500 µL potassium antimonyl solution, 1.5 mL ammonium molybdate solution and 3 mL ascorbic acid solution. The volume ratio of water sample to combined reagent used for all experiments was 1:0.16. Complex formation time was 10 minutes from time of reagent addition.

A water sample was collected from the River Tolka in Dublin City, Ireland. This sample site was selected to act as a low level phosphate sample for the sensor. It was filtered through a 0.45 µm filter prior to analysis on the system. An effluent sample was collected at the effluent point of Ringsend Waste Water Treatment Plant (WWTP) in Dublin City. A 1 in 5 dilution of the filtered WWTP sample was measured on the system. This acted as a high level sample for the sensor.

3.2.2 Instrumentation

Reference measurements for the sensor calibrations and environmental samples were obtained using a Shimadzu mini 1240 spectrometer (Shimadzu Corporation, Japan). Samples were run in parallel with the LOAD device for comparison of performance. BrandTech® cuvettes (Sigma Aldrich, Ireland) were used for optical path lengths of 10 mm. Absorbance spectra were recorded using a VWR UV-1600PC UV-vis spectrophotometer (VWR, Ireland).

The cuvette holder and the PhosphaSense system were 3D printed using a Stratasys uPrint Dimension SE 3D printer (Tri-Tech 3D, United Kingdom) from Acrylonitrile butadiene styrene (ABS) polymer, enabling rapid prototyping. For the path length study, glass cuvettes (Spectro Service Ltd., United Kingdom) were used. The path lengths of these cuvettes were 2, 5, 50 and 100 mm.

The optical detection system consists of an OSRAM Opto Semiconductors light emitting diode (LED) (purchased from Radionics Ltd., Ireland) and a Vishay silicon PIN photodiode (part number: BPW24R, purchased from Radionics Ltd., Ireland).

An 880 nm laser diode module (LM-104-E002, purchased from Roithner LaserTechnik GmbH) was used as an alternative light source for comparative purposes.

3.2.3 Disc design and fabrication

The centrifugal microfluidic disc was manufactured using PMMA sheets (Radionics™, Ireland), and PSA (Adhesives Research™, Ireland) respectively. It is made up of 5 layers, as shown in Fig. 3.1. The three PMMA layers, which contain the larger features, were cut using an Epilog Zing laser cutter (Epilog Corporation, CO, USA) (Fig. 3.1, yellow). These layers were adhered together using PSA, which contained the microfluidic channel features (Fig. 3.1, blue). This was cut using a Graphtec cutter plotter (Graphtec America Inc., CA, USA). The layers were assembled in a clean room, using a hot roll laminator (ChemInstruments, OH, USA) to activate the PSA.

Table 3.1. The LOD, linear range and attributes of centrifugal microfluidic water quality sensors with optical detection.[21,24-27]

Author	Analyte	LOD	Linear range	Attributes	Comments
Czugala[21]	pH	$2.5x10^{-4}$ M (BCP dye)	$2.5x10^{-6}$ – $5x10^{-5}$ M (BCP dye)	Portable, yields results on-site, LOD comparable with lab methods	Low power requirements, low cost detection system
	Turbidity	N/A	N/A	Excludes particles from optical detection chamber	
Czugala[24]	Nitrite	9.31 µg.L^{-1} NO_2^-	0.2-1.2 mg.L^{-1} NO_2^-	Portable, yields results on-site, LOD comparable with lab methods	Low power requirements, low cost detection system
Xi[25]	Nitrate	0.16 mg.L^{-1} NO_3-N	0.16-5 mg.L^{-1} NO_3^--N	Multiple sample capacity on one disc	High power requirements, more expensive detection system
	Nitrite	0.05 mg.L^{-1} NO_2-N	0.05-5 mg.L^{-1} NO_2^--N		

Hwang[26]	Nitrite	0.008 mg.L^{-1} NO_2^--N	0.027-10 mg.L^{-1} NO_2^--N	Multiple analytes on one disc	High power requirements, expensive detection system
	Nitrate + Nitrite	0.05 mg.L^{-1} NO_3^--N	0.07-10 mg.L^{-1} NO_3^--N		
	Ammonium	0.01 mg.L^{-1} NH_4^+-N	0.05-10 mg.L^{-1} NH_4^+-N		
	Ortho-phosphate	0.008 mg.L^{-1} PO_4^{2-}-P	0.024-1 mg.L^{-1} PO_4^{2-}-P		
	Silicate	0.19 mg.L^{-1}	0.79-100 mg.L^{-1}		
LaCroix-Fralish[27]	Nitrite	0.008 mg.L^{-1} NO_2-N	Up to 5 mg.L^{-1} NO_2-N	Calibration and multiple samples measured on one disc	High power requirements, more expensive detection system
	Chromium (VI)	0.03 mg.L^{-1}	Up to 5 mg.L^{-1}	Dry reagents stored on disc allow for single step analysis	

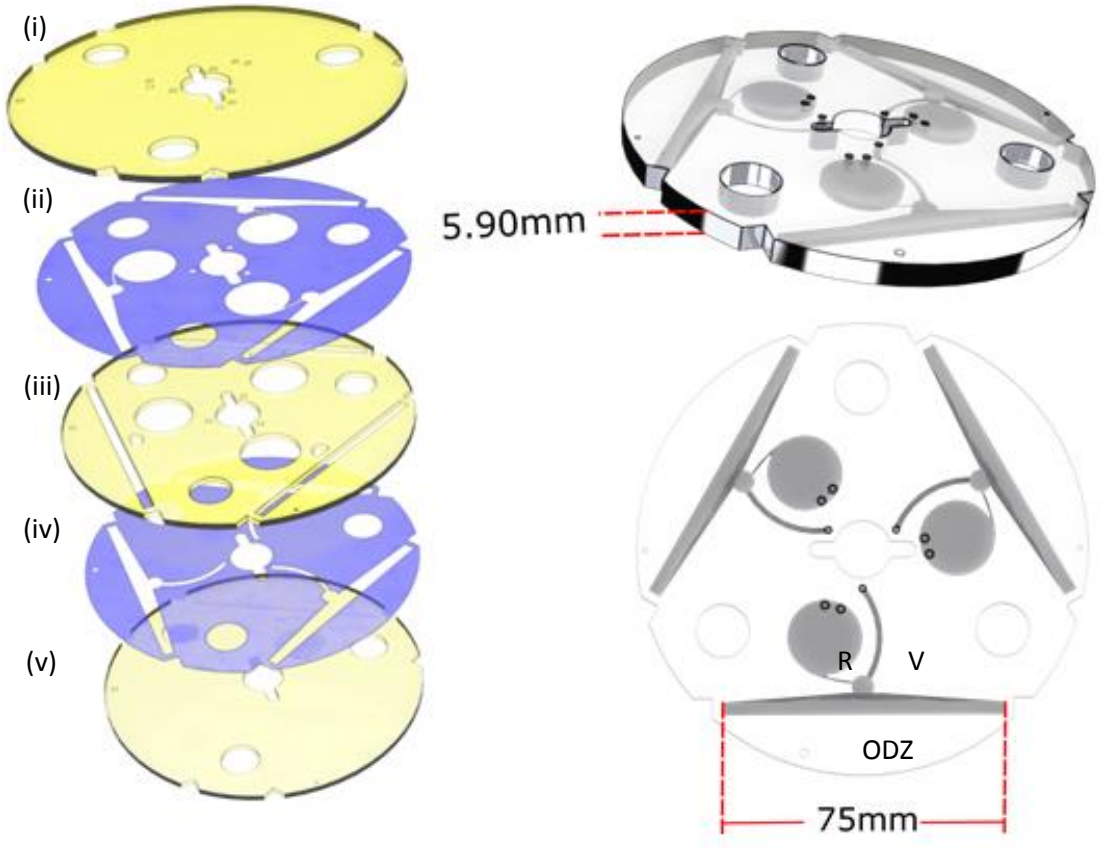

Fig. 3.1. (Left) Rendered image showing each layer of the microfluidic disc, where (i) is a PMMA layer with air vents and fluid inlets; (ii) is a PSA layer with microfluidic channels; (iii) is a PMMA layer with microfluidic channels; (iv) is a PSA layer with an air ventilation system; and (v) is a base PMMA layer. (Top right) Rendered image of the microfluidic disc showing thickness; (bottom right) schematic of the microfluidic disc, which consists of a mixing reservoir (R) with inlets for sample and reagent loading, a microfluidic channel through which the fluids flow into the 75 mm long optical detection zone (ODC), and an air vent (V) to release trapped air. The disc includes three alignment slots for precise optical alignment with the stage in Fig. 3.2.

The sample and combined reagent were added into the reservoir (R) of the disc, shown in Fig.3.1, using a micropipette with a combined volume of 600 µL, reaching the maximum capacity of the reservoir. On rotation of the disc at ~8 Hz, the sample and reagent were propelled through the microfluidic channels and into the 75 mm long optical detection zone (ODZ). As this detection zone filled, trapped air was released via a collapsible air ventilation system (V). This ventilation set-up was required to prevent the capture of air bubbles within the optical pathway. Air bubbles interfere with absorbance measurements, making their exclusion from the detection zone critical. The disc was allowed to gradually decelerate and was then aligned with the detection system using an alignment stage, which is shown in Fig. 3.2. The alignment pillars on this stage allowed for reproducible positioning of the detection zones in line with the LED-photodiode light pathway. Black acrylic paint was also applied to the PMMA each side of the detection window, to minimise light scattering and losses due to the disc materials.

3.2.4 PhosphaSense system design and fabrication

The 3D printed system was designed to directly complement the microfluidic disc. It was printed in 6 parts which were connected using screws. The system has a total mass of 2 kg, and dimensions of 20 x 18 x 14 cm. It contains a stage on which the disc is rotated by a motor. The optical detection system is configured for both LED-photodiode and LASER-photodiode pairing. Both pairings were carefully aligned to transmit light through the long optical detection zone of the disc. The transmitted light, at a reduced intensity due to absorption, then reaches the detection photodiode. A diagram of the PhosphaSense system is shown on the left in Fig. 3.2. The complementary system utilised a Wixel programmable module, (Cool Components, United Kingdom), to convert the outputted photodiode voltage into a digital signal, which can be interpreted and

recorded by the end-user via ExtraPuTTYsoftware. The Wixel is also capable of receiving live user commands, which was exploited to control the on-board motor rotational speeds. The electronics were stored in a separate compartment below the stage.

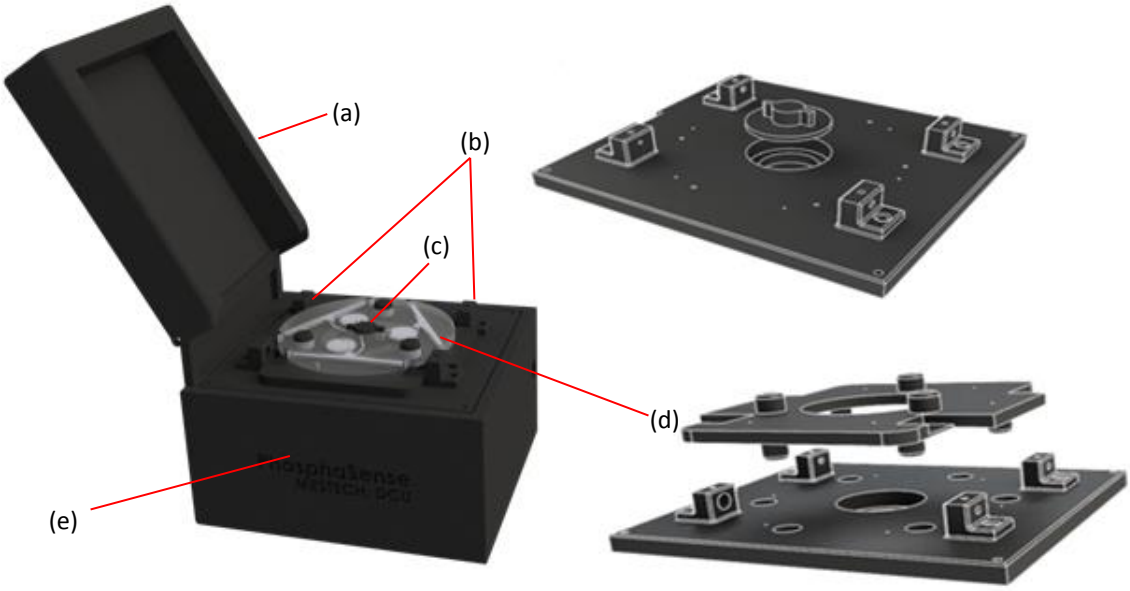

Fig. 3.2. (Left) Rendered image of the PhosphaSense system where (a) is the lid for ambient light exclusion; (b) is the optical detection system; (c) is the motor; (d) is the microfluidic disc; and (e) is the compartment for electronics. (Right) Rendered images of the 3D printed stage components of PhosphaSense, where the top image shows the stage component of the system, with the motor top piece, and the bottom image shows how the optical alignment stage is fitted on top of the primary stage. The pillars on this stage line up with slots on the microfluidic disc shown in Fig. 3.1 to facilitate precise alignment with the detection system.

3.2.5 Optimisation of optical path length

Optimisation of the path length for absorbance measurements within the microfluidic component was a critical step in platform development, to ensure that both maximum linear range and minimum LOD were achieved. To facilitate optimisation of this parameter using the LED-photodiode detection system, a custom-made cuvette holder was employed. The holder was designed to align the two light sources under investigation (an LED and a laser) with a detector (a photodiode for each light source). The experimental set up is shown in Fig. 3.3. The absorbance of a range of phosphate standards was measured at each path length, for each light source. The path lengths investigated were 2, 5, 10, 50 and 100 mm. The inside of the cuvette holder was painted black to minimise any light losses.

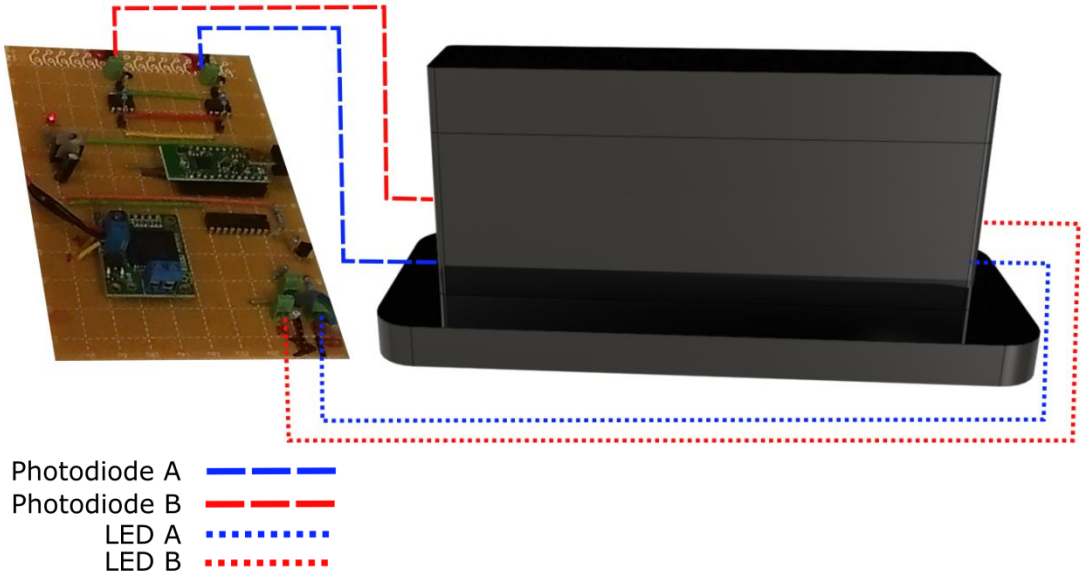

Fig. 3.3. Rendered image of the 3D printed cuvette holder with two light sources (an LED and a laser) and two detectors (photodiodes), precisely aligned for absorbance measurements over a range of optical path lengths.

3.2.6 Analytical method

The ascorbic acid method was adapted from reference 5 for use on this device. This method is based on the formation of a blue phosphomolybdenum complex with an absorption maximum in the near infra-red region of the electromagnetic spectrum. This method was selected from a range of standard analytical methods for phosphate measurement due to its high sensitivity, its ease of incorporation onto a microfluidic device, its stable product and its excellent reagent compatibility with the sensor materials.[5,28]

3.2.7 Signal processing

The ADC outputs from the photodiode were converted to absorbance values using Eq. 3.1, where *blank* is the average ADC reading of a reagent blank (where n=3), and *sample* is the ADC reading of the sample under the same conditions.

Equation 3.1. Absorbance = $\log_{10}\left(\frac{Blank}{Sample}\right)$

Equation 3.2. LOD = $\frac{3.3(S)}{m}$

The LOD was calculated using Eq. 3.2, where *S* is the standard deviation of the reagent blank (where n=3), and *m* is the slope of the calibration curve. The LOQ was calculated using 10 times *s*, divided by *m*.

3.3 Results and discussion

3.3.1 Calibration and evaluation of analytical performance

The calibration curve obtained using the fully optimised PhosphaSense system is shown in Fig. 3.4. This system displayed a linear response signal to phosphate concentration from 14-800 ug.L^{-1} PO_4-P. The LOD and LOQ values achieved were 5 and 14 µg.L^{-1}, respectively.

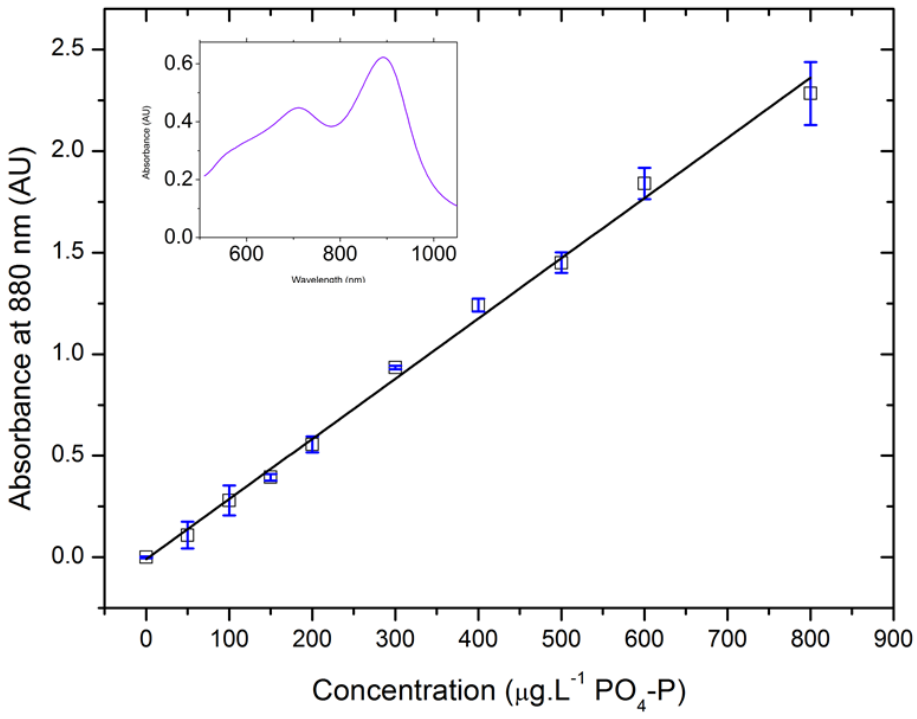

Fig. 3.4. Calibration curve obtained on the PhosphaSense system using prepared phosphate standards, where error bars show one standard deviation, with a slope of 0.003 AU.L.µg^{-1} and an R^2 of 0.9958.

The sensor's performance was compared to that of the same colourimetric method performed using a spectrophotometer. This comparison is shown in Fig. 3.5, with a more detailed comparison shown in Table 3.2.

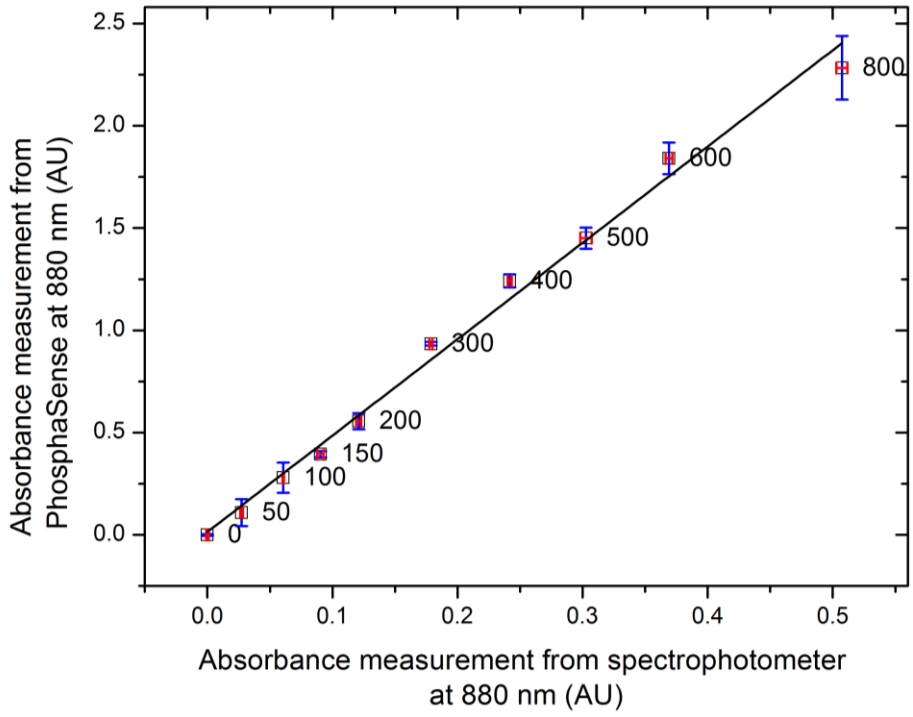

Fig. 3.5. Correlation plot for the measurement of the phosphate standards on PhosphaSense (n=3) and on a spectrophotometer (n=3), where each point is labelled with the concentration in $\mu g.L^{-1}$. Error bars show one standard deviation in blue for PhosphaSense and in red for the spectrophotometer, with an R^2 value of 0.9915 and a slope of 4.71.

From Fig. 3.5, the close agreement between PhosphaSense and the reference spectrophotometric measurements demonstrates the sensor's excellent analytical performance. This is further highlighted by the comparison in Table 3.2. PhosphaSense exhibited a sensitivity that was five times greater than that of

the spectrophotometric method. Although the standard deviation was higher for PhosphaSense, the LOD was half that of the spectrophotometric method, with a greatly improved LOQ. One drawback of PhosphaSense in this comparison was the diminished linear range in the upper region. This was due to the high percentage of light absorbed by the molybdenum blue species at higher concentrations. However, incorporation of a second, shorter optical path length through the width of the microfluidic disc would allow for measurement of these higher ranges without any changes to the microfluidic disc design. This could be easily incorporated into the next sensor prototype, as a second LED-PD pair located above and below the horizontal disc, measuring through the 2 mm path length of the disc.

Table 3.2. Comparison of the analytical performance of PhosphaSense and the reference spectrophotometric method

Analytical method	Path length (cm)	Slope ($AU.L.\mu g^{-1}$)	LOD ($\mu g.L^{-1}$ PO_4-P)	LOQ ($\mu g.L^{-1}$ PO_4-P)	Linear range ($\mu g.L^{-1}$ PO_4-P)	R^2
PhosphaSense	7.5	0.003	5	14	14-800	0.9958
Spectrophotometer	1	0.0006	10	150	150-1,300	0.9995

3.3.2 Application of PhosphaSense to phosphate determination in environmental water samples

The performance of the PhosphaSense system was demonstrated using water samples collected from two different water bodies, each of which represented a different phosphate level. This demonstrated the versatility of the PhosphaSense system for screening a variety of different water types. The river and WWTP effluent samples represented a low and a high phosphate level, respectively. The sensor output from these samples was compared to the spectrophotometric method, the results of which are shown in Table 3.3. It can be seen that the system measured both high and low level water samples with close agreement to spectrophotometric measurements. The standard deviation was low for both methods. Accuracy on PhosphaSense was good for both the Tolka and for the WWTP effluent samples, with a percentage error of 8% and 5%, respectively.

Table 3.3. Phosphate measurements from PhosphaSense (n=3) and the reference spectrophotometric method (n=3)

Sample ID	PhosphaSense ($\mu g.L^{-1}$ PO_4-P)	Spectrophotometer ($\mu g.L^{-1}$ PO_4-P)
Tolka	44 ± 3	48 ± 2
WWTP	620 ± 2	656 ± 1

PhosphaSense offers a range of advantages for on-site analyses. Its small dimensions and low mass make it portable and convenient to transport. Within 10 minutes, results from three different samples can be obtained from a single disc. No complex sample pre-treatment is required. A filtration of the sample

was carried out prior to analysis. This is typically done on-site during sample collection regardless of analysis method. The sensor's very low component cost and ease of use would make it an attractive option for researchers, local authorities or legislative bodies, where expertise is not required for use. Analysis on-site means that PhosphaSense is less prone to sample contamination and reduces work flow greatly, as the sample storage, transport and in-lab storage are removed from the analysis process.

3.3.3 Path length optimisation

The optical path length of the disc was optimised by comparing the LOD, sensitivity and saturation point (point at which 100% absorbance occurred) of five different path lengths, within the range investigated. The experimental set up is shown in Fig. 3.3. The results from this study are summarised in Table 3.4.

Table 3.4. The LOD, saturation point and sensitivity for the LED and laser at different optical path lengths.

Path length (mm)	LOD ($\mu g.L^{-1}$)	Saturation point ($\mu g.L^{-1}$)	Sensitivity ($AU.L.\mu g^{-1}$)
LED			
2	231.39	N/A	-0.00004
5	121.25	N/A	0.0004
10	49.63	N/A	0.0006
50	77.07	800	0.003
100	1.23	400	0.0063
Laser			
2	461.97	N/A	0.00007
5	25.48	N/A	0.0003
10	24.69	N/A	0.0007
50	84.37	800	0.0022
100	32.22	400	0.006

*N/A indicates that the saturation point was not reached within the concentration range investigated.

From the data shown in Table 3.4, it is clear that there must be a compromise between the linear range and the LOD achieved by the sensor. Sensitivity increased with increasing path length, however for path lengths of 50 mm and above, the saturation point was reached. Therefore, a path length of 75 mm was selected as it allowed for minimisation of LOD within the working dimensions of

the microfluidic platform. The linear range was diminished as a result, making this device more suited to measurements in water bodies where phosphate levels are typically below 800 µg.L^{-1}.

This study highlights the versatility of the system, whereby sensitivity can be selected for by designing microfluidic discs with a range of different path lengths. A long path length maximises sensitivity, making it best suited to measuring low levels of phosphate, while short path lengths allow for determination of high phosphate levels. A sampling site can be screened in order to approximate the phosphate range. The microfluidic disc with the predetermined optimal path length for this phosphate range can then be used for sample analysis.

3.4 Conclusions

A fully integrated, centrifugal, microfluidic optical sensor for phosphate determination in water has been developed. The use of a microfluidic disc was advantageous as it allowed the use of a long optical path length for improved sensitivity, while also enabling low reagent and sample volumes to be used. The detection limit achieved by the standard spectrophotometric ascorbic acid method is 10 µg.L^{-1} PO_4-P.[5] By adapting this method onto a microfluidic device, using a simple design to facilitate mixing and by including a long optical path length, a comparable LOD of 5 µg.L^{-1} has been achieved. However, the device has a diminished linear range of 14 - 800 µg.L^{-1}, compared to the spectrophotometric method range of 150 - 1,300 µg.L^{-1} PO_4-P.[5] This makes the system suitable for measurement of water bodies with low levels of phosphate. Future work will aim to incorporate a second absorbance measurement through the width of the disc, which has a short path length of 2 mm, thus extending the range of detection to the upper range. This addition will be included in the next version of the PhosphaSense system, making the system capable of measuring over a wide range of phosphate concentrations. The next prototype will also feature a lid

compartment for storage of all electronic components, rather than underneath the fluidic system which can lead to damage from leaks or splashes.

The LOD, LOQ, linear range and sensitivity show the system's good analytical performance when compared with the same method carried out using a spectrophotometer in a laboratory. The PhosphaSense system offers boundless opportunity for further tailoring of the microfluidic network and modification of detection wavelengths to permit determination of a wide array of analytes of interest through robust colourimetric methods.

References

1. V. H. Smith, Eutrophication of freshwater and coastal marine ecosystems: a global problem, Environ. Sci. Pollut. Res. Int. 10 (2003) 126–139. doi:10.1065/espr2002.12.142.

2. D. W. Schindler, The dilemma of controlling cultural eutrophication of lakes, Proc. R. Soc. B Biol. Sci. 279 (2012) 4322–4333. doi:10.1098/rspb.2012.1032.

3. J. Heisler, P. M. Glibert, J. M. Burkholder, D. M. Anderson, W. Cochlan, W. C. Dennison, Q. Dortch, C. J. Gobler, C. A. Heil, E. Humphries, A. Lewitus, R. Magnien, H. G. Marshall, K. Sellner, D. A. Stockwell, D. K. Stoecker, M. Suddleson, Eutrophication and harmful algal blooms: A scientific consensus, Harmful Algae. 8 (2008) 3–13. doi:10.1016/j.hal.2008.08.006.

4. B. L. Turner, M. J. Papházy, P. M. Haygarth, I. D. McKelvie, Inositol phosphates in the environment, Phil. Trans. R. Soc. Lond. B. 357 (2002) 449–469. doi:10.1098/rstb.2001.0837.

5. L. S. Clesceri, A. E. Greenberg, A. D. Eaton, Standard Methods for the Examination of Water and Wastewater, 20th ed., American Public Health Association, Washington, 1998.

6. B. Y. Spivakov, T. A. Maryutina, H. Muntau, Phosphorus Speciation in Water and Phosphorus speciation in water and sediments (Technical Report), Pure Appl. Chem. 71 (1999) 2161–2176. doi:10.1351/pac199971112161.

7. 7. A. M. Nightingale, A. D. Beaton, M. C. Mowlem, Trends in microfluidic systems for in situ chemical analysis of natural waters, Sensors Actuators, B Chem. 221 (2015) 1398–1405. doi:10.1016/j.snb.2015.07.091.

8. 8. C. Slater, J. Cleary, K. T. Lau, D. Snakenborg, B. Corcoran, J. P. Kutter, D. Diamond, Validation of a fully autonomous phosphate analyser based on a microfluidic lab-on-a-chip, Water Sci. Technol. 61 (2010) 1811–1818. doi:10.2166/wst.2010.069.

9. 9. S. C. Mukhopadhyay, A. Mason (Eds.), Smart Sensors for Real-Time Water Quality Monitoring, 978-3-642-37006-9, Springer, Heidelberg New York Dordrecht London (2013), 25–44.

10. 10. M. Bowden, D. Diamond, The determination of phosphorus in a microfluidic manifold demonstrating long-term reagent lifetime and chemical stability utilising a colorimetric method, Sensors Actuators, B Chem. 90 (2003) 170–174. doi:10.1016/S0925-4005(03)00024-8.

11. 11. D. Thouron, R. Vuillemin, X. Philippon, A. Lourenço, C. Provost, A. Cruzado, V. Garçon, An autonomous nutrient analyzer for oceanic long-term in situ biogeochemical monitoring, Anal. Chem. 75 (2003) 2601–2609. doi:10.1021/ac020696+.

12. 12. A. H. Barnard, B. Rhoades, C. Wetzel, A. Derr, J. Zaneveld, C. Moore, C. Koch, I. Walsh, Real-time and long-term monitoring of phosphate using the in-situ CYCLE sensor, OCEANS (2009), 1–6.

13. 13. Y. Udnan, I. D. McKelvie, M. R. Grace, J. Jakmunee, K. Grudpan, Evaluation of on-line preconcentration and flow-injection amperometry

for phosphate determination in fresh and marine waters, Talanta. 66 (2005) 461–466. doi:10.1016/j.talanta.2004.12.064.

14. 14. W. L. Cheng, J. W. Sue, W. C. Chen, J. L. Chang, J. M. Zen, Activated nickel platform for electrochemical sensing of phosphate, Anal. Chem. 82 (2010) 1157–1161. doi:10.1021/ac9025253.

15. 15. H. Guedri, C. Durrieu, Development of a Conductometric Algal Whole Cells Biosensor for Phosphate Monitoring, Sensor Lett., 7 (2009), 788–794. doi: 10.1166/sl.2009.1149

16. 16. R. C. H. Kwan, H. F. Leung, P. Y. T. Hon, J. P. Barford, R. Renneberg, A screen-printed biosensor using pyruvate oxidase for rapid determination of phosphate in synthetic wastewater, Appl. Microbiol. Biotechnol. 66 (2005) 377–383. doi:10.1007/s00253-004-1701-8.

17. 17. S. Berchmans, T. B. Issa, P. Singh, Determination of inorganic phosphate by electroanalytical methods: A review, Anal. Chim. Acta. 729 (2012) 7–20. doi:10.1016/j.aca.2012.03.060.

18. 18. X. Lin, X. Wu, Z. Xie, K. Y. Wong, PVC matrix membrane sensor for fluorescent determination of phosphate, Talanta. 70 (2006) 32–36. doi:10.1016/j.talanta.2006.01.026.

19. 19. G. Zhang, B. Lu, Y. Wen, L. Lu, J. Xu, Facile fabrication of a cost-effective, water-soluble, and electrosynthesized poly(9-aminofluorene) fluorescent sensor for the selective and sensitive detection of Fe(III) and inorganic phosphates, Sensors Actuators, B Chem. 171-172 (2012) 786–794. doi:10.1016/j.snb.2012.05.072.

20. 20. H. B. F. M. Nelissen, D. K. Smith, Synthetically accessible, high-affinity phosphate anion receptors, Chem. Commun. (Camb). 44 (2007) 3039–3041. doi:10.1039/b706227c.

21. M. Czugala, R. Gorkin III, T. Phelan, J. Gaughran, V. F. Curto, J. Ducrée, D. Diamond, F. Benito-Lopez, Optical sensing system based on wireless paired emitter detector diode device and ionogels for lab-on-a-disc water quality analysis, Lab Chip. 12 (2012) 5069. doi:10.1039/c2lc40781g.

22. M. Madou, J. Zoval, G. Jia, H. Kido, J. Kim, N. Kim, Lab on a CD, Annu. Rev. Biomed. Eng. 8 (2006) 601–628. doi:10.1146/annurev.bioeng.8.061505.095758.

23. R. Gorkin, J. Park, J. Siegrist, M. Amasia, B. S. Lee, J. -M. Park, J. Kim, H. Kim, M. Madou, Y. -K. Cho, Centrifugal microfluidics for biomedical applications, Lab Chip. 10 (2010) 1758–1773. doi:10.1039/b924109d.

24. M. Czugala, D. Maher, F. Collins, R. Burger, F. Hopfgartner, Y. Yang, J. Zhaou, J. Ducrée, A. Smeaton, K. J. Fraser, F. Benito-Lopez, D. Diamond, CMAS: fully integrated portable centrifugal microfluidic analysis system for on-site colorimetric analysis, RSC Adv. 3 (2013) 15928. doi:10.1039/c3ra42975j.

25. Y. Xi, E. J. Templeton, E. D. Salin, Rapid simultaneous determination of nitrate and nitrite on a centrifugal microfluidic device, Talanta. 82 (2010) 1612–1615. doi:10.1016/j.talanta.2010.07.038.

26. H. Hwang, Y. Kim, J. Cho, J. Y. Lee, M. S. Choi, Y. K. Cho, Lab-on-a-disc for simultaneous determination of nutrients in water, Anal. Chem. 85 (2013) 2954–2960. doi:10.1021/ac3036734.

27. A. LaCroix-Fralish, J. Clare, C. D. Skinner, E. D. Salin, A centrifugal microanalysis system for the determination of nitrite and hexavalent chromium, Talanta. 80 (2009) 670–675. doi:10.1016/j.talanta.2009.07.046.

28. J. Murphy, J. P. Riley, A modified single solution method for the determination of phosphate in natural waters, Anal. Chim. Acta. 27 (1962) 31–36.

Chapter 4:
ChromiSense

ChromiSense: A colourimetric lab-on-a-disc sensor for chromium speciation in water.

Gillian Duffy[a], Ivan Maguire[a], Brendan Heery[a], Pauline Gers[a], Jens Ducrée[b] and Fiona Regan[a]

[a] Marine Environmental Sensing Technology Hub, Dublin City University, Glasnevin, Dublin 9, Ireland

[b] School of Physical Sciences, Dublin city University, Glasnevin, Dublin 9, Ireland

Published: Talanta, 2017. DOI: 10.1016/j.talanta.2017.09.066

Aims and Objectives

Chapter 4 describes the design, fabrication and characterisation of a centrifugal, microfluidic sensor for speciation of chromium in water. The system was optimised for measuring low levels of chromium VI, and industrial levels of chromium III. As chromium VI is another analyte that is present at very low part per billion levels in water, the design and measurement approach that was successfully applied to phosphate could again be applied here. To demonstrate a more sophisticated system, it was shown that speciation of an analyte can be carried out simultaneously on-disc. This required some changes in the microfluidic disc design to facilitate two new colourimetric methods. The reservoir shape was changed to accommodate low-viscosity reagents. A heating step was included by incorporating heating pads into the complementary system. A long optical path length was used in order to maximise the sensitivity of the

colourimetric methods. The system was applied to the measurement of spiked river water samples.

Abstract

The development of a centrifugal device for quantitative analysis of both chromium (III) and (VI) species in water is reported. ChromiSense is a colourimetric sensor system that has been applied to the measurement of chromium in spiked river water samples. For analysis, the sample is loaded into a reservoir on the disposable microfluidic disc, along with reagents. A centrifugal force is created by spinning the disc to pump liquids through microchannels, causing them to mix and react to form a coloured product. The coloured product is then presented to a low-cost optical detection system, where absorbance measurements can be recorded. The optical detection system consists of a light emitting diode (LED) and photodiode (PD) couple. Chromium (III) was measured using 2,6-pyridine dicarboxylic acid as a ligand, forming a complex that was measured at 535 nm and at 335 nm. While measuring at 535 nm allowed for the use of a low cost LED, the sensitivity was improved 2.5 times by measuring at 335 nm. However, 335 nm also yielded a diminished linear range with little improvement in limit of deteciton (LOD), and required a lengthier manufacturing process due to the need for a UV-transparent material. Chromium (VI) was detected using 1,5-diphenyl carbazide (DPC). This standard analysis method was simplified for automation on-disc, and optimised to achieve a low LOD. The LOD for trivalent and hexavalent chromium using this device were 21 mg L^{-1} and 4 µg L^{-1}, respectively. The linear range for quantitative analysis was found to be 69-1000 mg L^{-1} for Cr(III) and 14-1000 µg L^{-1} for Cr (VI). While this range is high for Cr(III), incorporation of an off-disc pre-concentration method would make this technology suitable for environmental sample analysis. The device is simple to use, low in cost, and could provide rapid on-site measurements, with results comparable to those obtained using a benchtop spectrophotometer.

Keywords: Centrifugal, chromium, optical, sensor, water, microfluidic

4.1 Introduction

Chromium speciation refers to the quantitative analysis of chromium species. Although chromium exists in oxidation states from 0 to VI, it is primarily found in the (III) and (VI) states.[1] Chromium enters the environment through effluent discharged from industry (e.g. textile/electroplating) and cooling towers. It can enter drinking water supplies through corrosion inhibitors used in pipes or through contamination leaching from sanitary landfill.[2]

Changes in the oxidation state of an element can greatly change its bioavailability and toxicity.[2] Cr (III) is an essential micronutrient in the human diet, and is considered essential for maintenance of glucose, lipid and protein metabolism.[3] Cr (VI) is strongly oxidizing, exhibiting high toxicity, with carcinogenic and mutagenic properties.[4] According to the World Health Organisation (WHO), the recommended maximum allowable concentration for chromium (VI) is 0.05 mg L^{-1} in drinking water.[5]

Traditional laboratory-based measurements of chromium in freshwater are time and labour intensive, requiring expensive instrumentation and trained personnel. Commonly used techniques include atomic absorbance or emission spectroscopy, inductively coupled plasma mass spectrometry, ion chromatography, spectrophotometry, potentiometry and capillary electrophoreses. These methods can incorporate sample pre-treatments such as solid or liquid phase extraction, cloud point extraction, adsorbents or ion exchange.[2]

Handheld colourimeters for on-site measurements are a more convenient option for frequent monitoring; however the limit of detection (LOD) of these devices is typically higher than laboratory-based methods. A low LOD is essential for a chromium sensor as the recommended Cr (VI) limit is so low.

A centrifugal 'lab-on-a-disc' (LoaD) approach is employed for the development of an optical sensor for chromium speciation in water. The

disc contains microchannels guiding the flow. By rotation of the disc using a simple motor, a centrifugal field is created, which acts from the centre of the disc, radially outwards.[6] This force acts as a fluid pump, pushing fluids through the micro-channels. The philosophy behind these devices is to minimise and automate laboratory processes onto a compact, user-friendly and robust LoaD system that can be brought to the sampling site for simple and rapid analysis. The objective of this work was to design and fabricate an integrated optical sensor prototype that would be capable of simultaneous on-site measurement of both trivalent and hexavalent chromium in water.

A major concern for the minimisation of analytical protocols onto microfluidic analysers is the reduction in the optical path length from a typical 10 mm cuvette to approximately 2-5 mm, depending on the thickness of materials used in fabrication. This leads to a subsequent decrease in sensitivity and increase in detection and quantitation limits. Through using horizontal optical interrogation of the disk rather than vertical interrogation, this disc design overcomes this obstacle by incorporating an optical path length of 50 mm.

Chromium (III) is quantified by absorbance measurement following reaction with 2,6-pyridine dicarboxylic acid, which forms a [$Cr(PDCA)_2$] complex, as shown in Fig. 4.1. PDCA was selected due to its high selectivity for Cr(III) compared to other common ligands.[7] It has been used for Cr(III) for both pre- and post-column derivatisation to obtain a UV detectable complex.[7,8] Other ligands used for Cr(III) include EDTA for suppressed IC-ICP-MS, 2-hydroxybenzaldiminoglycine for colourimetric detection and Mo(VI) for UV detection after separation of Cr(III) and (VI) using CE.[9-11] The low molar extinction coefficient of this complex leads to poor sensitivity. Despite efforts to optimise the method and improve this sensitivity, the method does not reach environmentally relevant concentrations. This limits the applicability of the sensor to industrial run off or extracted samples from food.[2] The same DPC ligand as was used for Cr(VI) could be used to

determine Cr (III), however this reaction is inhibited by water, making its automation on a centrifugal system for water analysis challenging.[12]

Chromium (VI) is quantified using a modified version of the standard 1,5-diphenyl carbazide (DPC) protocol.[13] In this reaction, DPC is oxidised by chromium (VI) to form diphenyl carbazone (DPCO), with subsequent reduction of chromium (VI) to chromium (III), as show in Fig 4.2. A Cr(III)-DPCO complex then forms, which absorbs strongly at 535 nm. The positive charge on [Cr(DPCO)] is uncertain, and is written as $(3\text{-}n)^{+}$, where n is the unknown number of protons released in the complex formation.[14]

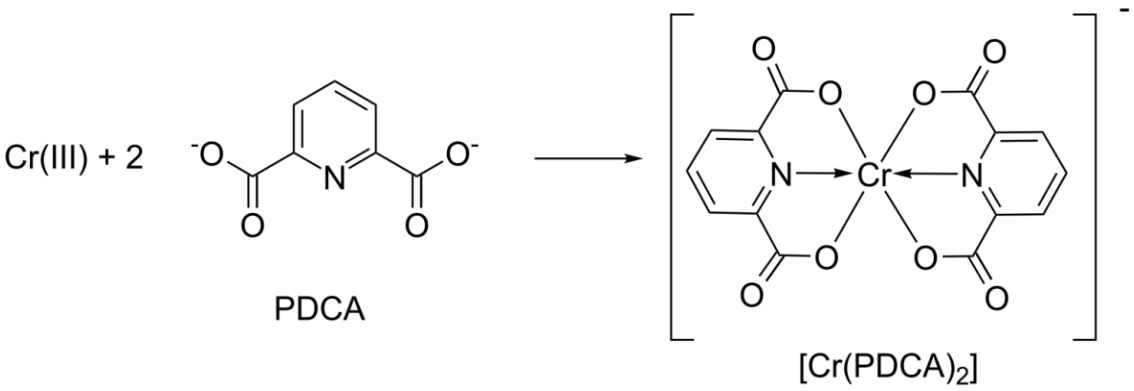

Fig. 4.1. Reaction of Cr (III) with 2 molecules of PDCA to form $[Cr(PDCA)_2]^{-}$.[15]

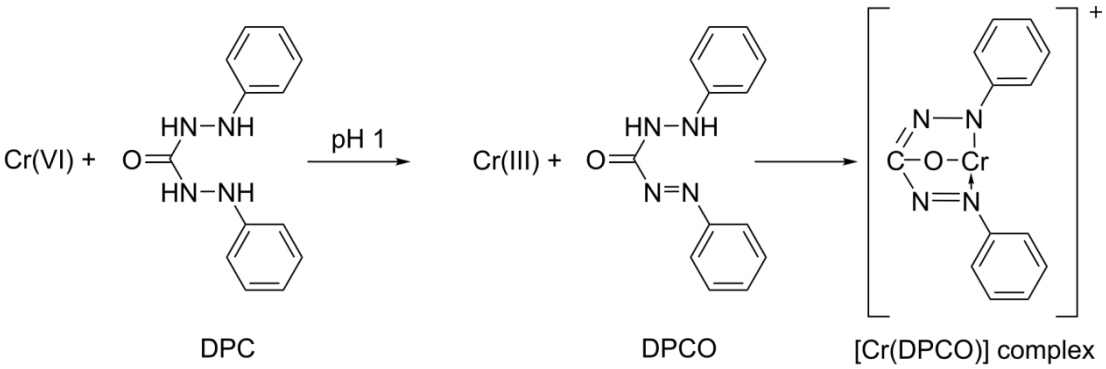

Fig. 4.2. Reaction of Cr (VI) with DPC to form $[Cr(DPCO)]^{+}$.[16]

Incorporation of a pre-concentration step for Cr (III), on- or off- disc, for subsequent complexation with PDCA would be a more straightforward approach to the issue. Pre-concentration has been achieved on microfluidic LoaD by incorporation of stationary phases such as C_{18}, porous carbon monoliths and ion exchange monoliths.[17-19] In 2009, LaFleur *et al.* demonstrated a disc that carried out SPE for heavy metal pre-concentration. It was capable of running 8 low volume samples on one disc, taking a total of 20 min. This type of pre-concentration could be done on-site, making it compatible with the ChromiSense system.[19]

4.2 Experimental

4.2.1 Materials and methods

All solutions were prepared using ultra-pure water (Elga Maxima®, 18.2 MΩ) and ACS grade reagents purchased from Sigma Aldrich, Ireland, unless otherwise stated. Working standards were prepared by dilution of stock solutions prepared from potassium dichromate and chromium (III) nitrate nonahydrate, respectively.

Chromium (VI) was quantified using a 0.02 M solution of 1,5-diphenyl carbazide (DPC) dissolved in HPLC grade methanol. The results from this were compared to the same concentration of DPC in acetone (ACS grade), which is the solvent used in the standard method.[5] A pH 1 ± 0.3 buffer was made by mixing 25 mL of 0.2 M KCl and 67 mL of 0.2 M HCl.

Chromium (III) was quantified using a 0.05 M solution of 2,6-pyridinedicarboxylic acid (PDCA) in methanol. A pH 10 buffer was made by mixing 50 mL of 0.05 M sodium tetraborate decahydrate and 18.3 mL 0.2 M sodium hydroxide.

For optimisation of reservoir filling capacity for low viscosity fluids, solutions covering a range of viscosities were prepared using ACS grade

acetone, HPLC grade methanol and ACS grade glycerol. The kinematic viscosity of each two liquid mixture was estimated using Gambill's method.[20]

Two river water samples were spiked with Cr(III) and Cr(VI). The first was made with 100 mg L^{-1} Cr(III) and 200 µg L^{-1} Cr(VI). The second was made with 800 mg L^{-1} Cr(III) and 800 µg L^{-1} Cr(VI). These were measured on ChromiSense, with reference measurements on the spectrophotometer.

4.2.2 Instrumentation

Reference measurements for the samples and sensor calibrations were obtained using a Shimadzu mini 1240 spectrometer with the same colourimetric methods as used on-disc using a 10 mm glass cuvette. Samples were run in parallel with the device for assessment of performance. Glass cuvettes with a variety of different path lengths were used (purchased from Spectro Service Ltd., UK).

Spectra were obtained using a VWR UV-1600PC UV-vis spectrophotometer (VWR, Ireland).

4.2.3 Disc design and fabrication

The centrifugal disc was fabricated from polymethyl methacrylate (PMMA) sheets (Radionics Ltd., Ireland) and pressure sensitive adhesive (PSA), (Adhesives Research Inc., Ireland). The 5 layer design is shown in Fig. 4.3. The three PMMA layers (Fig. 4.3, shown in purple) contain the larger reservoir features. They were cut using an Epilog Zing laser cutter (Epilog Corporation, CO, USA). These layers were adhered together using PSA (Fig. 4.3, shown in red) which contained the finer micro-channel features. This was cut using a Graphtec cutter plotter (Graphtec America Inc., CA, USA).

The layers were assembled in a clean room, using a hot roll laminator (ChemInstruments, OH, USA) to activate the PSA.

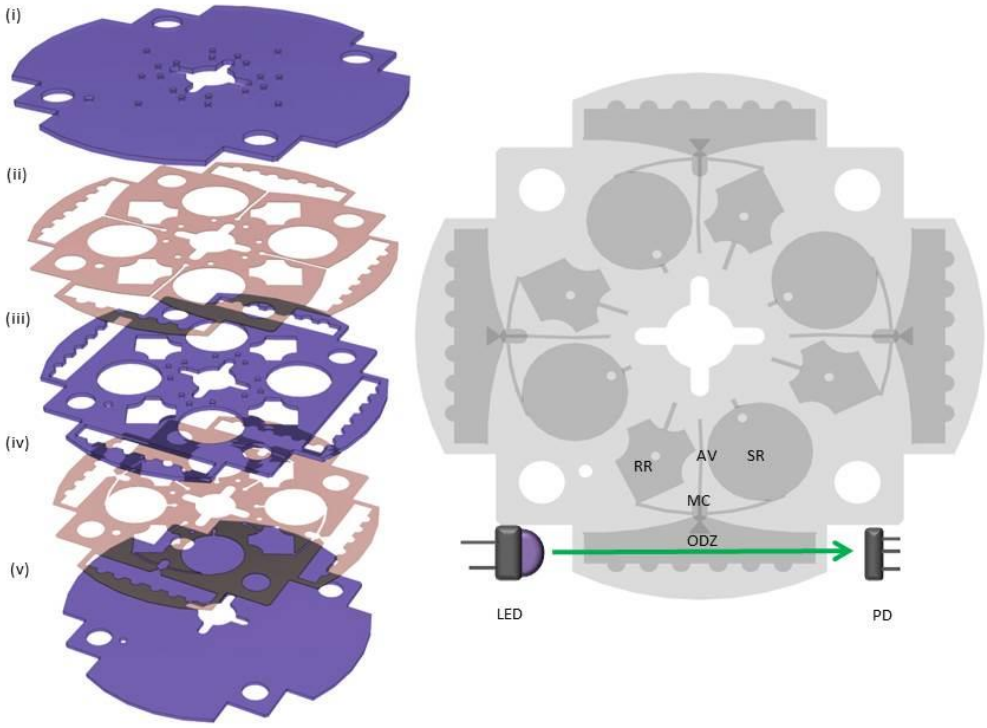

Fig. 4.3. (Left) A rendered image of the five disc layers, made from PMMA (shown in purple) and PSA (shown in red), where (i) contains inlets and air outlets; (ii) contains large reservoir features and air vents; (iii) contains large reservoir features; (iv) contains large reservoir features and microfluidic channels; (v) acts as the base. (Right) a schematic of the centrifugal disc (120 mm diameter), showing the sample reservoir (SR); reagent reservoir (RR); 500 µm wide micro-channels (MC); 5 x 50 mm optical detection zone (ODZ) with bubble traps; and 500 µm wide air ventilation system (AV). The light path for absorbance measurements is illustrated by an arrow through the ODZ, with LED and PD positions shown.

For determination of Cr (III) at 335 nm, a UV transparent material was required. For this purpose a reusable calibration disc was produced, which allowed for measurement of calibration solutions on-disc, with off-disc mixing. Half of the centre PMMA layer (containing 2 optical detection zones) was substituted with cyclic olefin copolymer (COP) (Zeonex® 408R, from Zeon Europe GmbH, Germany), so that both Cr(III) and Cr(VI) could be simultaneously analysed on one disc. A Roland MDX-40A Milling Machine was used to manufacture this layer. It then underwent solvent vapour treatment with cyclohexane for 4 min, followed by heat treatment at 65^{o}C for 30 min to smooth the optical features.[21] The design consisted of the optical detection zone, with a fluid inlet for insertion and removal of standards. A washing step was included to ensure no sample carry over occurred. This calibration disk allowed for the characterisation of the optical detection system and optical pathway as an intermediate step in sensor validation.

4.2.4 Integrated device prototype

The ChromiSense system was 3D printed using a Stratasys uPrint Dimension SE 3D printer, from Acrylonitrile butadiene styrene (ABS) polymer, enabling rapid prototype generation.

All parts were purchased from Radionics Ltd., Ireland, unless otherwise stated. The optical detection system for Cr (VI) consists of a Cree 535 nm LED module (Part no: C503B-GAN-CB0F0791) and a Vishay silicon PIN photodiode (part number: BPW21R). An Ocean Optics 74 series collimating lens was used with the 535 nm LED. The detection system for Cr (III) consists of a 330 nm LED (UVTOP325-HL-TO39, 330 ± 5 nm, with a hemispherical lens, purchased from Roithner LaserTechnik GmbH) and a Centronic full spectrum silicon photodiode (part number: OSD5.8-7Q).

In order to include a heating step within the sensor housing, two heating mats (RS Pro, stock no. 245-506) attached to heat sinks (Spreadfast, part no. SF-CHS-606015-PC) were placed below the disc, to use the air currents created by the disc's rotation as a fan to circulate this heat. A heat seal was formed using a foam sealant tape (Pro power PPC119 Tape, Farnell Ltd., Ireland) to prevent heat loss from the disc compartment, while the lid was lined with insulating foil.

The ChromiSense platform was designed to directly complement the disc design. The system has a total mass of 2 kg, and dimensions of 20 x 18 x 15 cm. For absorbance measurements, a secondary stage was applied to the system for precise optical alignment, shown in Fig. 4.4. The optical detection system was configured for LED-PD pairing. These pairs were precisely aligned to transmit light through the optical detection zone of the disc. A USB controlled Wixel programmable module, purchased from Pololu™, was used to convert the PD output voltage into a digital signal. The data was logged using ExtraPuTTY terminal software. This data was converted into absorbance values using Eq. 4.1, where *blank* is the average ADC (Analog-to-Digital Converter) reading of a reagent blank (where n=3), and *sample* is the ADC reading (rane = 0 to 2047) of the sample under the same conditions.

$$\textbf{Eq. 4.1:}\quad \textbf{Absorbance} = \boldsymbol{log10}\left(\frac{\boldsymbol{Blank}}{\boldsymbol{Sample}}\right)$$

Functions of the system were controlled by entering text in the terminal window. The electronics board was stored in a separate compartment below the stage. The system is currently powered by a 12V AC-to-DC mains

power supply, making future battery incorporation for in-field analysis simple.

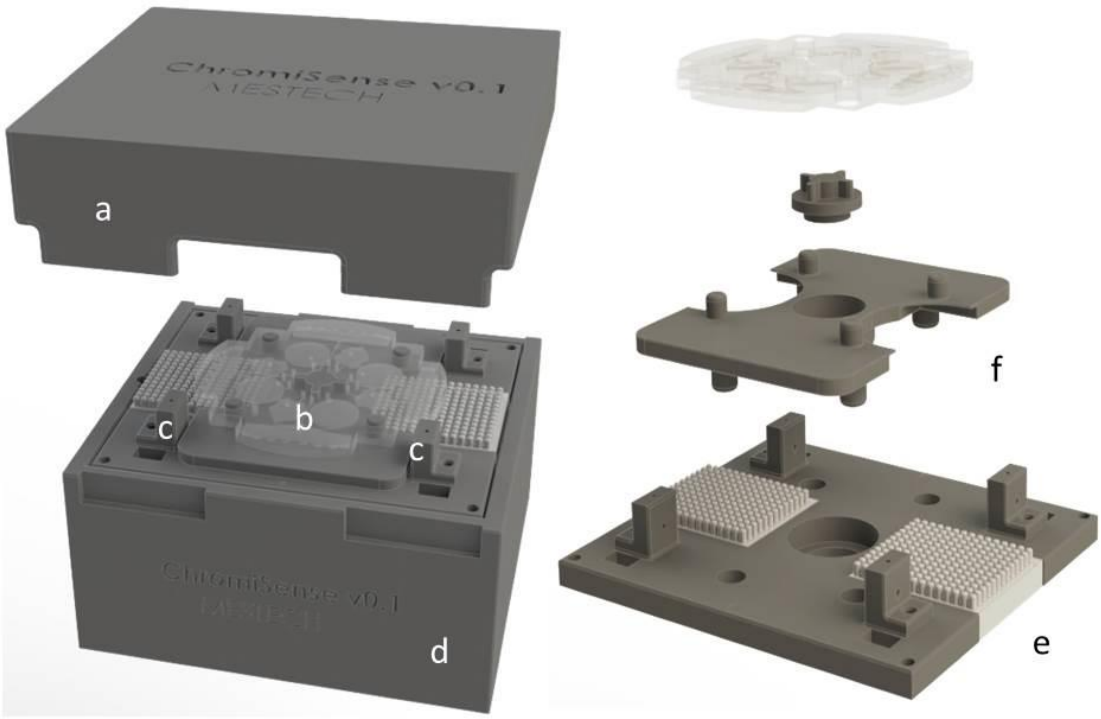

Fig. 4.4. A rendered image of the ChromiSense system (measuring 20 x 18 x 15 cm in total) where (a) is the lid for ambient light exclusion during optical measurements; (b) is the disc; (c) is the optical detection system consisting of an LED and PD couple; (d) is the compartment for storage of electronic components; (e) is the heating pads attached to heat sinks; (f) is the secondary stage for precise alignment of discs with the optical detection system.

4.2.5 Measurement on-disc

For Cr (VI), 910 µL of sample and 180 µL of pH 1 buffer were added into SA of the disc using a micropipette, and 455 µL of reagent were loaded into RR, as shown in Fig. 4.3. For Cr (III), 750 µL of sample and 180 µL of pH 10

buffer were placed in SR, and 400 µL of reagent was loaded in RR. When the disc was rotated at 10 Hz, the buffered sample and reagent were forced through the microchannels and into the ODZ. As this long reservoir filled, the air was displaced and released via a collapsible air ventilation system to prevent air bubble formation within the optical pathway.

Once the detection zone had filled, the disc was stopped and 5 min were allowed for complex formation. The disc was then rotated at 30 Hz to remove all air bubbles formed during the reaction. Any additional air bubbles remaining in the ODZ were moved into the bubble-trap structures at the bottom of the channel, which prevented them from affecting the absorbance measurements. The alignment stage shown in Fig. 4.3 was then used to accurately align the detection zone with the LED-PD light pathway. Cr(VI) was then measured. Once completed, the heating mats were switched on and the lid was closed. 20 min were allowed for heating the disc in order to drive the Cr(III)-PDCA reaction to completion. After one final rotation at 30 Hz to remove air bubbles, the alignment stage was reapplied for Cr(III) measurement.

Black acrylic paint was applied to the PMMA layers each side of the detection window to minimise light scattering and losses due to refraction. PMMA has a high refractive index of approximately 1.5, which can bend light away from the desired straight path.[22] The air vents and inlets were sealed using Loctite Silicomet AS 310 Transparent Silicone Sealant Paste (Radionics Ltd., Ireland) to prevent the solution from evaporating out of the disc.

The LOD and LOQ were calculated by multiplying the standard deviation of the reagent blank by 3 or 10, respectively, followed by division of this value by the slope of the calibration curve.

4.3 Results and discussion

The aims of this work were to design, fabricate and demonstrate the analytical performance of a centrifugal sensor for chromium speciation in water. This system was successfully fabricated and its analytical performance on lab standards and spiked real samples is presented. Two different analytical methods were automated on-disc, including a heating step, allowing for simultaneous measurement of two chromium species on one disc.

4.3.1 Calibrations and real samples

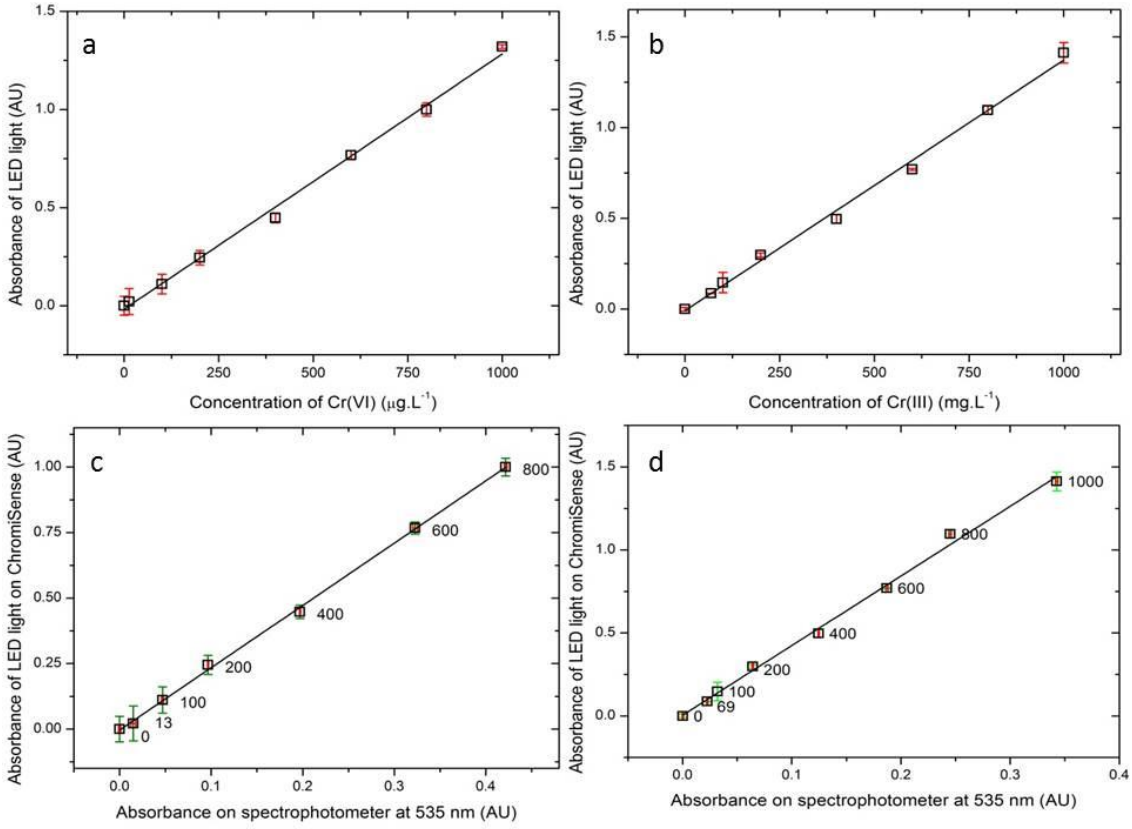

Fig. 4.5. Calibration curves for Cr(VI) (a) and Cr(III) (b), and correlation plots for the measurement of the Cr(III) (c, R^2=0.995) and Cr(VI) (d, R^2=0.999) standards on ChromiSense vs. using a spectrophotometer, where n=3.

A comparison between the analytical performance of ChromiSense and the same colourimetric methods measured using the spectrophotometer is summarised in Table 4.1, with calibration and correlation plots shown in Fig. 4.5. The longer optical path length of 50 mm on-disc contributed to the improved sensitivity of the system compared to the traditional 10 mm spectrophotometric method. Cr(VI) analysis was 2.6 times more sensitive on ChromiSense, while Cr(III) was 4.7 times more sensitive. While the LOD and LOQ values were lower for Cr(VI) on ChromiSense, the higher standard deviations seen for Cr(III) led to a higher LOD and LOQ compared to the spectrophotometric method (see Table 4.1). A wider linear range of 14-1000 µg L^{-1} was seen for Cr(VI) on ChromiSense compared to 23-800 µg L^{-1} on the spectrophotometer, while the same upper range limit of 1000 mg L^{-1} was observed using both methods for Cr(III). R^2 values above 0.99 were seen for all methods, showing excellent agreement to the linear response model, in agreement with the Beer-Lambert law. Standard deviations were higher for the ChromiSense prototype, as shown in the error bars in Fig. 4.5. As each disc was aligned and assembled by hand, this variation is to be expected. It could be improved upon in the future by using a more reproducible fabrication method such as injection moulding or 3D printing.

Table 4.1. Comparison of the analytical performance of ChromiSense and the reference spectrophotometric method, where Cr(VI) is in μg L^{-1} and Cr(III) is in mg L^{-1}.

Analytical method	Path length (mm)	Slope	LOD	LOQ	Linear range	R^2
ChromiSense						
Cr(VI)	50	0.0013	4	14	14-1000	0.996
Cr(III)	50	0.0014	21	69	69-1000	0.9957
Spectrophotometer						
Cr(VI)	10	0.0005	7	23	23-800	0.9976
Cr(III)	10	0.0003	6	19	19-1000	0.9931

ChromiSense was applied to the measurement of spiked river water samples. The results of this analysis are shown in Table 4.2. These measurements demonstrated good agreement with the spectrophotometric method, showing errors of 6% or less.

Table 4.2. Performance ChromiSense with reference measurements from the spectrophotometer, showing measurement and % error for spiked river water samples, where n=3.

Method	Concentration for low spike (mg L^{-1})	% error	Concentration for high spike (mg L^{-1})	% error
Cr(III)				
Spectrophotometer	93	11.7	804.4	1.7
ChromiSense	92.6	1.8	746	6
Cr(VI)				
Spectrophotometer	208.7	0.9	792.7	4.3
ChromiSense	209.7	4.3	801	3.2

4.3.2 Reusable calibration disc

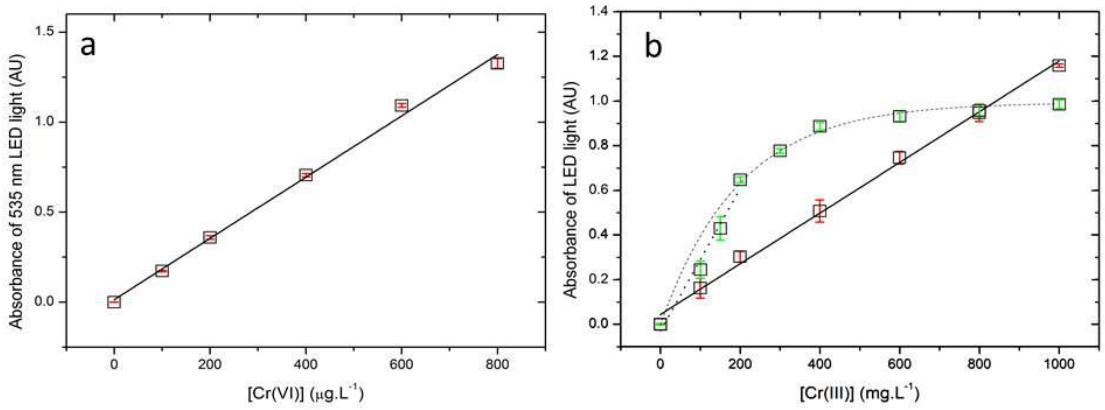

Fig. 4.6. Calibration curves for Cr(VI) (a) and Cr(III) (b) at 535 nm (solid line) and Cr(III) at 330 nm (dotted line for linear range, dashed line for exponential fit) using the calibration disc and ChromiSense optical detection system, n=3.

Fig. 4.6 shows the absorbance values obtained from the LED-PD pairs installed on the ChromiSense system, using the calibration disc. Mixing of sample and reagent was performed off-chip, allowing for testing of the detection system through the disc detection pathway, without any influence from on-disc mixing or heating efficiency. Table 4.3 shows the analytical performance of the detection system from this study. An LOD of 1.5 µg L^{-1} for Cr(VI) was achieved with this method. Only a small difference in LOD was seen for Cr(III) using the visible wavelength compared to the UV wavelength. The sensitivity was 2.5 times greater at the UV wavelength, however the linear range was greatly diminished from 1000 mg L^{-1} (at 535 nm) to 200 mg L^{-1} (at 330 nm). Additionally, the milling method of disc fabrication for COP (necessary for UV detection) added greatly to the manufacture time of the discs. For these reasons, 535 nm was used as the detection wavelength for both analytes.

Table 4.3. The analytical performance of ChromiSense using the calibration discs, with all measurements for Cr(VI) in µg L^{-1} and for Cr(III) in mg L^{-1}.

Analyte and wavelength (nm)	LOD	LOQ	R^2	Sensitivity	Upper limit of linear range measured
Cr(VI) at 535 nm	1.5	5	0.995	0.0017 AU L μg^{-1}	800
Cr(III) at 535 nm	4.5	15.2	0.992	0.0012 AU L mg^{-1}	At least 1000
Cr(III) at 330 nm	2.9	9.6	0.975	0.003 AU L mg^{-1}	200

4.3.3.System design and fabrication

A study was carried out to determine the optimal optical path length for absorbance measurements on-disc. This was carried out using a 3D printed cuvette holder, as described in a previous publication by this team.[23] The absorbance of a range of standards was recorded over a range of different path lengths. Based on the disc dimensions, the maximum path length that can be incorporated is 75 mm, as previously reported.[23] This would allow for one Cr(VI) zone and one Cr(III) zone per disc. By using the smaller path length of 50 mm, which performed well according to the above data in Table 4.4, two analytical zones per analyte were incorporated onto one disc. This path length gave excellent analytical performance for Cr(VI), and good performance for Cr(III), compared to the spectrophotometry data. The sensitivity increased linearly for all three methods with increasing path length. The LOD and LOQ decreased with increasing path length, while excellent agreement with a linear model was seen with most R2 values above 0.99.

Table 4.4. The LOD, LOQ, R^2 value and sensitivity for Cr(VI) at 535 nm and Cr(III) at 535 nm and 330 nm at different optical path lengths.

Path length (mm)	LOD	LOQ	R^2	Sensitivity
Cr (VI) at 535 nm	**µg L^{-1}**	**µg L^{-1}**		**AU L µg^{-1}**
1	110	366	0.9803	0.00005
2	80	268	0.9917	0.00009
5	40	134	0.994	0.0002
10	12	40	0.9958	0.0004
50	11	38	0.9996	0.002
100	13	42	0.9965	0.0039
Cr (III) at 535 nm	**mg L^{-1}**	**mg L^{-1}**		**AU L mg^{-1}**
1	110	366	0.9988	0.00003
2	80	268	0.9921	0.00005
5	40	134	0.9965	0.0001
10	12	40	0.9951	0.0002
50	6	20	0.9881	0.0014
100	7	21	0.991	0.0025
Cr(III) at 335 nm	**mg L^{-1}**	**mg L^{-1}**		**AU L mg^{-1}**
1	169	565	0.9945	0.0001
2	60	200	0.9994	0.0002
5	29	98	0.9997	0.0006
10	21	70	0.9999	0.0012
50	9	30	0.988	0.0043
100	8	25	0.9637	0.008

The reagent reservoir shape was optimised to facilitate ease of reagent loading, due to the low viscosity of the methanol-based reagent compared to aqueous solutions. As shown in Fig. 4.7, loading of low viscosity solutions into a circle-shaped reservoir was inefficient. Less than 50% of the fluid volume was successfully loaded into the reservoir. The proposed shield shape provided more surface area along the walls of the reservoir for the solution to come in contact with. This facilitated a greatly improved filling capability, reaching percentages much closer to 100%. Once the viscosity of water (0.89 mPa.s)[24] and above was reached, both reservoir shapes filled to 100% capacity. The greatest difference in loading success can be seen for the low viscosity liquids. Additionally, loading of two smaller volumes was found to be more efficient that one larger volume.

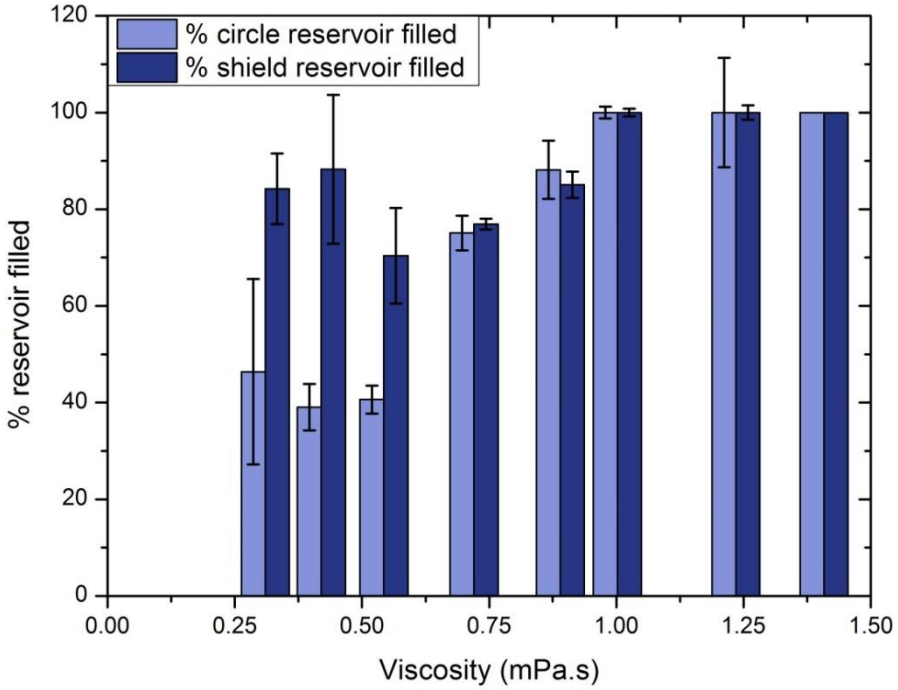

Fig. 4.7. A bar chart depicting the improved filling capability of the shield-shaped reservoir for low viscosity fluids, compared to that of the circle-shaped reservoir.

4.3.4 Analytical method development

Cr(VI)

In order to automate the standard diphenyl carbazide reaction on a centrifugal disc, the method was simplified. The standard colourimeteric method for Cr(VI) calls for addition of phosphoric acid, followed by the gradual addition of sulphuric acid to adjust the pH, using a pH meter. The sample is then diluted in a volumetric flask before the addition of the DPC reagent.[5] In order to simplify this method for incorporation onto a centrifugal disc, a KCl-HCl buffer was employed to achieve the recommended pH of 1.00 ± 0.3. This removed the need for both acids. The sample dilution step was also removed. The solvent for DPC was changed from acetone to methanol due to PMMA compatibility issues. A T-test was used to show that this change in solvent did not significantly change the absorbance values obtained, at a 95% confidence interval. Storage in methanol was found to reduce the stability of the reagent, compared to storage in acetone. The methanol-based reagent discoloured more rapidly, however both lasted several days while stored in the dark at 4^{o}C. If not stored in the dark, slight discolouration was seen after one day. This became more pronounced each day.

The ratio of buffer and ratio of reagent to the sample volume were optimised to minimise dilution of the coloured product and to maximise the sensitivity of the method, thus achieving a lower detection limit.

While the [Cr(DPC)] solution generated an orange colour over time, this did not affect the absorbance of the solution at 535 nm. The development of the orange colour can be seen at lower wavelengths in Fig. 4.8 (b). A decrease in absorbance of 1.3% was seen for a [Cr(DPC)] solution at 535 nm after 1 month, with no special storage conditions. The stability of the solution over 1 month is demonstrated in Fig. 4.8 (d).

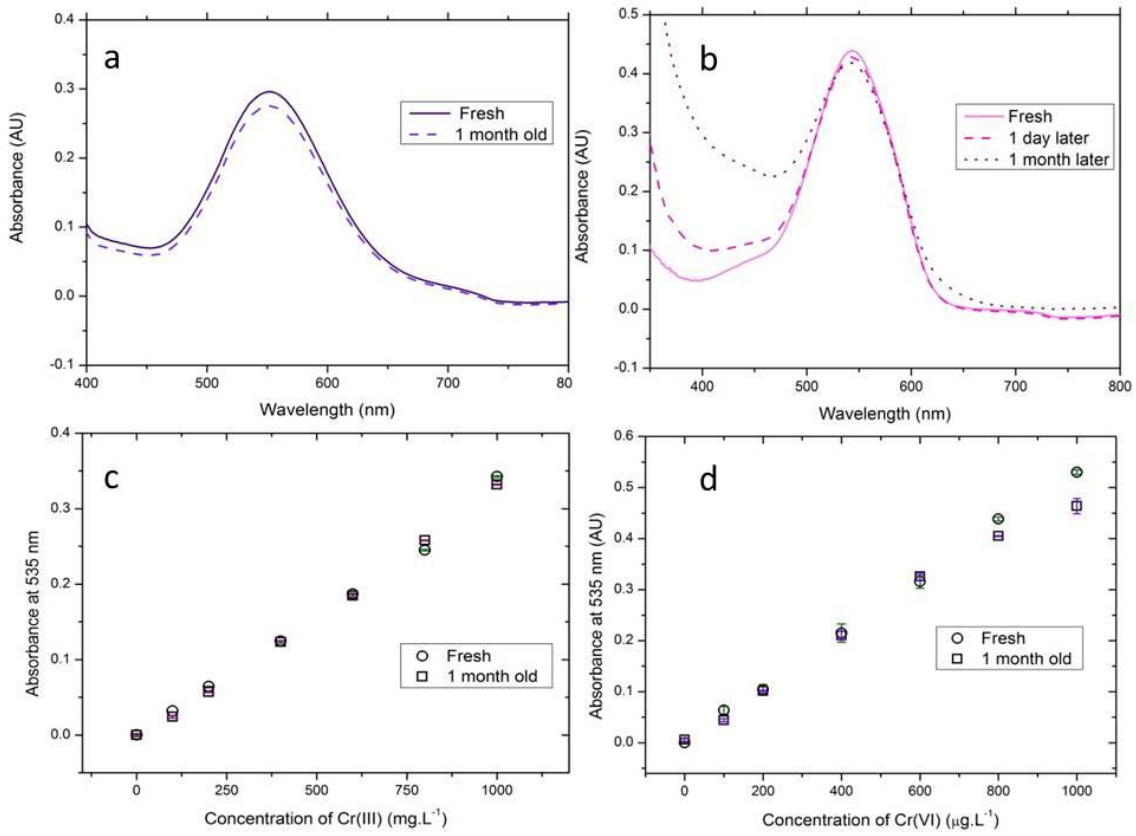

Fig. 4.8. The absorbance spectra of $[Cr(PDCA)_2]$ (a) showing a freshly made and a 1 month old solution of the purple coloured complex, and [Cr(DPC)] (b) showing a freshly made, a 1 day old and a 1 month old solution of the pink coloured complex, with calibration curves for freshly made and 1 month old solutions of $[Cr(PDCA)_2]$ (c) and [Cr(DPC)] (d).

Cr(III)

Fig. 4.8 (a) shows the good stability of the purple complex formed from Cr(III) and PDCA, with a decrease in absorbance of approx. 6% after 1 month, with no special storage conditions. A 3 month old PDCA solution stored under ambient conditions showed excellent correlation to the absorbance measurements

obtained using fresh PDCA solution, as shown in Fig. 4.8 (c). A T-test was used to show that they were not statistically different at a 95% confidence interval.

The method for chromium (III) was optimised in terms of solvent, reagent concentration, heating temperature, heating duration, pH and the volume ratio of buffer and reagent to sample.

Methanol proved to be the optimal solvent for this method as it dissolved the ligand with ease, and was compatible with the disc materials. A rapid complex formation time of 5 min at 65^{o}C was achieved. The heating temperatures of 50, 55 and 65^{o}C were tested. The highest temperature of 65^{o}C resulted in maximum absorbance after 5 min, compared to 10 min at 55^{o}C and 15 min at 50^{o}C. In the absence of applied heat, this reaction is very sluggish, and reaches only ~86% colour formation compared to that of the 65^{o}C sample, after 2 days at room temperature.

The optimal pH was found by measuring the absorbance of a Cr (III) sample over the pH range of 1-12, in increments of 1 pH unit. Maximum absorbance was measured at pH 10.

While the [Cr(PDCA)$_2$] complex absorbs strongly in the UV region, it also has a weaker, broad absorbance band that peaks at approximately 550 nm, meaning that it could also be measured at the same wavelength as that of the Cr (VI) detection LED-PD couple.

4.4 Conclusion

A fully integrated, centrifugal sensor with an optical detection system for chromium speciation was designed, fabricated and its performance was characterised. The sensor showed similar performance to that obtained when carrying out the same analytical methods using a spectrophotometer. The sensitivity on ChromiSense was 2.6 times greater for Cr (VI) and 4.7 times greater for Cr (III). An LOD and LOQ of 4 and 14 µg L^{-1} for Cr (VI) and 21 and 69 mg L^{-1} for Cr (III) were achieved. While this is

well below the legislative levels for Cr (VI) in drinking water, it is quite high for Cr (III). This makes the sensor suitable for measurement of industrial effluent waters. Incorporation of a pre-concentration method, such as those mentioned in the introduction, prior to on-disc analysis, could make this method suitable for analysis of environmental samples.

The performance of the system for Cr (III) was determined at 335 nm (using COP) and 535 nm (using PMMA). The linear range at 335 nm was greatly reduced at 10-200 mg L^{-1}, compared to 15-1000 mg L^{-1} at 535 nm. The LOD and LOQ only differed by 2 and 6 mg L^{-1}, respectively, making the visible wavelength a much better option.

The reservoir shape on the microfluidic disc was optimised for ease of loading for low viscosity liquids. The greater internal surface area along the walls of the shield-shaped reservoir allowed the methanol based reagents to be loaded with ease. Circular reservoirs were shown to perform better for loading of aqueous fluids, and poorly for low viscosity fluids.

This centrifugal colourimetric device acts as a proof-of-principle, where a simple change in disc design and LED detection wavelength enables new colourimetric methods to be carried out, and for new analytes to be determined, demonstrating the versatility of the system design. Future steps to improve this system would be to include a motor and to use a 12 V battery so that they system can be taken out of the lab and used to measure samples at the sampling site.

Notes and references

1. F.A. Byrdy, L.K. Olson, N.P. Vela, J.A. Caruso, Chromium speciation by anion-exchange high-performance liquid chromatography with both inductively coupled plasma atomic emission spectroscopic and

inductively coupled plasma mass spectrometric detection, J. Chromatogr. A. 712 (1995) 311–320. doi:10.1016/0021-9673(95)00528-U.

2. V. Gomez, M.P. Callao, Chromium determination and speciation since 2000, Trends Anal. Chem. 25 (2006) 1006–1015. doi:10.1016/j.trac.2006.06.010.
3. R. Świetlik, Speciation analysis of chromium in waters, Polish J. Environ. Stud. 7 (1998) 257–266.
4. K.-C. Hsu, C.-C. Sun, Y.-C. Ling, S.-J. Jiang, Y.-L. Huang, An on-line microfluidic device coupled with inductively coupled plasma mass spectrometry for chromium speciation, J. Anal. At. Spectrom. 28 (2013) 1320–1326. doi:10.1039/c3ja50030f.
5. 'Chromium in Drinking-water', Guidelines for drinking-water quality, 2nd ed. Vol. 2. Health criteria and other supporting information. World Health Organization, Geneva, 1996.
6. R. Gorkin, J. Park, J. Siegrist, M. Amasia, B.S. Lee, J.-M. Park, J. Kim, H. Kim, M. Madou, Y.-K. Cho, Centrifugal microfluidics for biomedical applications, Lab Chip. 10 (2010) 1758–1773. doi:10.1039/b924109d.
7. Z. Chen, R. Naidu, A. Subramanian, Separation of chromium (III) and chromium (VI) by capillary electrophoresis using 2,6-pyridinedicarboxylic acid as a pre-column complexation agent, Journal of Chromatography A, 927 (2001) 219–227.
8. C. Ehrling, U. Schmidt, H. Liebscher, Analysis of chromium(III)-fluoride-complexes by ion chromatography, Anal. Bioanal. Chem. 354 (1996) 870-873. doi:10.1007/s0021663540870.
9. H. Gürleyük, D. Wallschläger, Determination of chromium(III) and chromium(VI) using suppressed ion chromatography inductively coupled plasma mass spectrometry, J. Anal. At. Spectrom. 16 (2001) 926–930. doi:10.1039/B102740A.

10. K. Girish Kumar and R. Muthuselvi, Spectrophotometric Determination of Chromium(III) with 2-Hydroxybenzaldiminoglycine, J. Anal. Chem. 61 (2006) 28–31. doi:10.1134/S1061934806010072
11. Himeno, Sadayuki, Yoichi Nakashima, and Ken-ichi Sano, Simultaneous determination of chromium (VI) and chromium (III) by capillary electrophoresis. Analytical sciences, 14, 1998, 369-373.
12. R.T. Pflaum, L.C. Howick, The chromium-diphenylcarbazide reaction, J. Am. Chem. Soc. 78 (1956) 4862–4866. doi:10.1021/ja01600a014.
13. A. E. Greenberg, L. S. Clesceri, A. D. Eaton. Standard Methods for the Examination of Water and Wastewater. 18th ed. 1992.
14. G. J. Willems, N. M. Blaton, O. M. Peeters, C. J. De Ranter, The interaction of chromium (VI), chromium (III) and chromium (II) with diphenylcarbazide, diphenylcarbazone and diphenylcarbadiazone. Anal. Chim. Acta. 88 (1977) 345-352. doi: 10.1016/S0003-2670(01)95909-4.
15. N.M. Halim, V. Abramov, I. Pantenburg, G. Meyer, Two New Chromium (III) Complexes with the Pincer-type Pyridine-2,6-dicarboxylate Ligand, Z. Naturforsch. 66 (2011) 685–688. doi: 10.1515/znb-2011-0706.
16. K. Ashley, A.M. Howe, M. Demange, O. Nygren, Sampling and analysis considerations for the determination of hexavalent chromium in workplace, J. Environ. Monit. 5 (2003) 707. doi:10.1039/b306105c.
17. E. Duffy, R. Padovani, X. He, R. Gorkin, E. Vereshchagina, J. Ducrée, E. Nesterenko, P.N. Nesterenko, D. Brabazon, B. Paull, M. Vázquez, New strategies for stationary phase integration within centrifugal microfluidic platforms for applications in sample preparation and pre-concentration, Anal. Methods. (2017). doi:10.1039/C7AY00127D.
18. M. Vázquez, D. Brabazon, F. Shang, J.O. Omamogho, J.D. Glennon, B. Paull, Centrifugally-driven sample extraction, preconcentration and

purification in microfluidic compact discs, Trends Anal. Chem. 30 (2011) 1575–1586. doi:10.1016/j.trac.2011.07.007.

19. J.P. Lafleur, E.D. Salin, Pre-concentration of trace metals on centrifugal microfluidic discs with direct determination by laser ablation coupled plasma mass spectrometry, J. Anal. At. Spectrom. 24 (2009) 1511–1516. doi:10.1021/ac8010582.
20. W.R. Gambill, How to estimate mixtures viscosities, Chem. Eng., 66 (1959) 151-152.
21. I.R.G. Ogilvie, V.J. Sieben, C.F.A. Floquet, R. Zmijan, M.C. Mowlem, Reduction of surface roughness for optical quality microfluidic devices in PMMA and COC, J. Micromechanics Microengineering. 20 (2010) 1–8. doi:10.1088/0960-1317/20/6/065016.
22. J. M. Cariou, J. Dugas, L. Martin, and P. Michel, Refractive-index variations with temperature of PMMA and polycarbonate, Applied Optics, 25 (1986) 334-336.
23. G. Duffy, I. Maguire, B. Heery, C. Nwankire, J. Ducrée, F. Regan, PhosphaSense: A fully integrated, portable lab-on-a-disc device for phosphate determination in water, Sensors Actuators B Chem. 246 (2016) 1085–1091. doi:10.1016/j.snb.2016.12.040.
24. L. Korson, W. Drost-Hansen, and F. J. Millero. Viscosity of water at various temperatures, J. Phys. Chem. 73 (1969) 34-39. doi:10.1021/j100721a006.

Chapter 5:
AutoPhos

Field-based assessment of the analytical performance of novel phosphate sensors for water monitoring.

G. Duffy,[a] P. McCluskey[b], U. H. Mahl[c], N. Kent[b], J. Tank[c], D. Diamond[b] and F. Regan[a]

[a] Marine Environmental Sensing Technology Hub, Dublin City University, Glasnevin, Dublin 9, Ireland

[b] Insight, Centre for Data Analytics, National Centre for Sensor Research, Dublin City University, Dublin 9, Ireland

[c] University of Notre Dame, Department of Biological Sciences, Notre Dame IN, 46556, USA

Prepared for Submission to peer reviewed journal.

Aims and Objectives

Chapter 5 describes the field-based characterisation of two novel phosphate sensors. PhosphaSense, first introduced in Chapter 3, was applied to the measurement of field samples and compared to the performance of an autonomous phosphate sensor (AutoPhos) developed in collaboration with Prof. Dermot Diamond's research group in DCU. These systems were taken from DCU to University of Notre Dame, Indiana, USA, as part of a collaboration with Prof. Jennifer Tank. Phosphate is typically found at very low part per billion levels in

stream water (< 70 µg L^{-1}). While this can be measured using PhosphaSense, it is below the detection limit of AutoPhos. However, during pollution events such as run-off during a storm, levels can reach the mg L^{-1} range, which lies above the linear range of PhosphaSense. However, it is now within the wide measurement range of the AutoPhos system. Field samples were collected from an agricultural stream while a nutrient pulse was performed. This pulse meant that water samples across a wide range of concentrations would be collected for analysis, covering the analysis range of both sensor systems, and representing the range of concentrations that can be encountered in the environment. The use of an autonomous and a handheld sensor system was compared in this chapter, showing the pros and cons of each sensing approach from a development point of view. The in-field performance of AutoPhos was demonstrated and compared with its in-lab performance, and the in-lab performance of PhosphaSense.

Abstract

Autonomous sensors for phosphate measurement in water are currently expensive to purchase and to run. The alternative, lower cost hand-held sensors for in-field measurements typically cannot measure low concentrations of phosphate. High frequency monitoring of phosphate is essential for effective water catchment management. The performance characterisation and comparison of two phosphate sensors is reported; one autonomous and one handheld. A centrifugal microfluidic disc system based on the molybdenum blue colourimetric method (PhosphaSense) was shown to have higher sensitivity and a lower, narrower linear range, while a syringe pump driven, microfluidic chip system based on the vanadomolybdophosphoric acid colourimetric method (AutoPhos), responded linearly at a higher concentration range with a higher detection limit. While PhosphaSense was designed as a handheld analyser for in-field analysis, AutoPhos was designed for long-term deployment for continuous, unattended measurement. Stability and robustness of the sensors was demonstrated by comparing the calibration curves obtained on two different continents. The LOQ of PhosphaSense and AutoPhos were found to be 18 µg L^{-1} and 0.4 mg L^{-1} PO_4-P, respectively. The linear range of PhosphaSense was 18-800 µg L^{-1}, while it was 0.4-10 mg L^{-1} for AutoPhos. In order to provide water samples that both systems could detect, a nutrient pulse experiment was performed within an agricultural stream. This nutrient pulse could represent a pollution event such as that during a storm event or from events such as discharge from a waste water treatment plant. Both sensor systems were applied to the measurement of collected field samples from this nutrient pulse, yielding average percentage error for field sample measurements of 1.7% for PhosphaSense and 9% for AutoPhos, within their stated operating ranges. PhosphaSense was also used for in-field analysis, where it yielded average percentage errors of 13%.

5.1 Introduction

Phosphorus (P) monitoring in environmental waters and industrial effluent is essential due to its growth limiting nature. P is an essential nutrient used by all living organisms for growth and energy transport. Intensive agriculture has resulted in an increased demand for P for use as fertiliser. Some of this P is transported from soil into streams and rivers by rain water. Elevated levels of P in water bodies stimulates excessive growth of plants and algae leading to eutrophication, hypoxia, death of biota and harmful algal blooms.[1-3]

There is a growing demand for reliable, low-cost P sensors as populations grow, agriculture intensifies further and water resources become even more valuable. Fertiliser use has increased hugely since the 1940s in order to meet the food demands of a rapidly growing population. This has resulted in accumulation of P in catchments, with negative environmental consequences.

In order to understand accumulation and depletion of P in a catchment, long-term monitoring is required.[4]

The phosphate concentrations encountered in surface waters range from 0.01-0.07 mg L^{-1} for unpolluted waters, with levels greater than 0.1 mg L^{-1} being indicative of accelerated growth.[5] The range of phosphate concentrations observed from different anthropogenic sources in water was summarised by Withers *et al.* in 2008, revealing that the mean concentration of phosphates observed were as follows; wastewater (6.63 mg L^{-1}), septic tanks (10.2 mg L^{-1}), road/track runoff (2.39 mg L^{-1}), farmyards (30.8 mg L^{-1}), field surface runoff (1.29 mg L^{-1}) and field tile drains (0.79 mg L^{-1}).[6]

An affordable network of phosphate sensors for continuous, real-time monitoring, providing temporal and spatial variations in phosphate levels, is essential for the management of water quality. However this is currently a very expensive undertaking. In order for sensor networks to become feasible, the cost per sensor and per measurement must decrease. Alternatively, systems capable of in-field, rapid sample-to-answer measurements are also a more convenient alternative to traditional grab sampling with laboratory-based analysis, removing

the sample transport and storage steps from the process. This article compares the analytical performance of one autonomous and one handheld phosphate sensor, both of which were developed in-house, based on their analytical performance both in the laboratory calibrations and on field samples.

There are multiple standard colourimetric methods for phosphate determination in water. The syringe pump-driven microfluidic chip-based sensor (AutoPhos) operates using the vanadomolybdophosphoric acid method (or simply the 'yellow method'), while the centrifugal sensor (PhosphaSense)[7] operates using the ascorbic acid 'blue method'. Both sensors measure the absorbance of the coloured product using a low-cost detection system consisting of a light emitting diode (LED) and photodiode (PD) pair.

The vanadomolybdophosphoric acid method involves the addition of one reagent to a water sample in a 1:1 volume ratio. Under acidic conditions, phosphate reacts with ammonium molybdate to form molybdophosphoric acid ($H_3Mo_{12}O_{40}P$), a keggin structure heteropoly acid.[8] In the presence of vanadium, vanadomolybdophosphoric acid is formed, which absorbs in the yellow region of the spectrum.[9]

This method has been successfully applied to the development of deployable phosphate analysers due to the stability of the reagent (over 1 year), the stability of the yellow product, vanadomolybdophosphoric acid (days), and its insensitivity to temperature fluctuations.[9-13] As AutoPhos is intended for long-term deployments, this method was used.

In contrast, PhosphaSense is intended for in-field measurements, and therefore reagent stability is not an issue. The ascorbic acid method involves the addition of a combined reagent to a water sample in a 1:6.25 volume ratio, resulting in a phosphomolybdenum blue complex that absorbs strongly at 880 nm.[7,14] The combined reagent is stable for only a few hours, while the ascorbic acid component alone is stable for up to one week, if refrigerated.[10] The other components of the combined reagent are stable for months. According to another source, ascorbic acid in water is stable for 18 days.[14] This poor stability

makes it unsuitable for long-term deployments, however the superior sensitivity of the method makes it a good option for use in the handheld system, allowing for a lower LOD to be achieved. This method is used on the Wetlab's Cycle-P phosphate sensor, which claims a reagent stability of over 3 months, showing that with special storage, this method can be used for longer term sensor deployments also.[15]

There are several examples of centrifugal microfluidic sensor systems with optical detection that were applied to water analysis in the literature. The analytes or parameters measured include nitrate, nitrite, phosphate, silicate, ammonium, pH, turbidity and hexavalent chromium.[16-20] However some of these examples incorporate expensive light sources and detectors. Substitution with low-cost LEDs and PDs, as shown with the PhosphaSense or CMAS systems, allows for a significant reduction in the component cost of the sensor.[16,17,20]

Colourimetric chemical analysis has also been applied to microfluidic systems for long-term deployment. Some analytes measured in this manner include nitrate, nitrite, pH, phosphate, ammonium and silicate.[11,12,21, 22-27] These systems use fluid pumps (solenoid, syringe, peristaltic) for sample and reagent delivery to a microfluidic chip, followed by absorbance measurements using an LED and PD or spectrophotometric detection system. While the need for multiple fluid pumps can increase the component cost for these systems, the microfluidic chip is reused. This differs from the disposable microfluidic discs, most of which contain solid reagents sealed within reservoirs, ready for single use. Data was either stored on a memory card or sent wirelessly to the user. Applications of autonomous microfluidic systems in environmental monitoring was reviewed by Campos *et al.* in 2013.[28]

5.2 Experimental

5.2.1 Reagents and standards

In Ireland, standards were made from a 50 μg L^{-1} PO_4-P stock solution of potassium diphosphate monobasic (Sigma Aldrich, Ireland). All reagents were ACS grade and were purchased from Sigma Aldrich, Arklow, Ireland. All solutions were made in ultra-pure water (Elga Maxima®, 18.2 MΩ). The reagent for the vanadomolybdophosphoric acid method was made of 0.02 M ammonium molybdate tetrahydrate, 0.01 M ammonium metavanadate and 4 M HCl. The reagents for the ascorbic acid method were prepared as previously published.[7]

In the USA, the same reagents and concentrations were used, all purchased from Fisher Scientific, except for potassium antimonyl tartrate, which was purchased from Sigma Aldrich. Sulfuric and hydrochloric acids were both purchased from VWR. All reagents were ACS grade. Standards and reagents were prepared in Nanopure deionised water (Barnsted®, 18.0 MΩ).

5.2.2 AutoPhos system

This system operates using motor driven syringe pumps, as illustrated in Fig. 5.1. A similar design to this was previously published in 2016.[21] Using a two-way valve (DCV114-001, Nordson Medical), the 1 mL syringe could be filled from a reagent bottle, and then emptied into tubing leading to the microfluidic chip.

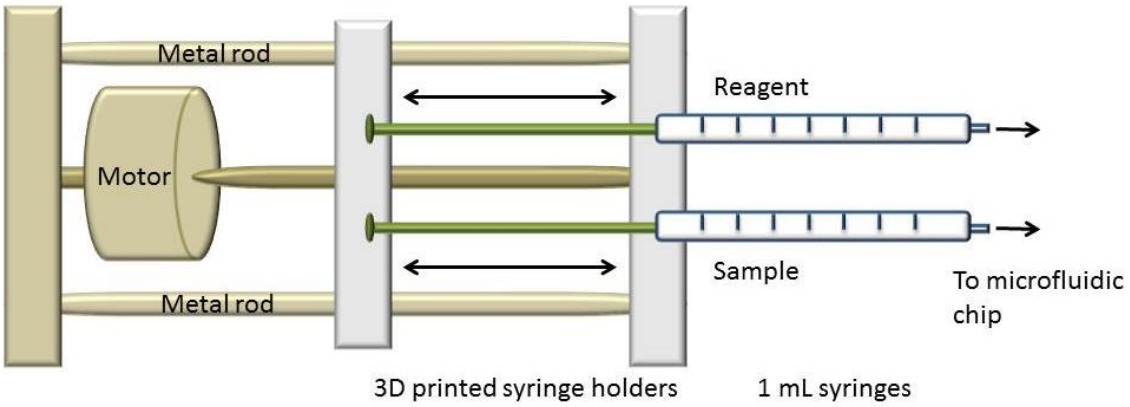

Fig. 5.1. A schematic of the syringe pump system, where the motor rotates a metal screw, which moves the 3D printed syringe holder up and down along the crew threads, along the metal rods.

As shown in Fig. 5.1, the plunger is secured into the 3D printed holder. It is either pulled out of or pushed into the barrel of the syringe when the motor rotates the central screw rod, moving the plunger holder along the screw threads. The direction of the motor dictates whether the syringe is filled or emptied.

Sample measurement frequency was 1 sample every 10 min. This allowed for 1 min of pumping time for sample and reagent onto the chip, 6 min of colour development time, 1 min of absorbance measurement time, and 2 min of chip flushing time to prevent sample carryover to the next measurement.

Between the microfluidic chip and the syringe, a one-way valve (SCV67220, Nordson Medical) was included in the tubing (1.6 mm inner diameter Tygon® formula 2375, Sigma Aldrich) to prevent backward flow of fluid from the chip.

An Arduino programmable module was used to control the motors, LED and photodiode function. The system could be programmed to run autonomously, with data storage on an SD card.

The reagent, phosphate standard and deionised water for the reagent blank and for channel flushing were stored in the system in polystyrene containers, with tubing connecting them to the syringe pump intake valve. This meant that the

system could be calibrated with the phosphate standad and a reagent blank in between sample measurements.

A sample intake system was incorporated to allow for unattended monitoring. It consisted of a Xylem Flojet Pump (Radionics Ltd., Ireland, stock no. 705-9324), a Flojet strainer to remove debris and larger particles (Raptor Supplies Ltd, item no. GR0498359), and a Whatman Polycap HD 36 Polypropylene Capsule Filter for removal of fine particles. A 12 V lead acid battery (Yuasa NP12-12) was used to power the sensor in-field. The sensor was enclosed within a 1600 PeliCase water tight and crush proof protective case.

5.2.3 AutoPhos Chip

The chip contains 3 T-junctions for mixing of sample and reagent. This provides separate mixing channels for a high standard, a reagent blank and a sample on the chip. Each of these T-junctions is connected to a pair of syringe pumps, as shown in Fig. 5.1. Only one of these mixing channels is used at a time, as there is only one detection zone. The mixed product moves from the T-junction towards the waste outlet. When flow is stopped, the optical detection channel, located just before the waste outlet, is filled with the coloured product, ready for measurement with the LED-PD detection system. This detection system is carefully aligned to direct light through a microfluidic channel and onto the PD.

The chip was fabricated using tinted PMMA (Plexiglas GS 7F60, Röhm) and composed of three layers. The two main layers contained microchannels and optical components, while a smaller cap was used to attach PTFE tubing directly to the chip. Channels were 300 µm deep and 200 µm wide, with the exception of the measurement channel which was 300 µm wide. All features were created using a LPKF mill. The two main layers were bonded using a solvent vapour bonding method. The LED (a 385 nm LED from Farnell, Ireland) and photodiode (AMS - TSL257-LF) were aligned by hand and bonded to the chip using UV-curable optical adhesive (Norland NOA-78).

A similar microfluidic chip was previously published for determination of pH in water, and is here applied to determination of phosphate.[21] A schematic of the chip is shown in Fig. 5.2.

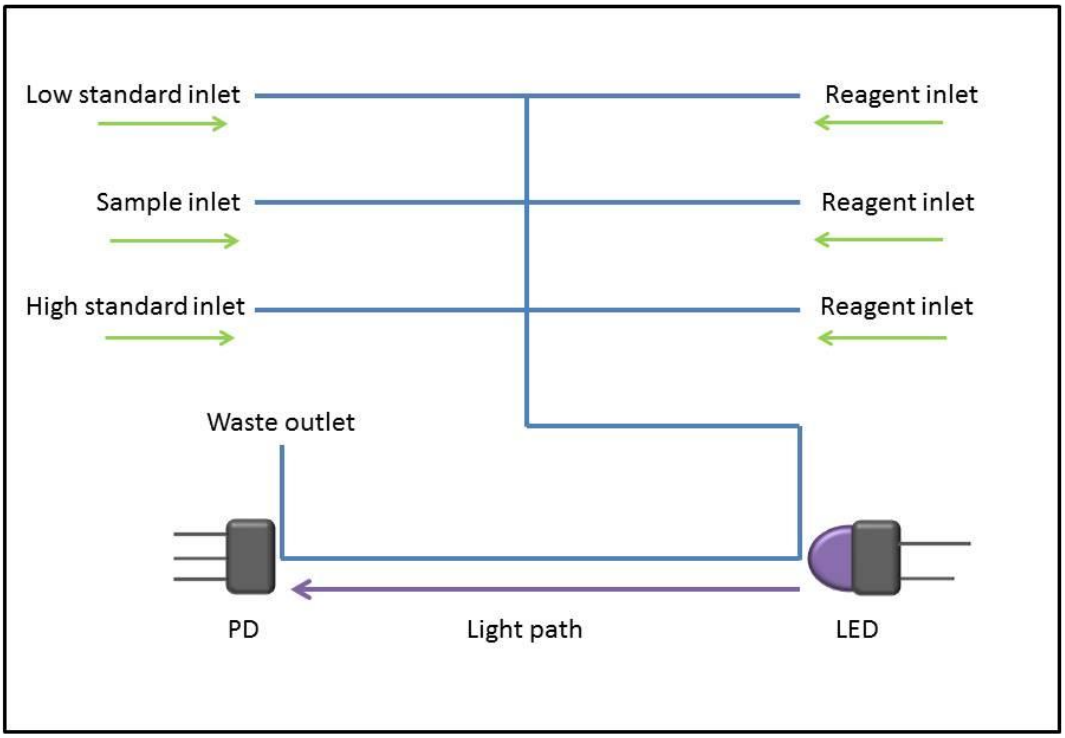

Fig. 5.2. A schematic of the microfluidic chip, showing 6 inlets, 1 outlet, 3 T-junctions for mixing, and 1 optical detection channel with an LED-PD pair for absorbance measurements.

5.2.4 PhosphaSense

PhosphaSense design, fabrication and performance was previously published.[7] The system consists of a disposable microfluidic disc on which the ascorbic acid method for phosphate determination is carried out. This disc is spun by an on-system motor in order to mix the sample and reagent. It is then precisely aligned with the LED-PD detection couple for absorbance measurements. Data is logged using a laptop, via a USB connection. Within 10 minutes, 3 sample measurements can be made.

A comparison of the two sensor systems in summarised in Table 5.1, as well as shcematics of their function shown in Fig. 5.3 and 5.4.

Table 5.1. Comparison of features of the sensors used in this study.

Feature	PhosphaSense	AutoPhos
Mode of Operation	Hand-held	Autonomous
Analytical method	Molybdenum blue	Yellow
Optical path length	75 mm	13.7 mm
Chip type	Disposable microfluidic disc	Reusable microfluidic chip
Chip material	Clear PMMA bonded with PSA	Tinted PMMA, solvent bonded
Pump method	Centrifugal force	Syringe pumps
Sample volume	500 µL	2 mL
Sample throughput	3 samples in 10 min	1 sample in 10 min
Power source	12 V mains supply	12 V lead acid battery
Sample intake	Manual	Automated
Mass	2 kg	13 kg
Dimensions	20 x 18 x 14 cm	54 x 44 x 20 cm
Component Cost	Approx. €150	Approx. €2000

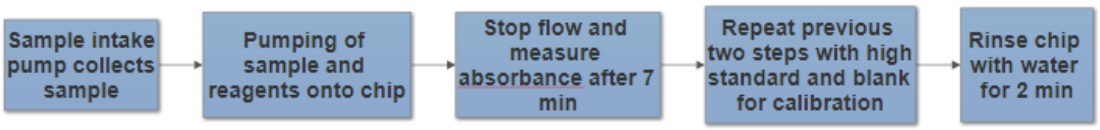

Fig. 5.3. A schematic of the steps involved for AutoPhos to make a measurement.

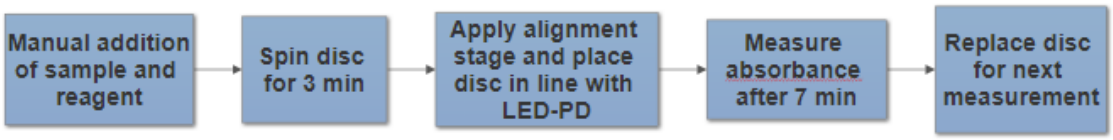

Fig. 5.4. A schematic of the steps involved for PhosphaSense to make a measurement.

5.3 Experimental

5.3.1 Sensor validation

All standards were validated using the vanadomolybdophosphoric acid method on a Shimadzu UV mini-1240 spectrometer **(**Shimadzu Corporation, Japan**).** Field samples were validated using a Lachat QC8500 Flow Injection Autoanalyzer (Lachat Instruments, Loveland, Colorado, USA) as described below.

5.3.2 Sensor calibration

Both sensors were calibrated in the laboratory in both Ireland and the USA. A comparison between these calibrations was made in order to show sensor reliability and stability. The same concentration of phosphate standards and reagents were prepared for the calibrations in each continent.

For PhosphaSense, calibration was carried out within its operating range of 8-1000 µg L^{-1} PO_4-P. For AutoPhos, a higher operating range of 0.4-20 mg L^{-1} PO_4-P was measured. The LOD and LOQ were calculated as 3 times or 10 times the standard deviation of the blank, respectively, divided by the slope of the calibration curve.

5.3.3 Off-chip mixing

In order to demonstrate the performance of the optical detection system of the AutoPhos sensor, without any influence from the mixing efficiency of the microfluidic chip, standards were mixed with reagent off-chip in triplicate, and then injected onto the chip for absorbance measurement. This allowed for a step by step transition from the laboratory to on-chip mixing and measurements.

5.3.4 Field Deployment

Site Description

The field portion of this study was conducted in Shatto Ditch, which is a tributary of the Tippecanoe River in north-central Indiana, USA. Shatto is typical of agricultural streams in the Midwest region of the USA and has historically been maintained as a drainage ditch with steep slopes and an incised, trapezoid-shaped channel. The surrounding landscape is primarily tile-drained row crop agriculture in a maize-soy bean rotation. As a result, Shatto has a flashy hydrograph and high concentrations of dissolved inorganic nutrients.

5.3.5 Pulse addition method

In order to evaluate sensor function in the field, a nutrient enrichment experiment was performed using a pulse addition method in Shatto Ditch (based on Tank *et al.* 2008)[29]. In order to determine travel time, ensure adequate mixing of the release solution across the stream channel, and determine the quantity of KH_2PO_4 needed for the nutrient pulse, a conservative tracer (100 g of sodium chloride, NaCl- dissolved in 1 L of stream water) was first released and downstream changes in conductivity were measured using a Pro30 Conductivity meter (YSI®). The nutrient pulse was added by dissolving 170 g of KH_2PO_4 in 20 L of stream water in a carboy, and this P-enriched solution was poured into the

stream. The aim for the peak concentration during the pulse was about 6 mg PO_4-P L^{-1} so that samples collected during the pulse would span the detection ranges for both sensors. This resulted in a rapid increase in P-concentrations followed by a gradual return to background P-concentrations which we characterized by measuring conductivity and taking grab samples every 30 – 120 s as the pulse passed by a sampling station located 50 m downstream of the nutrient addition.

Field samples were filtered into acid washed centrifuge tubes imediately after collection using glass fiber filters (1 µm nominal pore size; Pall, Ann Arbor Michigan, USA) and then stored on ice before returning to the laboratory after which they were transferred to a refrigerator (4°C). Field samples were analyzed within 24 hours after collection both using sensors, and with the molybdate blue method on a Lachat QC8500 Flow Injection Autoanalyzer.

Samples were measured using the Autophos Sensor in manual collection mode in the field as well as in the laboratory to compare function in the field with laboratory results. Manual collection was used because the sample time for autonomous mode (10 min) was too long to adequately characterize the nutrient pulse (~15 min). However, the sample frequency for autonomous mode would be appropriate for field monitoring given that P-concentrations are relatively stable during baseflow and storm pulses typically occur over a longer time frame (several hours to several days). Samples were also measured in the laboratory with the PhosphaSense system. Conductivity measurements were used to determine which sensor should be used for sample measurement based on expected P concentrations.

5.4 Results and discussion

5.4.1 Calibration of AutoPhos sensor

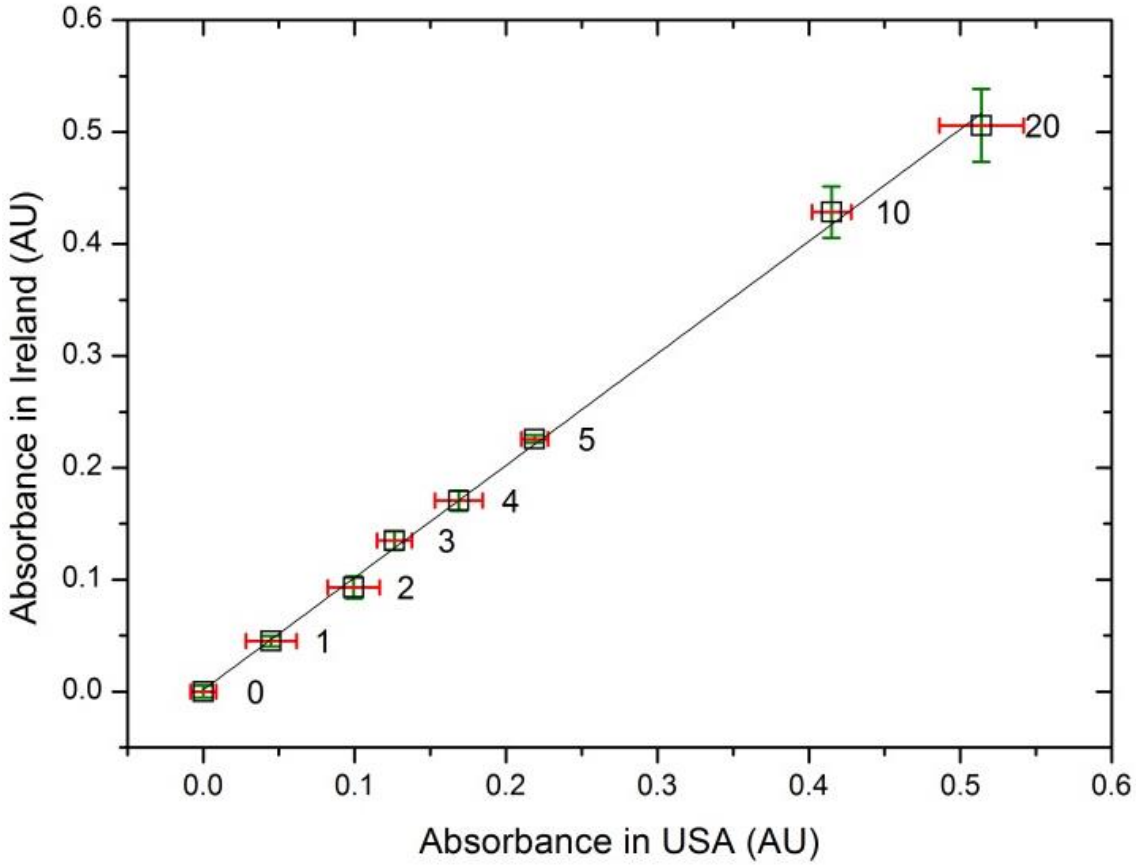

Fig. 5.5. A correlation plot between the calibration carried out on the AutoPhos system in Ireland vs. that carried out in the USA, yielding an R^2 value of 0.998, where the phosphate concentration is shown in mg L^{-1}, and error bars represent standard deviation, where n=3.

As shown in Fig. 5.5, inter-laboratory and inter-continental sensor stability was demonstrated. Correlation with an R^2 value of 0.998 is reported from 0-20 mg L^{-1}, using different batches and suppliers of reagents. This excellent sensor performance between continents shows that the system is robust enough for transport, and reliable enough for consistent analytical performance within two different climates.

5.4.2 Off-chip mixing

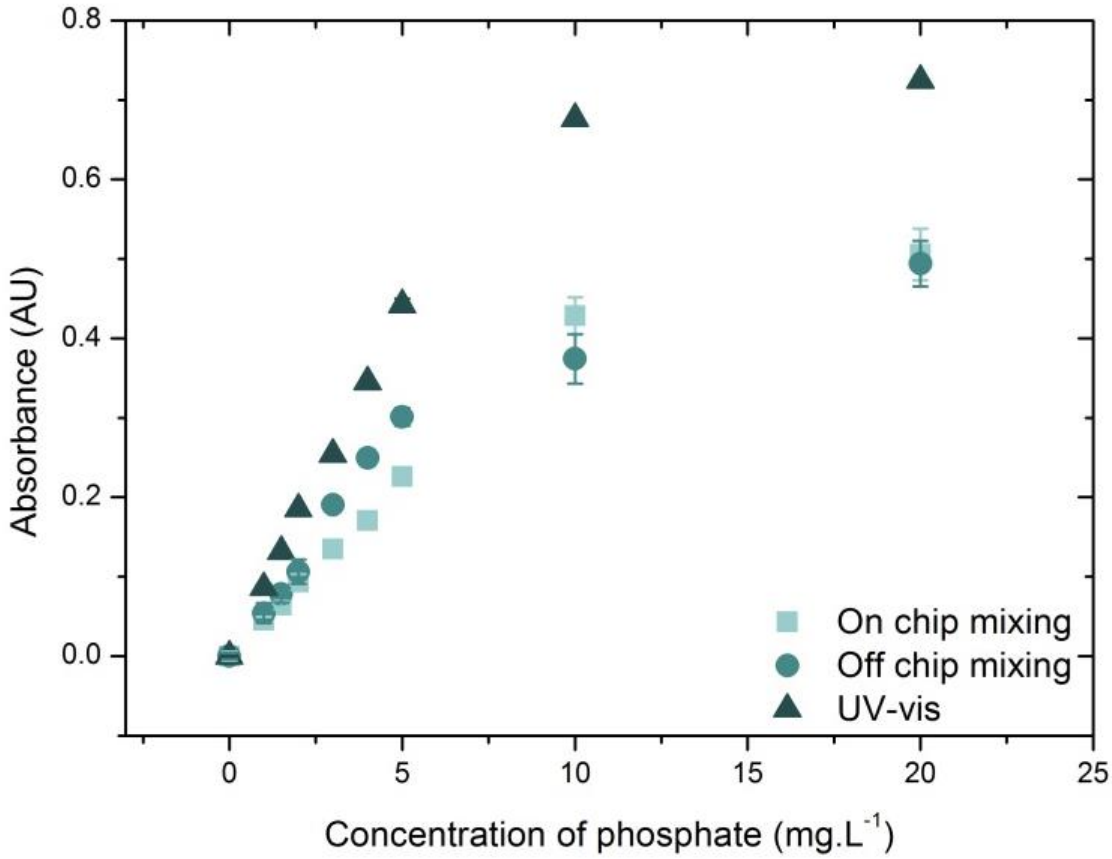

Fig. 5.6. On-chip mixing, off-chip mixing and UV-vis absorbance measurements for a range of phosphate concentrations, with error bars showing the standard deviation, where n=3.

In order to progressively move from sample analysis on the UV-vis spectrophotometer to analysis on the AutoPhos sensor, an off-chip mixing step was included as an intermediate validation. As shown in Fig. 5.6, UV-vis measurements were the most sensitive, showing the greatest slope. This was followed by off-chip mixing, while on-chip mixing showed slightly lower absorbance values. This is because diffusional mixing occurs on-chip, which is less efficient than mixing off-chip. More time must therefore be allowed for on-chip mixing. The linear range was wider for on-chip analysis, reaching as high as

10 mg L^{-1}, while the other two methods only reached 5 mg L^{-1}. The LOD, LOQ, linear range and R^2 value for each validation stage are summarised in Table 5.2.

Table 5.2. A comparison of the analytical performance of UV-vis spectrophotometer with off- and on-chip mixing, where concentrations are given in mg L^{-1}.

Method	LOD mg L^{-1}	LOQ mg L^{-1}	Linear range mg L^{-1}	R^2	Sensitivity
UV-vis	0.019	0.064	0.064 -5	0.998	0.09
Off-chip mixing	0.199	0.663	0.663 -5	0.990	0.06
On-chip mixing	0.414	1.382	1.382 - 10	0.999	0.04

For on-chip measurements, the calculated LOD and LOQ were greater than the experimentally determined values, where three of the prepared standards with concentrations below the calculated LOQ were measurable in triplicate, fitting on the linear portion of the response curve. This is shown in Fig. 5.7.

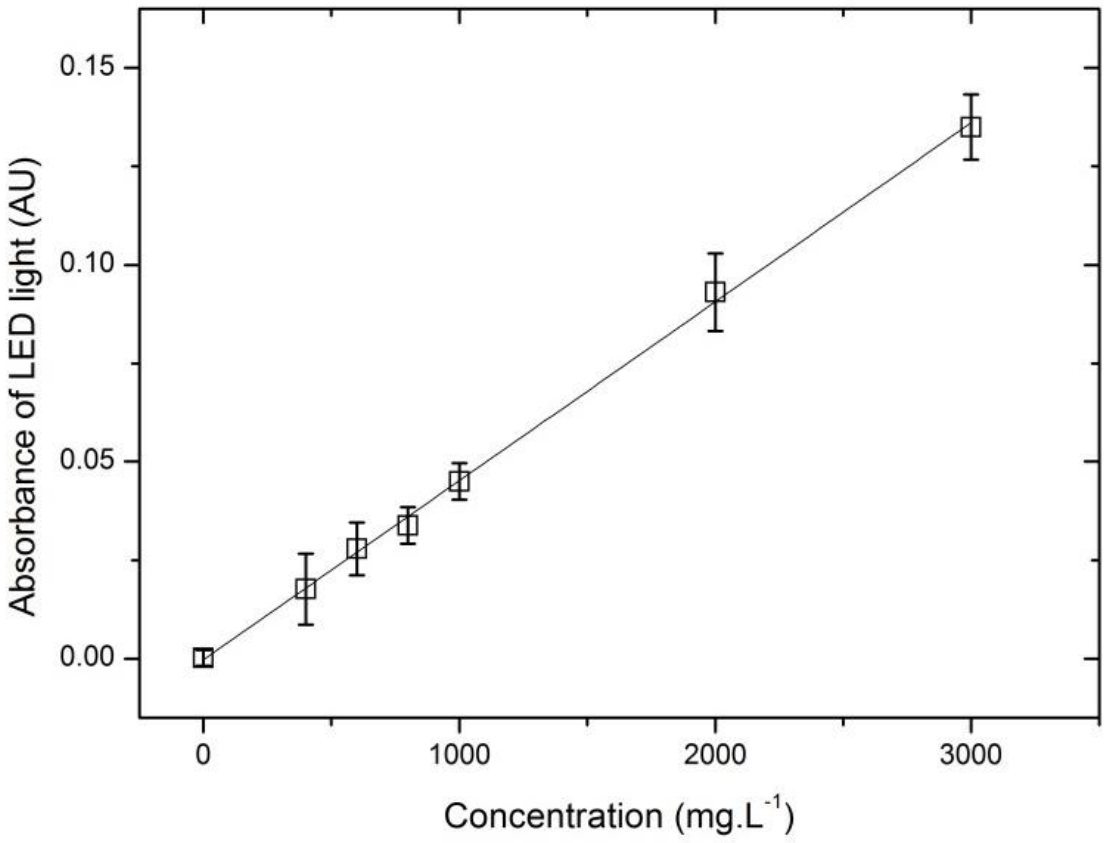

Fig. 5.7. Calibration curve including standards below the calculated LOQ, with and R^2 value of 0.999, where n=3.

5.4.3 Calibration of PhosphaSense

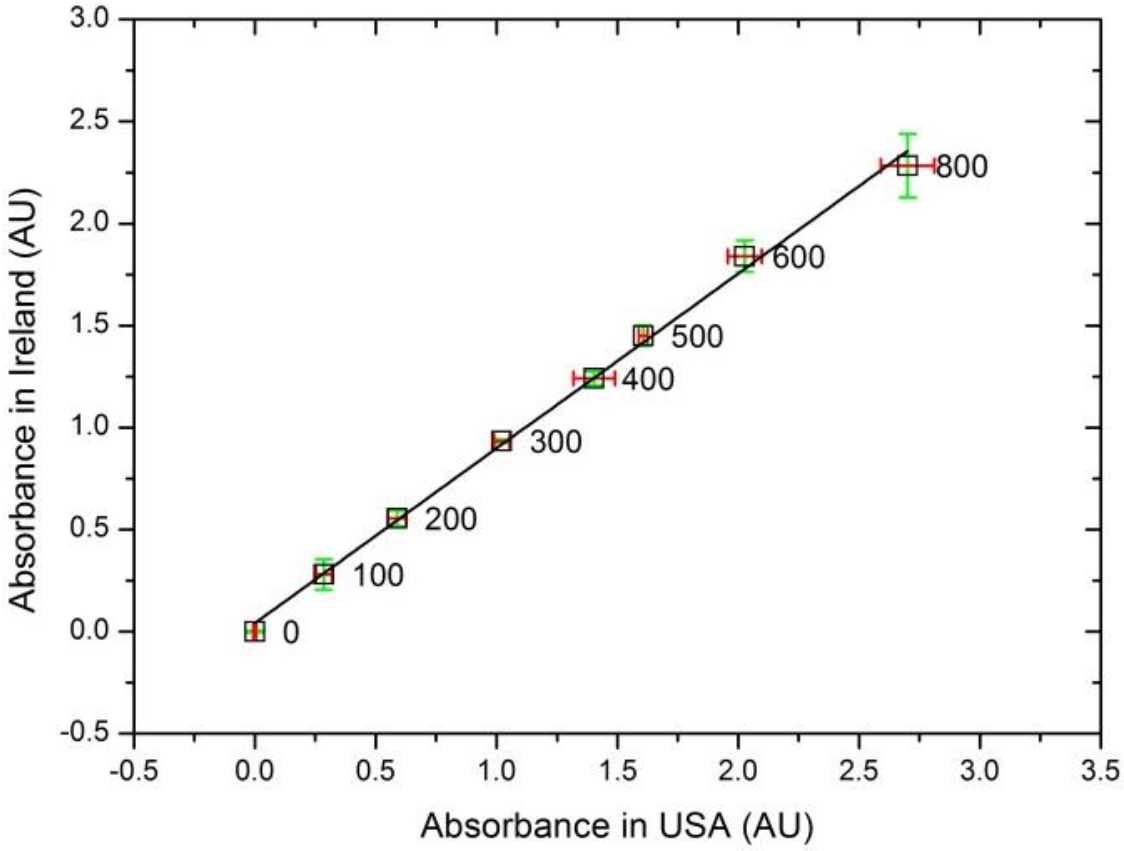

Fig. 5.8. A correlation plot for PhosphaSense between calibration carried out in Ireland (previously published)[7] vs. that carried out in the USA with an R^2 of 0.997, where the phosphate concentration is shown in µg L^{-1}, and error bars represent standard deviation, where n=3.

The calibration of PhosphaSense yielded data that correlated closely with previously published calibration data obtained in Ireland, as shown by Fig. 5.8, where the R^2 was 0.997 and the slope was 0.9.[7] The calibration yielded data that is summarised in Table 5.3.

Table 5.3. A comparison of the analytical performance of PhosphaSense in two different continents, where concentrations are given in µg L^{-1}.

Location	LOD	LOQ	Linear range	R^2	Sensitivity
	$\mu g L^{-1}$	$\mu g L^{-1}$	$\mu g L^{-1}$		AU L μg^{-1}
Ireland[7]	5	14	14-800	0.996	0.0030
USA	5	18	18-800	0.997	0.0034

The performance of PhosphaSense in both locations was very similar. A slightly higher LOQ of 18 µg L^{-1} was obtained from the USA data compared with 14 µg L^{-1} in Ireland, and a slightly higher sensitivity of 0.0034 AU L μg^{-1} was obtained in the USA, compared to 0.003 AU L μg^{-1}.

5.4.4 In-field measurements

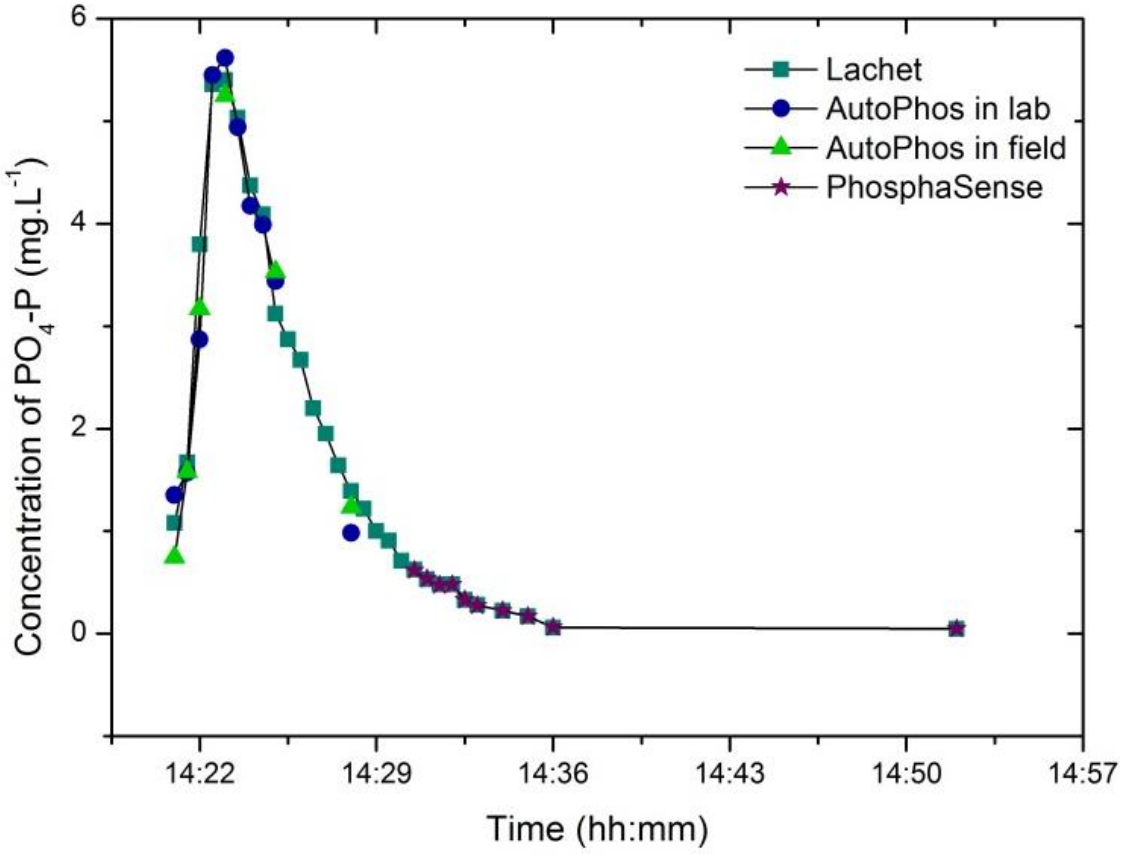

Fig. 5.9. A plot of the data obtained by measuring field samples in-field and in the lab on the AutoPhos sensor, on PhosphaSense, and on the Lachet system.

There was good agreement between the Lachet data and both sensor systems, as shown in Fig. 5.6. The AutoPhos sensor underestimated the concentration of some samples, with average percentage error of 13%. However, the overall shape of the response matched closely to that of the Lachet system, meaning that the sensor could capture the event well. Excellent agreement was seen between PhosphaSense and the Lachet system for samples within the sensor's predetermined measurement range, with an average percentage error of 1.7%. In-lab measurements on the AutoPhos system yielded average percentage error of 9%. Furthermore, these results show that calibration of both sensors with DIW standards yielded accurate measurements for P in a fresh water matrix.

5.5 Conclusions

The aim of this work was to field-test two novel phoshate sensors. The systems are designed to measure concentrations in the range 18-800 µg L^{-1} and 0.4-10 mg L^{-1}, which are relevant for the wide concentration ranges evident in agricultueral catchments. Good correlation was seen between the two novel sensors and the validation method, showing that both sensors could capture valuable data for field samples, within their measurement ranges. Good correlation was also seen between calibrations carried out in two different continents, showing the excellent stability and robustness of the sensors.

This study showed that by using different colourimetric methods on different types of microfluidic platforms, different ranges of phosphate concentrations could be effectively measured. The highly sensitive molybdenum blue colourimetric method on centrifugal disc with a long optical path length of 75 mm performed well on field samples, yielding average percentage error of 1.7%. Its measurement range was 18-800 µg L^{-1}. This contrasted with the less sensitive yellow method on microfluidic chip with a 13.7 mm optical path length, which yielded a much wider linear measurement range of 0.4-10 mg L^{-1}, with average % error of 13% for field sample measurements, and 9% for in-lab measurements. Inter-continental calibration agreement showed that both sensors were robust enough for transport and travel, yielding high correlation between the two calibration sets.

Two different low-cost pumping methods were demonstrated: motor driven syringe pump pairs for AutoPhos, and a single motor for PhosphaSense. The single motor on PhosphaSense pumped 3 separate samples, allowing for 3 simultaneous measurements within 10 min. This meant that it had a higher sample throughput than AutoPhos. AutoPhos was restricted to one sample measurement every 10 min. However, AutoPhos was capable of continuous, unattended monitoring, while PhosphaSense required manual input of sample and reagent, and manual placement of the alignment stage for absorbance measurements.

The disposable nature of the microfluidic disc means that PhosphaSense has a higher running cost, while the reusable microfluidic chip on the AutoPhos sensor means that reagents are the only consumables. However, the component cost is significantly lower for PhosphaSense, with parts costing less than €150, while components for the AutoPhos system costed approx. €2000. This is a significant reduction in costs relative to commercially available PO4 sensors (eg. $17,000 per unit with operating costs of $2,500 per sensor per year) and has the potential to increase access to high frequency monitoring, which, to date, has been limited due to high costs. Because peak nutrient export from agricultural watersheds occurs during storms due to fertiliser runoff from fields, high frequency measurements during these critical periods would improve both estimates for annual nutrient export and our ability to detect the effects of agricultural management and conservation on water quality.[30]

Acknowledgements

The authors would like to thank the Naughton Graduate Fellow-ship Program 2013 in the University of Notre Dame, USA, and DCU Educational Trust and Faculty of Science & Health for funding this project.

Notes and references

1. P. Worsfold, I. McKelvie, P. Monbet, Determination of phosphorus in natural waters: A historical review, Anal. Chim. Acta. (2016) 8–20. doi:10.1016/j.aca.2016.02.047.
2. P.J.A. Withers, H.P. Jarvie, Delivery and cycling of phosphorus in rivers: A review, Sci. Total Environ. 400 (2008) 379–395. doi:10.1016/j.scitotenv.2008.08.002.

3. C. Warwick, A. Guerreiro, A. Soares, Sensing and analysis of soluble phosphates in environmental samples: A review, Biosens. Bioelectron. 41 (2013) 1–11. doi:10.1016/j.bios.2012.07.012.
4. P.M. Haygarth, H.P. Jarvie, S.M. Powers, A.N. Sharpley, J.J. Elser, J. Shen, H.M. Peterson, N.I. Chan, N.J.K. Howden, T. Burt, F. Worrall, F. Zhang, X. Liu, Sustainable phosphorus management and the need for a long-term perspective: The legacy hypothesis, Environ. Sci. Technol. (2014) 8417–8419. doi:10.1021/es502852s.
5. UK Technical Advisory Group, 2012, *Phosphorus Standards For Rivers,* available from: https://www.wfduk.org/sites/default/.../Phosphorus%20standards%20for%20rivers.pdf (accessed on 11/08/17)
6. P.J.A. Withers, H.P. Jarvie, Delivery and cycling of phosphorus in rivers: A review, Sci. Total Environ. 400 (2008) 379–395. doi:10.1016/j.scitotenv.2008.08.002.
7. G. Duffy, I. Maguire, B. Heery, C. Nwankire, J. Ducrée, F. Regan, PhosphaSense: A fully integrated, portable lab-on-a-disc device for phosphate determination in water, Sensors Actuators B Chem. 246 (2017) 1085–1091. doi:10.1016/j.snb.2016.12.040.
8. N. Lingaiah, K.M. Reddy, P. Nagaraju, P.S.S. Prasad, I.E. Wachs, Influence of vanadium location in titania supported vanadomolybdophosphoric acid catalysts and its effect on the oxidation and ammoxidation functionalities, J. Phys. Chem. C. 112 (2008) 8294–8300. doi:10.1021/jp7119476.
9. J. Cleary, D. Maher, D. Diamond. 2013. Development and deployment of a microfluidic platform for water quality monitoring. In: Mukhopadhyay, Subhas C. and Mason, Alex, (eds.) Smart Sensors for Real-Time Water Quality Monitoring. Smart Sensors, Measurement and Instrumentation. Springer-Verlag, Berlin Heidelberg 2013, 125-148.

10. A. E. Greenberg, L. S. Clesceri, A. D. Eaton. Standard Methods for the Examination of Water and Wastewater. 18th ed. 1992.
11. C. Slater, J. Cleary, K.T. Lau, D. Snakenborg, B. Corcoran, J.P. Kutter, D. Diamond, Validation of a fully autonomous phosphate analyser based on a microfluidic lab-on-a-chip, Water Sci. Technol. 61 (2010) 1811–1818. doi:10.2166/wst.2010.069.
12. F.E. Legiret, V.J. Sieben, E.M.S. Woodward, S.K. Abi Kaed Bey, M.C. Mowlem, D.P. Connelly, E.P. Achterberg, A high performance microfluidic analyser for phosphate measurements in marine waters using the vanadomolybdate method, Talanta. 116 (2013) 382–387. doi:10.1016/j.talanta.2013.05.004.
13. A.T. Law Al, S.B. Adeloju, Progress and recent advances in phosphate sensors: A review, Talanta. 114 (2013) 191–203. doi:10.1016/j.talanta.2013.03.031.
14. L. Drummond, W. Maher, Determination of phosphorus in aqueous solution via formation of the phosphoantimonylmolybdenum blue complex Re-examination of optimum conditions for the analysis of phosphate, Anal. Chim. Acta. 302 (1995) 69–74.
15. Sea-Bird Scientific HydroCycle-PO_4 data sheet 'In situ dissolved phosphate' 2017. Available at: http://wetlabs.com/hydrocycle (accessed 30/04/17)
16. M. Czugala, D. Maher, F. Collins, R. Burger, F. Hopfgartner, Y. Yang, J. Zhaou, J. Ducrée, A. Smeaton, K.J. Fraser, F. Benito-Lopez, D. Diamond, CMAS: fully integrated portable centrifugal microfluidic analysis system for on-site colorimetric analysis, RSC Adv. 3 (2013) 15928–15938. doi:10.1039/c3ra42975j.
17. A. LaCroix-Fralish, J. Clare, C.D. Skinner, E.D. Salin, A centrifugal microanalysis system for the determination of nitrite and hexavalent chromium, Talanta. 80 (2009) 670–675. doi:10.1016/j.talanta.2009.07.046.

18. H. Hwang, Y. Kim, J. Cho, J.Y. Lee, M.S. Choi, Y.K. Cho, Lab-on-a-disc for simultaneous determination of nutrients in water, Anal. Chem. 85 (2013) 2954–2960. doi:10.1021/ac3036734.
19. Y. Xi, E.J. Templeton, E.D. Salin, Rapid simultaneous determination of nitrate and nitrite on a centrifugal microfluidic device, Talanta. 82 (2010) 1612–1615. doi:10.1016/j.talanta.2010.07.038.
20. M. Czugala, R. Gorkin III, T. Phelan, J. Gaughran, V.F. Curto, J. Ducrée, D. Diamond, F. Benito-Lopez, Optical sensing system based on wireless paired emitter detector diode device and ionogels for lab-on-a-disc water quality analysis, Lab Chip. 12 (2012) 5069. doi:10.1039/c2lc40781g.
21. Isabel M. Perez de Vargas Sansalvadora, Cormac D. Fay, John Cleary, Adrian M. Nightingale, Matthew C. Mowlem, Dermot Diamond, Autonomous reagent-based microfluidic pH sensor platform, Sensors & Actuators B: Chemical, 2016, 225, 369-376.
22. D. Thouron, R. Vuillemin, X. Philippon, A. Lourenço, C. Provost, A. Cruzado, V. Garçon, An autonomous nutrient analyzer for oceanic long-term in situ biogeochemical monitoring, Anal. Chem. 75 (2003) 2601–2609. doi:10.1021/ac020696+.
23. V.M.C. Rérolle, C.F.A. Floquet, A.J.K. Harris, M.C. Mowlem, R.R.G.J. Bellerby, E.P. Achterberg, Development of a colorimetric microfluidic pH sensor for autonomous seawater measurements, Anal. Chim. Acta. 786 (2013) 124–131. doi:10.1016/j.aca.2013.05.008.
24. E. Taylor, J. Bonner, R. Nelson, C. Fuller, W. Kirkey, S. Cappelli, Development of an in-situ total phosphorus analyzer, Ocean. MTS/IEEE Washingt. (2016) 1–4. doi:10.23919/OCEANS.2015.7404384.
25. A.D. Beaton, C.L. Cardwell, R.S. Thomas, V.J. Sieben, F.-E. Legiret, E.M. Waugh, P.J. Statham, M.C. Mowlem, H. Morgan, Lab-on-chip measurement of nitrate and nitrite for in situ analysis of natural waters., Environ. Sci. Technol. 46 (2012) 9548–9556. doi:10.1021/es300419u.

26. D. Cogan, C. Fay, D. Boyle, C. Osborne, N. Kent, J. Cleary, D. Diamond, Development of a Low Cost Microfluidic Sensor for the Direct Determination of Nitrate Using Chromotropic Acid in Natural Waters, Anal. Methods. 7 (2015) 5396–5405. doi:10.1039/C5AY01357G.
27. D. Cogan, J. Cleary, T. Phelan, E. McNamara, M. Bowkett, D. Diamond, Integrated flow analysis platform for the direct detection of nitrate in water using a simplified chromotropic acid method, Anal. Methods. 5 (2013) 4798–4804. doi:10.1039/c3ay41098f.
28. C.D.M. Campos, J. A. F. da Silva, Applications of autonomous microfluidic systems in environmental monitoring, RSC Adv. 3 (2013) 18216. doi:10.1039/c3ra41561a.
29. P.J. Mulholland, A.M. Helton, G.C. Poole, R.O Hall, S.K. Hamilton, B.J. Peterson, J.L. Tank, L.R. Ashkenas, L.W. Cooper, C.N. Dahm, W.K. Dodds, S. E. G. Findlay, S. V. Gregory, N. B. Grimm, S. L. Johnson, W. H. McDowell, J. L. Meyer, H. M. Valett, J. R. Webster, C. P. Arango, J. J. Beaulieu, M. J. Bernot, A. J. Burgin, C. L. Crenshaw, L. T. Johnson, B. R. Niederlehner, J. M. O'Brien, J. D. Potter, R. W. Sheibley, D. J. Sobota & S. M. Thomas, Stream denitrification across biomes and its response to anthropogenic nitrate loading. Nature, 2008, 452, 202-205. doi:10.1038/nature06686
30. L.E. Gentry, M.B. David, T. V Royer, C.A. Mitchell, K.M. Starks, Phosphorus transport pathways to streams in tile-drained agricultural watersheds., J. Environ. Qual. 36 (2007) 408–415. doi:10.2134/jeq2006.0098.

Chapter 6:

Conclusion

Overall Summary & Conclusion

The aim of this thesis was to develop low-cost, microfluidic, colourimetric sensors for environmental water quality monitoring. The development of low-cost sensors for maintenance and management of environmental water resources is of critical importance worldwide. Autonomous and handheld sensor systems allow for more frequent and widespread monitoring to be carried out, enabling large data set collection and larger-scale studies. This thesis presented the development of both autonomous and handheld sensors for the measurement of phosphate and chromium (III) and (VI) in water. Colourimetric, wet chemistry-based determination methods coupled with microfluidic technology were shown to be an excellent means for reliable and viable sensor development. Accuracy and repeatability of measurements were demonstrated on all systems, using environmental water matrices to demonstrate method robustness in real water samples.

Three sensors were developed and characterised: two hand-held analysers suitable for in-field measurements and one autonomous system suitable for deployment in a water body. Centrifugal microfluidic technology was chosen as the optimal design for hand-held systems as they require no fluidic pumps, only a motor for disc rotation. These handheld analysers were fabricated for the measurement of phosphate, and for the speciation of chromium in water. For the deployable sensor system, the more expensive approach of a microfluidic chip with syringe pumps for fluid delivery was chosen due to the reusable nature of the chip in this format. This system was characterised, alongside the hand-held phosphate sensor, using field samples collected from an agricultural stream in Shatto Ditch, Indiana, USA, as part of a collaboration with Prof. Jennifer Tank in University of Notre Dame. Its in-field performance was compared to its performance on grab samples analysed in the laboratory environment.

A major challenge for the development of low-cost sensors for in-field use is the limit of detection that can be achieved using a simple, low-cost LED-PD detection

system. The majority of microfluidic sensing systems with absorbance detection use expensive, polychromatic light sources and sensitive detectors such as a photodiode array system or a spectrometer coupled with fibre optic technology. This not only increases the system cost and power consumption greatly, but it also reduces portability of the system, making it unsuitable for in-field sensors. This challenge was overcome in a number of ways. The sensitivity of each system was maximised by optimisation of the wet chemistry methods (eg. pH optimisation, reagent concentration optimisation, inclusion of a heating step etc.), by optimisation of lighting conditions (eg. collimation lenses, tinted PMMA, reduction of light scattering and refraction) and by the incorporation of long optical path lengths within the microfluidic systems for absorbance measurements. Optimisation of LED light intensity and photodiode measurement range was essential for optimisation of measurement ranges and LODs. The use of well validated colourimetric methods with fewer steps in the reaction meant that the complexity of the microfluidic design and sensor design could be minimised, ensuring reliability for in-field use or long-term deployments, and user-friendly devices.

The low cost of these sensor systems was achieved in a number of ways. The use of low-cost fabrication methods and sourcing of low-cost materials and components contributed to the low component cost. The detection systems used costed less than €4, a great reduction compared to the alternative options. The incorporation of microfluidics allowed for reduction of running costs by reducing the volume of reagent consumed and the waste produced per sample. The handheld systems achieved a significantly lower component cost than the AutoPhos system as they did not need to withstand very harsh environmental conditions, and some manual steps were included, reducing the complexity of electronic components and system automation required. A 3D printed housing was sufficient for these analysers, while the AutoPhos system required a fully waterproof, strong housing to withstand storms and harsh environmental conditions. AutoPhos required multiple syringe pumps to deliver reagents and

samples to different inlets, while manual addition of sample and reagents on the disc-based systems allowed for one motor to be used for all fluid manipulation.

These sensors demonstrate the versatility of microfluidic technology for the automation of colourimetric chemistry methods, coupled with low-cost detection systems for determination of a wide range of different analytes in water. This versatile modular design approach can be used to automate a range of different colourimetric methods by a simple change in microfluidic design and in detection wavelength, enabling a suite of sensors to be developed for wide scale environmental analysis.

“Begin at the beginning, and go on till you come to the end:

then stop.”

Lewis Carroll